Controlled Release of Dexamethasone to the Inner Ear from silicone-based Implants

——

Libération contrôlée de dexaméthasone à partir des implants en silicone pour l'oreille interne

THESE DE DOCTORAT

Soutenue le 29 Janvier 2016 à Lille

MARIA GEHRKE

Dirigée par:

Dr. Florence Siepmann – Directrice

Prof. Christophe Vincent – Co-directeur

Composition du Jury :

Monsieur SIEPMANN Juergen   Président de Jury
Professeur à l'Université de Lille 2

Monsieur VERVAET Chris   Rapporteur
Professeur à l'Université de Gand

Madame BOCHOT Amélie   Rapporteur
Professeur à l'Université Paris-Sud

Madame PIEL Géraldine   Examinatrice
PhD à l'Université de Liège

Madame SIEPMANN Florence   Directrice de Thèse
Maître de conférences, HDR à l'Université de Lille 2

Remerciements

Je tiens à remercier vivement tous les personnes qui m'ont accompagné durant mes trois ans de thèse.

Je tiens à remercier Dr. Florence Siepmann pour avoir accepté d'encadrer ce travail. Merci beaucoup pour l'encouragement et les discussions très ouvertes (p.ex. pour détourner l'utilisation du matériel de laboratoire) et pour m'avoir laissé beaucoup de liberté au sein du laboratoire. Merci de m'avoir encouragée à toujours garder un équilibre entre la recherche scientifique et la vie de famille.

Je remercie aussi le Professeur Christophe Vincent qui m'a encadré comme co-directeur de thèse pour m'avoir donné toujours beaucoup d'idées. De plus, il m'a donné l'opportunité de travailler avec plusieurs étudiants de son équipe qui ont grandement aidé à l'avancement de ce projet de thèse. Merci beaucoup!

Je voudrais remercier le Professeur Jürgen Siepmann pour m'avoir accueilli dans son équipe internationale. Dès le premier jour de mes six mois d'Erasmus à Lille, et jusqu'à la fin de ma thèse, j'ai beaucoup apprécié sa gentillesse d'une part, et ses connaissances scientifiques d'autre part. Merci mille fois!

J'exprime toute ma reconnaissance envers les Professeurs Amélie Bochot de l'Université Paris-Sud et Chris Vervaet de l'Université de Gand qui m'ont fait le grand plaisir de juger ce travail en tant que rapporteurs et membres de mon jury de thèse.
Je tiens également à remercier Dr. Géraldine Piel de l'Université de Liège pour avoir accepté d'évaluer ma thèse en tant que membre de jury.

Je remercie beaucoup les personnes avec qui j'ai eu la possibilité de travailler pendant ma thèse et qui m'ont chacune et chacun grandement aidé : particulièrement le Professeur Stefan Plontke de l'Université de Halle de m'avoir accueillie dans son laboratoire pour apprendre les techniques d'implantation, mais aussi Florence Danède et Jean-François Willart de l'Université de Lille 1 pour l'aide concernant la réalisation et l'évaluation des analyses de calorimétrie différentielle à balayage et de diffraction des rayons X.

Table of Contents

List of Abbreviations

AIED	Autoimmune Inner Ear Disease
BDNF	Brain-derived neurotrophic factor
DNQX	6,7-dinitroquinoxaline-2,3-dione
DXM	Dexamethasone
GOM	Glycerolmonooleate
LSR	Liquid Silicone Rubber
NIHL	Noise-Induced Hearing Loss
OWM	Oval window membrane
PEG	Polyethyleneglycol
PLGA	Poly(lactic-co-glycolic acid)
RWM	Round window membrane
SNHL	Sensorineural Hearing Loss
SPION	Superparamagnetic iron oxide nanoparticle
SSNHL	Sudden Sensorineural Hearing Loss

1.   Introduction

The ear is responsible for the perception of sound and the sense of balance. In 2015, the WHO estimated that worldwide 360 million people (over 5 % of the population) are suffering from disabling hearing loss, meaning a loss of 40 or 30 dB in the better hearing ear in adults and children respectively (1). In the USA 15 % of the population over 18 reported at least minor changes in hearing capacities (classification from "a little bit of trouble hearing" to "deaf") (2).

Hearing loss can have several causes: The loss before or soon after the birth of a child is one of the most frequent birth defects since 0.1 to 0.3 % of all neonates are born with congenital hearing loss (3,4). Nevertheless, hearing impairment nowadays can also be related to the certain employments of people: It has been reported that especially professional soldiers often suffer from hearing loss, tinnitus or other noise-related comorbidities following their service in the armed forces (5–7).

Additionally, a lot of employees in the manufacturing sector suffer from occupationally induced hearing loss. In 2010, about 16 million people have been working in the manufacturing sector in the USA (8). Those 16 million people have reported 42 700 cases of nonfatal occupational illness in 2013, therein - representing the majority - 13 400 cases of hearing loss in 2013 (9). That means that nearly one third of the reported illnesses in the manufacturing sector is related to hearing loss.

Importantly, hearing impairment can not only be related to the working situation but also to free time activities. The WHO states that 1.1 billion people have a high risk to suffer from hearing loss in the future due to excessive consumption of loud music in their free time, referred to as "recreational noise" (10). The use of audio devices or the attendance in a night club can lead to high noise levels over 85 dB that can damage the inner ear. E.g., the attendance to one single rock/pop concert with an average of 98.5 dBA resulted in a threshold shift of 10 dB or greater in 33.3 % of the examined persons in at least one ear compared to the data collected before the concert (11).

The treatment of diseases of the inner ear remains a challenging topic: People from all over the world are affected by hearing loss, tinnitus or other diseases related to inner ear disorders. The impact on the personal lives of patients is tremendous: They might suffer from social exclusion which could lead to psychological, educational and economic problems. Furthermore, the patients might experience violence due to stigmatization or prejudices regarding this invisible illness (12).

Despite the personal challenge, the overall costs for the society should not be underestimated: Higher unemployment rates in combination with lower income of patients who receive insufficient treatment of their disorder are estimated to cause lost taxes of over 18 billion US dollar annually in the USA (13). Especially the governments of developing countries sometimes seem to have difficulties providing the public with sufficient material and trained staff to treat hearing related illnesses. Therefore, children often receive appropriate treatment too late, e.g., in the LAUTECH Teaching Hospital (Osogbo, Nigeria), 109 (48.9 %) cases of hearing impairment in children could have been prevented by an appropriate treatment (14).

The examples cited above make it obvious why research on inner ear diseases remains a global challenge. To understand the underlying processes and find matching strategies to treat and help people whose daily lives are strongly affected by inner ear diseases will be a major topic in the upcoming years.

Before describing current strategies to deliver drugs to the inner ear (section 1.2.), a brief introduction of the anatomy and physiology of the ear will be given in the following chapter.

1.1. Anatomy and Physiology of the Ear

The ear is divided into three main parts: the outer, the middle and the inner ear (Figure 1.1.). The outer ear consists of the auricle which is the visible part of the ear and the 2.5 cm long ear canal that connects the outer ear with the tympanic membrane, also called ear drum (15).

The middle ear is limited by the tympanic membrane which is connected to the malleus, the incus and the stapes, the tiny chained up ossicles in the tympanic cavity. The stapes at the end of the ossicular chain stays in connection with the oval window. The air filled tympanic cavity has a volume of 1 to 2 cm^3 and is connected via the Eustachian tube with the oral cavity. Via this tube differences in pressure between the outer and the middle ear are compensated.

The middle ear is connected to the inner ear via the round window membrane and the oval window membrane. Those are two semi-permeable membranes through the petrous bone which surrounds the inner ear.

The inner ear consists of the cochlea where sound perception takes place and the vestibular system which is involved in the process to maintain the balance.
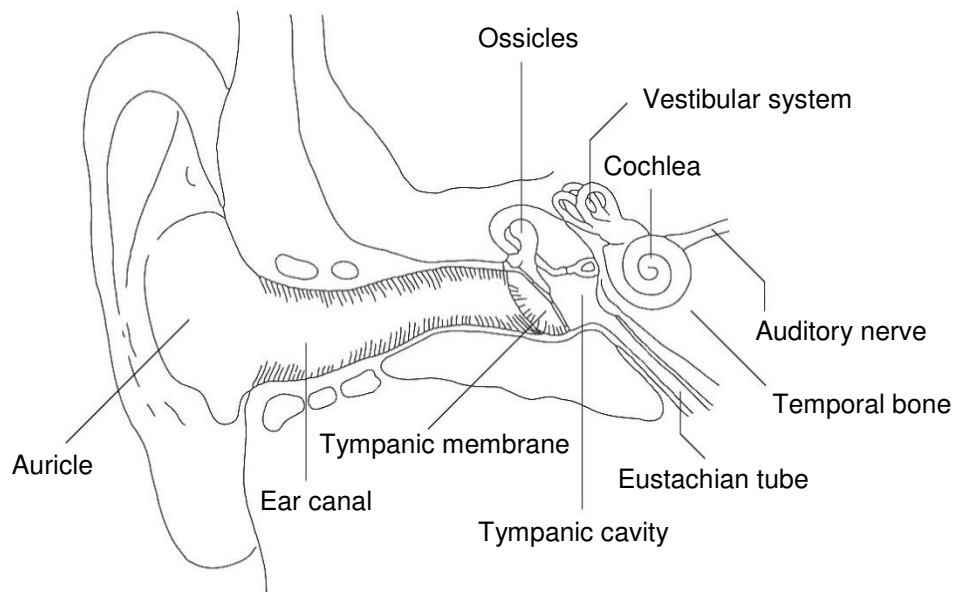
Figure 1.1. Anatomy of the ear: division into the outer (Auricle, Ear Canal, Tympanic membrane), the middle (Tympanic cavity, Ossicles, Eustachian tube) and the inner ear (Cochlea, Vestibular system), adapted from (16).

The cochlea has the form of a snail and consists of three fluid filled canals with a length of 31 to 37 mm coiled up in the cochlea (16,17): scala tympani and scala vestibuli are filled with perilymph which has a composition similar to other extracellular fluids whereas the scala media situated between the two other scalae is filled with endolymph (Figure 1.2.a). The latter has an unusual composition with a high concentration of potassium ions of 150 mM leading to a high potential in the endolymphatic fluid. The scalae tympani and vestibuli are connected at the apex of the cochlea via the helicotrema and have a volume of 70 µL in humans and 2.78 µl in gerbils which in both species is nearly ten times higher than the volume of the endolymphatic space (Table 1.1.).

To separate the three scalae from each other there are two membranes in the inner ear: Reissner's membrane between scala vestibuli and media as well as the basilar membrane between scala media and tympani (Figure 1.2.b). In the middle, the organ of Corti is situated in the scala media. The highly specialized inner and outer hair cells situated on the basilar membrane of the organ of Corti (Figure 1.2.c) are responsible for the translation of mechanical waves into electrical signals leading to the perception of sound in the brain (16).

a)

Scala vestibuli (perilymph)
Scala media (endolymph)
Scala tympani (perilymph)

Spiral ganglion (auditory nerve)

b)

Reissner's membrane

Scala media

Organ of Corti

Tectorial membrane

Basilar membrane

c)

Inner hair cell

Outer hair cell
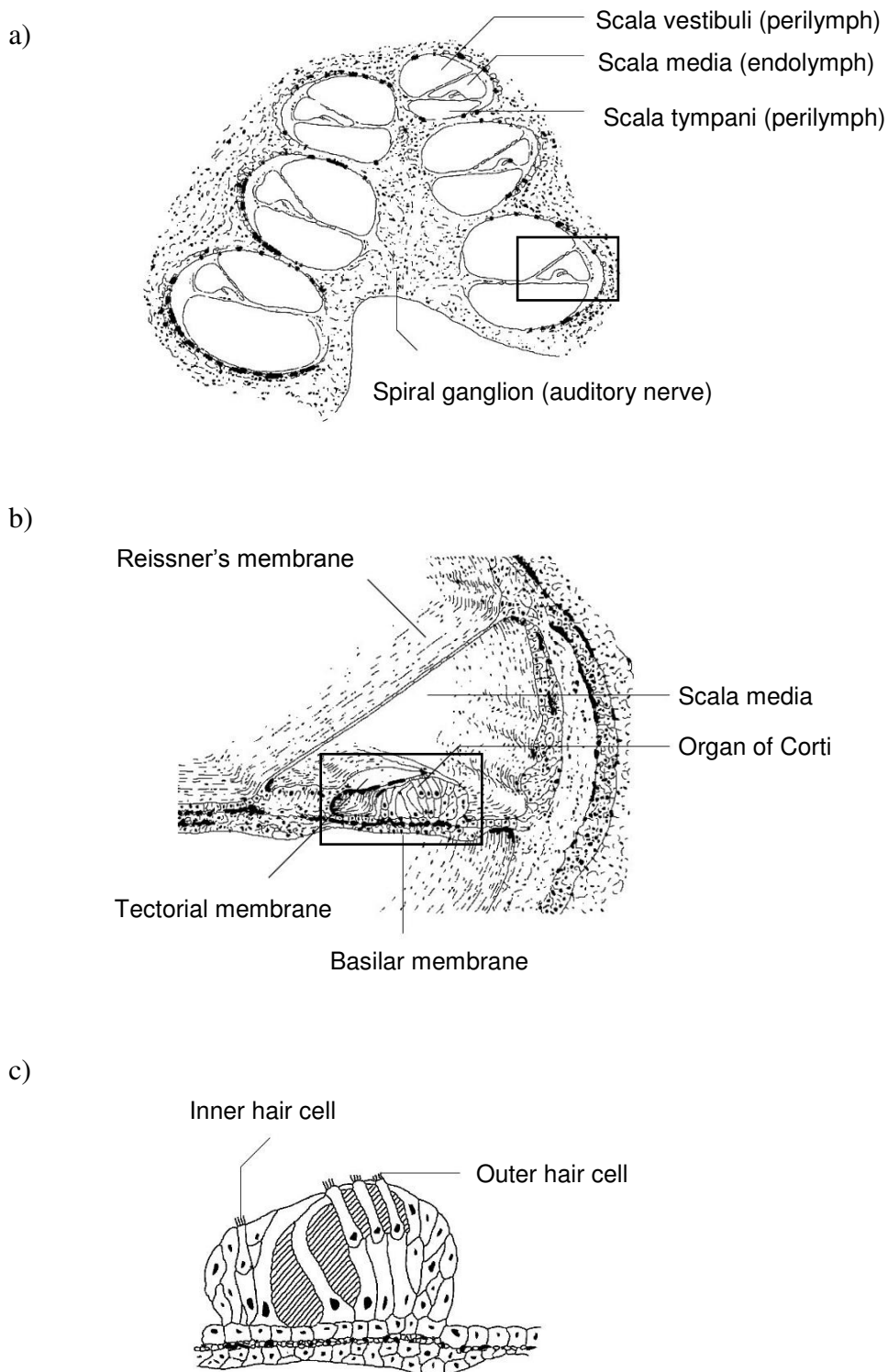
Figure 1.2. Anatomy of the cochlea: Section through the cochlea: a) cochlea with three coiled up fluid filled spaces: scala vestibuli, media and tympani; b) zoom into the scala media with the Organ of Corti – the organ containing the sensory cells; c) zoom into the Organ of Corti with three rows of outer hair cells and one row of inner hair cells, adapted from (16).

Table 1.1. Characteristics of fluids inside the cochlea: Perilymph and Endolymph in humans, adapted from (18,19).

	Perilymph	Endolymph
Volume, µL	70	8
Volume (gerbil), µL	2.78	0.38
Na^+, mM	160	1
K^+, mM	4-5	150
Cl^-, mM	120	130
H_2CO_3, mM	20	30
Ca^{2+}, mM	1.2	0.02
Glucose, mM	4	0.5
Proteins, g L^{-1}	1	0.15
pH	7.4	7.4
Osmolality, mOsm kg^{-1}	290	315
Potential, mV	0	+80

The vestibular system consists of the three semicircular canals as well as the vestibule which comprises of the utricle and saccule. It stays in contact with the fluids of the cochlea. That is why the inner ear can also be divided into the bony labyrinth, filled with perilymph, and the membranous labyrinth, filled with endolymph (20,21) (Figure 1.3.). The perilymph of the bony labyrinth stays in contact with the cerebrospinal fluid and surrounds the membranous labyrinth (22). Nevertheless, the flow of the inner ear fluids is very low which means that the local conditions in the vestibular system and the cochlea are maintained locally in each compartment of the two labyrinths (23).

Part of the membranous labyrinth of the vestibular system are the semicircular canals: the superior, the horizontal and the posterior canal. They are arranged at right angles to each other and open out into correspondent ampullae leading to the utricle (Figure 1.3. on the left hand side). The ampullae, the utricle and the saccule contain specialized hair cells detecting movement of the head: the macula is situated in the utricle and saccule whereas the crista ampullaris is situated in the ampullae (21).
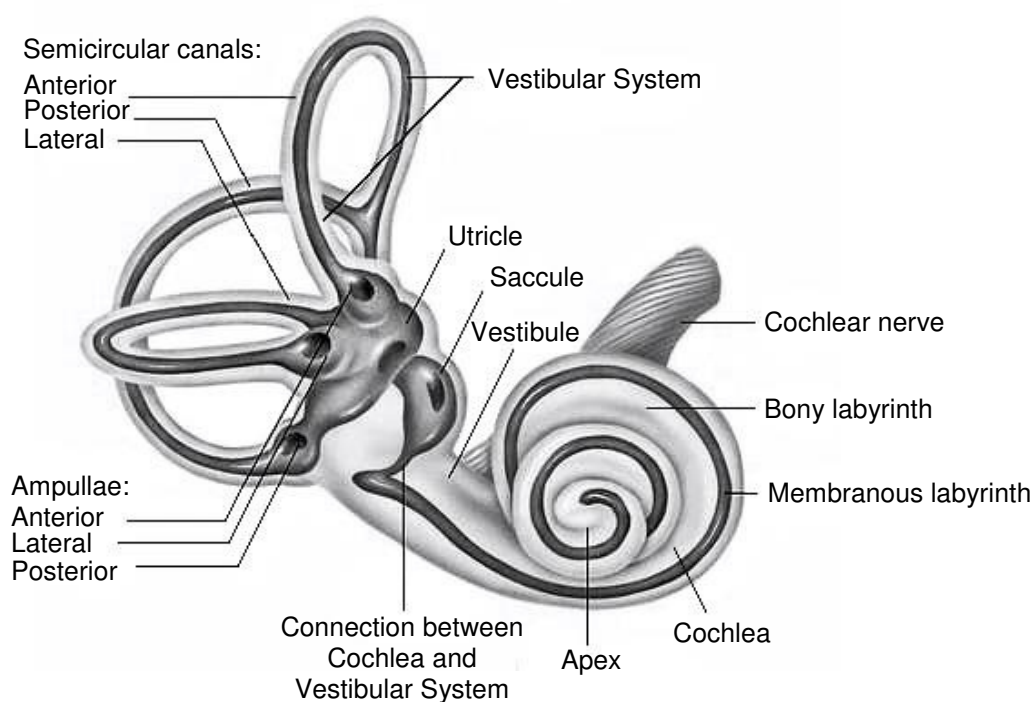
Figure 1.3. Anatomy of the inner ear: The fluids of the cochlea (right) stay in contact with the fluids of the vestibular system (left). The bony labyrinth with the Perilymph (light grey) surrounds the membranous labyrinth containing Endolymph (dark grey), adapted from (22).

This system reacts very sensitive to potentially toxic changes and, though, is protected by several barrier systems described in the following chapter.

1.1.1. Barriers of the Inner Ear

The highly sensitive inner ear is protected via three different barriers: The Blood-cochlea barrier, the tympanic membrane as well as the oval and the round window (18).

The blood-cochlea barrier, also called the blood-perilymph barrier, is similar to the blood-brain barrier: Diffusion of drugs from the systemic blood circulation into the inner ear is limited due to the special composition of the capillary endothelium of the blood vessels. It is blocking the entrance of drugs from blood stream into the cochlea via tight junctions without fenestrations (24–26). Furthermore, p-glycoprotein (p-gp) as well as multidrug resistance protein 1 (MRP1) has been detected in the inner ear indicating that it is also protected by efflux pumps (27,28). The impact on clinical results is important, e.g., dexamethasone administered i.v. resulted in significant lower cochlear concentrations compared to drug administered intratympanically (29). Nevertheless, it seems that drugs can enter the inner ear depending on their chemical characteristics. Small lipophilic drugs can

enter the perilymph more easily than big hydrophilic, charged or protein binding drugs (25). Finally, positively charged drugs are less likely to enter the endolymphatic space from the perilymph because of the electrical gradient (Table 1.1.) (25). Importantly, various conditions can disturb the blood-cochlea barrier, e.g. noise exposure, inflammation, the administration of diuretics or several osmotic agents (18).

The tympanic membrane (Figure 1.1.) protects the middle ear from toxic substances entering through the ear canal of the outer ear and has an area of 85 to 90 mm^2. It consists of an outer epidermal layer, followed by a fibrous layer as well as an inner mucosal layer and has an almost oval and conical shape (15,30). During intratympanic injection this membrane is damaged.
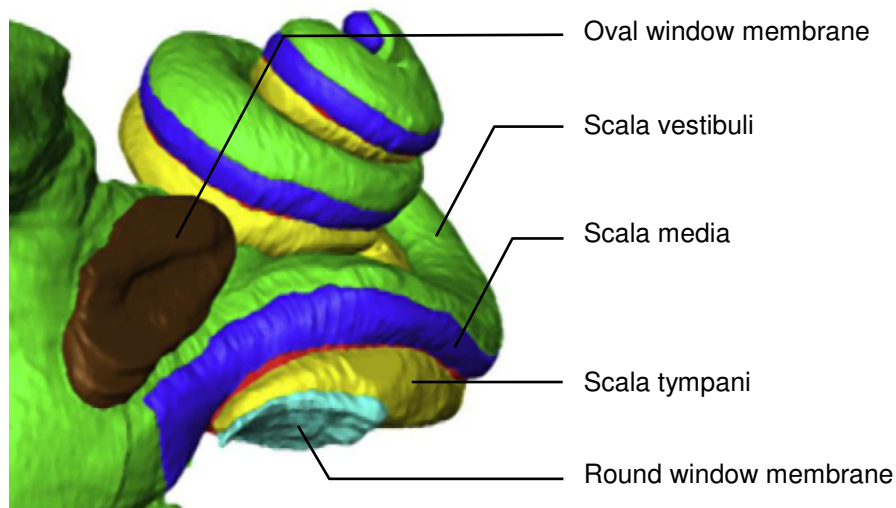
Figure 1.4. Barriers of the inner ear: 3D-reconstruction of a human inner ear. The round window membrane (RWM) stays in contact with the scala tympani whereas the oval window membrane (OWM) is connected to the scala vestibuli, adapted from (31).

The round and the oval window connect the middle ear with the cochlea which is surrounded by the petrous bone (Figure 1.4.). Unfortunately, drug delivery to the inner ear through the petrous bone – one of the densest bones in the body – seems to be limited in humans. Importantly, drug delivery through this bone seems to be overestimated in animal experiments because the bone in animals is very thin compared to the bone in humans (32).

Both, the round and oval window membrane, are not only barriers but also a potential target for local drug delivery. The round window is connected to the scala tympani at the basal turn of the cochlea. It consists of three layers, an outer epithelium with a single layer of cells, a middle layer of connective tissue containing fibroblasts, blood vessels, collagen and

elastic fibers as well as an inner layer consisting of squamous epithelium (18). The round window niche has an opening width of about 0.5 to 3 mm, the membrane has a thickness of about 50 - 100 µm in humans compared to 10 to 14 µm in rodents (18,33,34). The ovoid surface of the round window is around 2.2 mm^2 in humans compared to 1 mm^2 in rodents and can have various shapes (18,34). Unfortunately, the round window membrane is often plugged by a pseudomembrane, a fat plug or fibrous tissue which makes the quantification of drug delivery quite challenging. From 85 patients, 22 % had obstructions in both ears whereas only 56 % of the examined patients had no obstacle in both ears at the round window niche (35). Additionally, the transport of a drug through the round window membrane depends highly on the size, concentration, solubility, electrical charge and uptake mechanism of the drug (18) which makes the development of an appropriate drug delivery system very challenging and time consuming.

The second membrane connecting the middle with the inner ear is the oval window which stays in contact with the perilymph of the scala vestibuli at the base of the stapes. The stapes' footplate is attached to the oval window by the annular ligament and has a normal thickness of 0.3 to 0.5 mm in humans (33). The length of the footplate has been measured to be 2.5 to 3.36 mm compared to a width of 0.7 to 1.66 mm (36). It has been calculated that the surface area of the stapes footplate is about 3.97 mm^2 (36). In the past, clinicians thought that the drug enters the inner ear mainly through the round window membrane. Recent studies indicate that drugs can also enter the inner ear via the stapes footplate (37): It has been calculated that the ionic marker trimethylphenylammonium (TMPA) enters the inner ear mainly through the round window membrane, but, importantly, one third of the drug enters through the oval window membrane (31).

Those barriers protect the inner ear, more precisely the inner ear hair cells. This mechanoreceptor cells are responsible for the auditory perception that will be described in the following chapter.

1.1.2. Auditory perception

The sound that is processed in the inner ear and detected in the brain depends on the characteristics of the sound waves arriving at the outer ear. Sound waves can be described regarding the amplitude (or intensity), the wavelength, the frequency and the phase (16). Briefly, the sound wave is collected by the auricle, passes the ear canal where it is amplified and, subsequently, causes movement of the tympanic membrane (15). This movement is

converted into mechanical vibrations that are – again – amplified and transferred via the ossicles to the oval window membrane. The movement of the stapes is converted at the oval window into a pressure wave which is spread throughout the fluid filled cochlea - from the oval window of the scala vestibuli via the apex of the cochlea to the round window of the scala tympani.

Inside the cochlea, the sound wave causes vibration of the basilar and the tectorial membrane. Depending on the frequency of the sound wave, especially the cells in the corresponding area of the cochlea are stimulated: Human beings can detect low frequencies from approximately 20 Hz at the apex until high frequencies of 20 000 Hz at the base of the cochlea (Figure 1.5.) (15). Mongolian gerbils have a hearing frequency range of 100 to 60 000 Hz (38). In humans, the ability to detect high frequencies is typically decreasing with age.
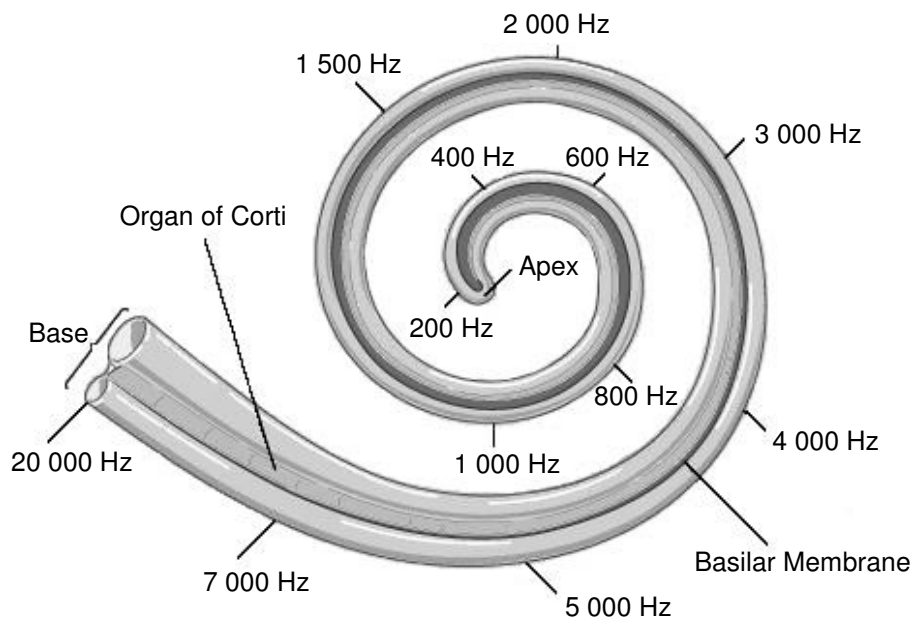
Figure 1.5. Perception of sound inside the cochlea depending on the frequency of the sound wave in humans: High frequencies stimulate the hair cells at the base whereas low frequencies vibrate the hair cells at the apex of the cochlea, adapted from (39).

The difference between the vibration of the basilar and the tectorial membrane causes a shearing force. Subsequently, this mechanical signal is translated into an electrical signal in the specialized outer and inner hair cells of the organ of Corti: The stereocilia situated on top of the hair cells vibrates depending on the mechanical wave. This vibration causes the hair cells to depolarize and repolarize by opening of potassium and calcium channels. The sound is amplified by the outer hair cells which leads to vibration and release of transmitters from the

inner hair cells that activate receptors in the nerve leading to the brain. Subsequently, this signal is transferred to the brain where the sound is perceived (16,40).

Along with this first perceptional system situated in the cochlea, the second main system in the inner ear, the vestibular system, is responsible for the equilibrioception and will be described in the following chapter.

1.1.3. Sense of balance

The semicircular canals and the vestibule of the inner ear (Figure 1.3.) are part of the system maintaining the balance of the body. Not only the inner ear is involved in this process but also the eyes, muscles, the brainstem, the cerebellum and the cortex (21,41). In this context, the inner ear hair cells play a major role in translating the movement of the head into electrical signals which can be interpreted by superordinate systems.

Therefore, two types of hair cell containing membranes exist in the vestibular system: the macula, also called otolitic organ, and the crista ampullaris. The mechanosensitive hair cells inside those membranes consist of a kinocilium and 70 to 100 stereocilia (21).

Macula membranes exist inside the utricle and the sacculus of the vestibule and are responsible for the detection of linear acceleration and head tilt (41). Those membranes contain not only hair cells but also "heavy" calcium carbonate crystals, so called otoliths. They are embedded in the otolitic membrane which covers the gelatinous layer containing the hair cells. When the head is leaned forwards or moved linearly these crystals are displaced. They cause a shearing force between the otolitic membrane and the macular surface leading to a bending of the hair cells followed by an electrical signal which can be detected in the brain (21).

The crista ampullaris inside the ampullae at the end of the semicircular canals detect angular acceleration. Since the three semicircular canals are arranged orthogonal to one another the hair cells in each ampulla can detect movement in the three dimensions (22). Therefore, the hair cells are embedded into a gelatinous structure, the cupula, similar to the macula. In contrast to the otolitic structure of the macula, the hair cells of the crista ampullaris are bent due to the movement of the endolymph of the membranous labyrinth and contain no calcium carbonate crystals. When the head is moved the endolymph inside the semicircular canals flows in the opposite direction of the movement causing the bending of the cupula. In consequence, the hair cells are bent and stimulated (Figure 1.6.). A continued uniform movement of the head results in a return of the cupula to the original position, stopping the

motion results in a bending of the cupula in the opposite direction with correspondent hair cell polarization (21). The signals from the vestibular system are transduced via the nerve to the brain where head and eye movement are matched to maintain the balance of the body (22).
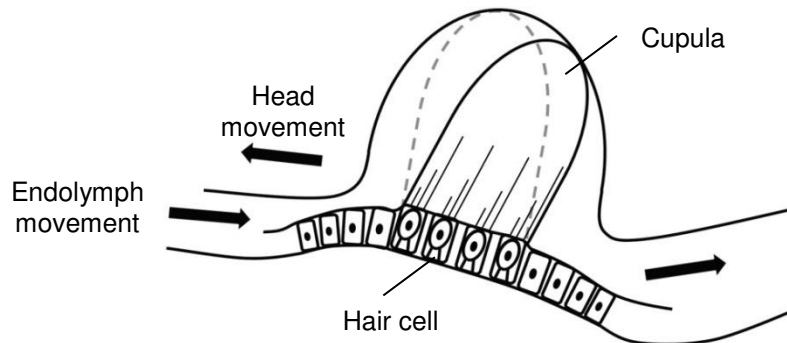
Figure 1.6. Function of the crista ampullaris: Rotation of the head causes endolymph flow inside membranous labyrinth in the opposite direction. The cupula waves depending on the flow leading to a stimulation of the hair cells (21).

Damage in the cascade of auditory perception or the sense of balance in only one step can lead to inner ear disorders that are described in the next chapter.

1.2.   Diseases of the inner ear

Current strategies to treat inner ear diseases aim at the treatment of Noise Induced and Sudden Sensorineural Hearing Loss (NIHL and SSHL respectively), of Autoimmune Inner Ear Disease (AIED), Tinnitus or Meniere's Disease and the protection of the inner ear, e.g., during aminoglycoside or anti-cancer therapy. In this introduction a major focus will be on Hearing Loss. Additionally, a short overview on other illnesses will be given here.

Autoimmune Inner Ear Disease causes bilateral, generally asymmetric, progressive or fluctuating hearing loss that is often combined with a systemic autoimmune disease of the patient as well as vestibular symptoms and responds to immunosuppressive therapy (42,43). Researchers assume that the etiology of the disease includes inflammation, vascular and cochlear tissue damage (e.g., Stria vascularis, Spiral ganglion, Organ of Corti) due to a disproportionate Th1 immune response (42). Therapy includes systemic and intratympanic administration of corticosteroids for a prolonged period. Sometimes other immunosuppressive agents like methotrexate or cyclophosphamide seem to be beneficial for the patient by reducing the dose of steroids. Recent research focuses on fusion proteins and monoclonal

antibodies to block the inflammatory reaction. A second promising approach might be the application of stem cell and gene therapy to repair damaged inner ear tissues (43).

Tinnitus is defined as the perception of sound without an external acoustic stimulation (44,45). The cause of the disease is unclear, researchers discuss not only a peripheral but also a central neural origin (46). This disease can occur following to excessive noise exposure or during the normal process of aging and can be associated with additional symptoms like hearing loss, sleep disturbance, hearing loss, anxiety and depression (45). Therapy aims at interrupting or masking the "phantom" sound via sound therapy (47) but also includes an appropriate treatment of the additional symptoms. This treatment might involve supply with hearing aids, education, psychological support, relaxation and cognitive behavioral therapy for the patient (44,45). Research on drugs that might be promising for the treatment of Tinnitus focuses on corticosteroids, e.g., dexamethasone, local anesthetics, e.g., lidocaine, and n-Methyl-d-aspartate receptor antagonists (18).

Patients suffering from Meniere's disease report intermittently occurring episodes of vertigo, often associated with hearing loss, tinnitus or an aural pressure (48). This illness has an enormous impact on patient's lives and researchers still discuss about its origin. Autoimmune reactions or viral infections might cause endolymphatic hydrops as well as fibrosis and tissue degeneration leading to the major symptoms of Meniere's disease (48). The treatment with intratympanic Aminoglycoside antibiotics, e.g., gentamicin, seems to reduce vertigo but increases the risk to suffer from hearing loss (49). Also transtympanic injection of steroids seems to have a beneficial effect on vertigo attacks but further studies should be performed to proof those promising results (50).

Otoprotective actions should be taken to prevent hearing loss due to Cisplatin or Aminoglycoside related toxicity. Both groups of drugs cause similar damage to the inner ear hair cells. Mainly outer hair cells inside the cochlea are degraded, while the damage is increasing from the apex to the base of the cochlea (51). Therefore, an increasing hearing impairment at the correspondent frequencies can be observed. Hearing Loss due to Cisplatin administration during anti-cancer therapy is not only age- (very young and the elder patients are more affected) but also dose-dependent (25): Administration of the ototoxic drug via an osmotic pump with concentrations from 0 to 300 µg/mL respectively resulted in greater and faster hearing loss when a higher concentration is administered (52). Spiral ganglion cells can also be affected. Additionally to this hearing loss, during aminoglycoside administration vestibular toxicity can be observed. The mechanism behind seems to be an excessive level of reactive oxygen species damaging especially outer hair cells (25). Local administration of

antioxidants seems to be promising but systemically administered methionine or sodium thiosulfate decreases the effectiveness of the cisplatin therapy (25). Furthermore, the use of cytoprotective agents, e.g., amifostine, has not been proven to prevent hearing loss due to cisplatin therapy in children (53). During aminoglycoside therapy, otoprotection can be achieved by the administration of antioxidants as well as steroids (25).

Hearing loss can be related to all of the inner ear illnesses described above and, thus, will be discussed in detail in the following chapter.

1.2.1. Hearing Loss

Especially when it occurs suddenly, hearing loss is a frightening disorder for the patient. In addition to the hearing loss patients may report tinnitus ("ringing" of the ears), dizziness or fullness of the ear (54).

According to the World Health Organization there are five grades of hearing impairment (Table 1.2.): no, slight, moderate, severe and profound impairment (Grades 0 to 4 respectively). Following this classification, disabling hearing impairment occurs when the patient has at least a hearing loss of Grade 2. This moderate impairment with a loss of 41 dB or more on the better hearing ear means that words can still be understood and repeated at 1 m distance with a raised voice (55).

Table 1.2. Hearing impairment according to the definition of the WHO: with a grade exceeding grade 1 hearing aides are recommended, adapted from (55).

Grade	Threshold shift of the better ear, dB	Effect
0	25 or better	No/slight problems, even whispers are heard.
1	26 to 40	Words spoken in 1 m distance with normal voice can be heard and repeated.
2	41 to 60	Words spoken in 1 m distance with raised voice can be heard and repeated.
3	61 to 80	Some words can be heard when shouted.
4	81 or greater	No words can be heard and understood even when shouted.

The causes of hearing loss are various. In general, they can be classified as congenital or acquired (1). Congenital hearing loss refers to causes occurring during or shortly after birth, e.g., rubella, toxoplasmosis or other infections of the mother as well as treatment with

inappropriate drugs during pregnancy, asphyxia and low weight of the newborn (56). Importantly, genetic factors also play a major role in 25 % of the cases, over 400 gene related syndromes have been identified (4,56). Unfortunately, in 57 % of the cases the cause of congenital hearing loss still remains unknown (4).

Acquired hearing loss refers to cases occurring at every age of the patient and can develop suddenly or over a long period. Hearing loss can develop due to infections, e.g. meningitis, measles, mumps or otitis media, as well as traumata of the head or the ear following an accident or surgery (1,55,57). Other causes can be autoimmune diseases, e.g. systemic lupus erythematosus, tumor growth and treatment, neurologic diseases, e.g. Multiple sclerosis, or vascular events (58–61). Additionally, certain drugs can have a toxic effect on the ear, e.g. aminoglycoside antibiotics as well as several chemotherapeutic agents and anti-malaria drugs (51,62,63). Importantly, also acute or long term noise exposure can cause noise-induced hearing loss (NIHL), e.g. recreational noise during a sport event or from a MP3-Player and noise from machines or explosions. Also, a certain degree of hearing loss is age-related (64) and can be considered as a normal process: It was estimated that 30 % of the men and 20 % of the women over 70 suffer from hearing loss (threshold shift of at least 30 dB) in Europe (65). Frequently, patients are also diagnosed with hearing loss due to excessive ear wax stuck in the ear canal (66). Nevertheless, only in 7 to 45 % of patients with Sudden Sensorineural Hearing Loss (SSNHL with a threshold shift of at least 30 dB over three continuous frequencies during 72 h) the cause can be identified, a major part of cases remains idiopathic (57).

Table 1.3. Types of hearing loss with the concerned region, according to (15).

Type of hearing loss	Concerned region
Conductive	Disease of external and/or middle ear
Sensorineural	Disease of the cochlea and/or nerve
Mixed	Combination of conductive and sensorineural
Central	Disease of the auditory pathway higher than the auditory nerve

Depending on the region, there are several types of hearing loss (Table 1.3.) (15). Conductive loss occurs when the stiffness of the outer or middle ear is changed, e.g. when the ear canal is stuck with ear wax or in case that the ossicular chain is damaged because of

otosclerosis (67). Sensorineural hearing loss (SNHL) occurs when the cochlea or the nerve is damaged, e.g. this is the case when hair cells of the organ of Corti are damaged due to gentamicin administration (37). A combination of conductive and sensorineural is a so called mixed hearing loss. When the auditory system is damaged in higher regions than the auditory nerve a central hearing loss occurs.

Nevertheless, the cause of hearing loss is unknown in most of the cases and therapy still remains challenging. Ongoing research on different strategies to treat hearing loss is discussed in the following chapter.

1.3. Drug delivery to the inner ear

Current strategies used in clinic focus mainly at treating Sudden Sensorineural Hearing Loss and autoimmune diseases as well as at a protection of the inner ear (25). Besides the strategy of providing the patient with appropriate medical devices, e.g., hearing aids or cochlear implants to cure persistent hearing loss, different drug delivery tools are a major topic in research.

Since the rate of spontaneous recovery from Sudden Sensorineural Hearing Loss is relatively high (32 to 65 %) and the etiology of Hearing Loss is not fully understood yet, clinicians discuss about the appropriate treatment of hearing loss. Nevertheless, in case that the cause is known, the patient should be treated accordingly (57,66). In the case of Idiopathic Hearing Loss, current therapeutic strategies often include systemic or local administration of steroids but also antivirals, diuretics, vasodilators, antioxidants, hyperbaric oxygen treatment, middle ear surgery and bedrest are used to treat hearing loss (57,66).

Systemic drug delivery (described in section 1.3.1.) is still used to treat inner ear diseases but is progressively replaced by local drug delivery (described in section 1.3.2.) to avoid adverse events caused by high systemic blood concentrations of the drug.

1.3.1. Systemic drug delivery

Unfortunately, the systemic administration of both, steroids, optionally combined with antivirals, and vasodilators did not show a significant improvement in Cochrane Reviews (54,68,69). This may be partially due to insufficient patient numbers and inconsistent inclusion criteria or study designs.

However, oral steroids may be useful in the treatment of sudden sensorineural hearing loss but their influence on hearing recovery remains uncertain. Only one of three studies

included in the Cochrane Review showed a significant effect of oral steroids on hearing recovery with a hearing improvement of 61 % compared to 32 % in the placebo/untreated group (70). In two other studies no improvement of hearing loss can be seen when oral steroids are administered (71,72).

The systemic administration of antivirals to treat idiopathic sudden sensorineural hearing loss neither shows improvement: Two studies included in a Cochrane review showed no improvement when aciclovir was administered additionally to prednisolone (73,74). Accordingly, patients treated with valaciclovir in addition to prednisone, or aciclovir administered additionally to hydrocortisone, showed no hearing improvement (75,76). Nevertheless, animal studies support the assumption that an early treatment of patients with antivirals could be beneficial. Unfortunately, in clinical practice most patients present very late so the impact of the treatment with antivirals may be difficult to prove (54).

The administration of vasodilators or vasoactive substances could be beneficial for the treatment of hearing loss but due to the small number of patients included in the studies the benefit remains unproven (68). A significant hearing improvement has been reported for patients receiving carbogen additionally to several other drugs compared to no inhalation of carbogen (77). In a study where patients received Prostglandin E1 additionally to hydrocortisone only the hearing in higher frequencies was improved (78). The hearing in lower frequencies was improved by the administration of low molecular weight Dextran with additional Naftidrofuryl (79). Those results are promising clinicians should be aware of potential side effects of drugs whose benefit for the patient is not yet approved in clinical practice (66).

In addition to the unknown cause of the disease in most of the cases, during systemic administration of drugs side effects are more likely to occur. The patient often needs an elevated dose to enhance absorption of the drug into the inner ear to reach therapeutic drug concentrations. This is due to the barriers protecting the highly sensitive inner ear as described before (chapter 1.1.1. Barriers of the Inner Ear). Additionally, the small volume of the inner ear fluids and its complicated anatomical access make local drug delivery very difficult.

Nevertheless, local drug delivery seems to be a promising approach to limit adverse events during the treatment of hearing loss and will be discussed in the following chapter.

1.3.2. Local drug delivery

Local inner ear drug delivery has been the topic of several reviews in the last years (Table 1.4.). Most reviews concentrate on either intratympanic or intracochlear administration of drugs: El Kechai et al. recently published an interesting update focusing on intratympanic administration and in vivo studies (18), whereas Ayoob and Borenstein focused on intratympanic drug delivery (26). The review of Salt and Plontke deals with the pharmacokinetics of the inner ear (80). Salt also provides a program to simulate cochlear fluids of several species (81).

Table 1.4. Reviews on inner ear drug delivery, adapted from (82).

Main focus of the review	Author	Reference
Overview on inner ear drug delivery systems	Swan et al. 2008	(25)
Pharmacokinetics of the inner ear	Salt and Plontke, 2009	(80)
Historical background, current strategies	McCall et al., 2010	(83)
Drug delivery using nanoparticles	Pyykkö et al., 2011	(84)
Drug delivery using micropumps	Leary Pararas et al., 2012	(85)
Intratympanic drug delivery	Liu et al., 2013	(82)
Intracochlear administration	Ayoob and Borenstein, 2015	(26)
Intratympanic administration, in vivo studies	El Kechai et al., 2015	(18)

The two major strategies to deliver drugs locally to the inner ear are intratympanic and intracochlear drug delivery. Depending on the intended treatment both systems have various benefits and drawbacks.

During intratympanic delivery the drug is placed inside the tympanic cavity where the drug is absorbed mainly via the round but also by the oval window. The advantage of this strategy is the relatively save, usually ambulatory administration, often requiring no general anesthesia, allowing for short and mid-term drug delivery to the middle or inner ear. Unfortunately, the preparation might be washed away through the Eustachian tube or degraded rapidly and, though, often requires repeated application. These repetitions increase the risk of introducing pathogens into the inner ear. Additionally, the anatomy of the ear

varies from patient to patient leading to different drug concentrations in the inner ear. Depending on the characteristics of the drug, a gradient along the length of the cochlea can occur (18,25).

Intracochlear delivery allows for the release of drugs directly inside the cochlea and requires a cochleostomy. The main advantage of this administration is the direct access to the inner ear ensuring a defined long term drug delivery during months or years bypassing inter-patient anatomical differences. Importantly, the characteristics of the drug only play a minor role since the drug is not obliged to pass the barriers protecting the inner ear. However, the patient has to stay in hospital during the treatment which is rather invasive and the surgeon risks to introduce pathogens during the operation (18,25).

1.3.2.1.   Intratympanic drug delivery

Today, intratympanic administration of a drug loaded solution is commonly used in clinical practice. Therefore, the tympanic cavity is filled with the solution which is injected via the tympanic membrane using a thin needle. The outcome is promising: Patients suffering from Sudden Sensorineural Hearing Loss whose first line treatment with oral steroids failed could benefit from a treatment with intratympanic steroids which has led to a reduction in hearing thresholds (86). Other diseases of the inner ear might be treated accordingly using aminoglycosides, glutamate receptor antagonists, protease inhibitors, antioxidants or neurotrophins (25).

Unfortunately, the drug solution is often eliminated very fast from the middle ear cavity. To enhance the residence time at the round window membrane, promising devices are the Silverstein MicroWick®, the Round Window µ-Cath[TM] and the Round Window E-Cath[TM]. Another strategy is to place biodegradable polymers loaded with either a drug solution or nanoparticulate systems inside the middle ear, e.g., close to the round window membrane (18,87).

Medical devices

MicroWick®

The MicroWick® is a cylinder (dimensions 9 or 19 x 1 mm) consisting of polyvinyl acetate. It stays in contact with the round window membrane and passes through a perforation in the tympanic membrane. A drug solution (that can be administered dropwise into the ear canal of the outer ear by the patient himself) is absorbed by the polymer and, thus, transported

to the round window (25). The device is often used to treat vertigo occurring during Meniere's disease with gentamicin (88), but also patients suffering from Sudden Sensorineural Hearing Loss can profit from a prolonged drug delivery: 26 patients receiving methylprednisolone during 10 days (after failure of the conventional therapy against hearing loss) had improved mean speech discrimination scores. The score recorded at 40, 55 and 70 dB improved by 24.2 ± 8.7 % (89). Despite these promising results, the application of the MicroWick® might result in a permanent perforation of the tympanic membrane (82,83). Additionally, the risk of infection of the middle ear is increased due to the connection to the outer ear (83). The compliance of the patient is important because the drug solution is administered usually several times per day during weeks.

µ-Cath^{TM} and E-Cath^{TM}

The microcatheters can be used to deliver drugs intratympanically and via an intracochlear approach. They have two different canals: The first serves to infuse a solution, the other to withdraw fluids. The E-Cath^{TM} has a third canal that can be used to insert an electrode to control inner ear function during surgery (25). The tip of the microcatheter is inserted through a tunnel drilled into the temporal bone and fixed near the round window. This device has been used successfully to treat Sudden Sensorineural Hearing Loss (90). To facilitate the removal of plugs blocking the round window niche and the intratympanic injection of drug preparation, an otoendoscope has been developed that can visualize the middle ear during surgery. It has two canals: the first one serves removing mucosal adhesions, via the second one a drug solution can be injected into the middle ear (91). After treatment during several weeks, the catheter can be removed (83). Potential drawbacks are the risk of catheter dislocation or obstruction, the formation of granulation tissue and a potentially permanent perforation of the tympanic membrane (83).

Polymeric matrices

Hydrophilic polymers are widely used in research since the residence time of the formulation at the round window compared to intratympanically injected solutions is increased. These polymers can not only be administered in the form of solid sponges or discs but also as injectable in situ forming gels. The drug is released through degradation of the matrix, diffusion of the drug or a combination of both mechanisms (82). Thus, drug

concentration inside the cochlea seems to be more consistent, the concentration gradient along the scala tympani seems to decrease.

Gelfoam®

Gelfoam® is a compressed biodegradable sponge based on purified porcine gelatin which is used because of its hemostatic and fluid absorbing properties. Prior to the use as a drug delivery device, the polymer is soaked in drug solution. Promising results have been reported for the delivery of brain-derived neurotrophic factor (BDNF): Guinea pigs have been deafened and treated with a sponge that was loaded with BDNF and placed onto the round window. This treatment increases spiral ganglion cell survival in the basal turn of the cochlea after 2 and 4 weeks, thus, provides a protection to inner ear cells. Unfortunately, this effect in lower compared to studies working with an intracochlear approach (92). Silverstein et al. treated patients suffering from Meniere's disease with a Gelfoam® sponge loaded with gentamicin solution. Vertigo was controlled in 75 % of the patients; hearing was preserved in 90 % of the cases (93).

Seprapack™

Seprapack™ is a bioresorbable device consisting of carboxymethyl cellulose and hyaluronic acid. Several studies evaluated the capacity of dexamethasone loaded Seprapack™ gels to reduce hearing loss due to trauma, e.g., during cochlear implantation (82). The administration of dexamethasone-loaded Seprapack™ before the implantation resulted in detectable drug concentrations inside the cochlea what was not the case when other types of delivery beads were applied. Dexamethasone protects residual hearing during cochlear implantation (94). In another study, it was confirmed that an administration of the dexamethasone-loaded device before the implantation resulted in increased hearing thresholds from 2 to 32 kHz. Importantly, protection increased with longer application time of the drug loaded device. Also, higher concentrations of dexamethasone applied onto the round window membrane resulted in better hearing protection in the second turn of the cochlea (95).

Hydrogels

Hydrogels can also be administered to the inner ear via intratympanic injection of the gel itself or in the form of an in situ forming gel. Various polymers have been tested to adjust drug delivery from the gels, e.g., gelatin, chitosan glycerophosphate, hyaluronic acid, alginate, siloxane, poloxamer 407 and collagen (25,82,83).

Chitosan, a non-toxic cationic polymer, has been used to deliver dexamethasone to the inner ear of mice. In vitro, the chitosan-glycerophosphate hydrogel released 92 % of the drug during 4 days. In vivo, dexamethasone has been detected during 5 days. Reversible hearing loss has been reported after surgery but mice recovered spontaneously after 10 days (96).

Gelatin is not only administered as the solid Gelfoam® but also as a gel: The biodegradable polymer has been used to deliver the recombinant human insulin-like growth factor 1 (rhIGF-1) to prevent damage of the inner ear cells upon excessive noise exposure. Histological evaluation confirmed a higher survival of outer hair cells when the gel is applied onto the round window membrane (97).

An interesting approach to prolong drug delivery is to use temperature-sensitive systems: The formulation can be injected intratympanically at room temperature as a liquid solution and forms a gel at body temperature (sol-gel-transition), e.g., on the round window membrane. Poloxamer has been used to provide prolonged dexamethasone release to the inner ear by forming an in situ forming gel. Concentration gradients along the scala tympani were lower compared to when injecting a solution. This can be partially due to a formation of the gel at the thin bone at the apex of the cochlea (which is more permeable in rodents than in humans) but can possibly related also to an extended release of the drug (98). This promising formulation is currently under clinical evaluation in Phase IIb to treat Meniere's disease with a sustained release of dexamethasone (OTO-104, Otonomy) (18,99).

Other candidates for clinical practice are two formulations based on hyaluronic acid to cure Noise Induced Hearing Loss and Tinnitus, administering dexamethasone and esketamine (AM-111 and AM-101 respectively, Auris Medical) (18). Additionally, a gelatin-based preparation releasing IGF-1 to cure Sudden Sensorineural Hearing Loss is clinically evaluated (18).

A potential drawback concerning hydrogel-based drug delivery could be that the formulation has to be placed precisely at the round window niche. Another problem might occur when excessive gel in the middle ear cavity causes transient hearing loss by blocking the ossicular chain. Quick elimination of the formulation via the Eustachian tube might limit application of hydrogels to treat chronic diseases (83).

Nanoparticles

Nanoparticles are drug delivery systems with diameters of less than 1000 nm, typically a diameter of 200 nm or smaller is requested for otological use (83). They should be incorporated into formulations or devices that sustain drug release and prevent the elimination

via the Eustachian tube, e.g., by using hydrogels or microcatheters. Different drug delivery systems have been investigated to treat inner ear illnesses, e.g., silica nanoparticles, PLGA- or GMO-based systems, liposomes, lipid nanocapsules, hyperbranched polylysine nanoparticles, polymerosomes, as well as dendrimer-based nanoparticles and SPIONs (18,26). Nanoparticles can be used to counteract low drug solubility, problems with degradation, with passage of the round window membrane or short half-life of the drug (18). Functionalization of the nanoparticles' surface offer interesting possibilities to target single cell types inside the inner ear. An interesting approach to enhance diffusion through the round window membrane might be to combine PLGA-nanocarriers with magnetite to release dexamethasone-acetate. After the administration of the nanoparticles on the round window niche, a permanent magnet was placed on the opposite site of the round window. Drug transport through the membrane has been increased using magnetic nanocarriers with a magnet compared to pure diffusion (100). For further interesting studies on drug release from nanoparticles the author refers to the review published by El Kechai et al. were a vast amount of different strategies are discussed in detail (18).

1.3.2.2.   Intracochlear drug delivery

In contrast to intratympanically administered drugs which have to be absorbed via the round window membrane, intracochlear delivery offers the potential to release drugs directly to the inner ear. Strategies include direct intracochlear injection, drug release using osmotic pumps or microcatheters (described in section 1.3.2.1. Intratympanic drug delivery), as well as reciprocating perfusion systems and cochlear prosthesis-mediated drug delivery. A rather invasive cochleostomy through the round window or the temporal bone is needed to provide access to the inner ear (26).

Intracochlear injection

The intracochlear injection of drugs is mainly used for research, e.g., to conduct pharmacokinetic studies or to study the effect of new drugs on inner ear cells. Therefore, a few microliters of the drug solution are injected via cochleostomy. Potential drawbacks are the short period of drug delivery as well as a possible leakage of cochlear fluids that might wash the drug solution out of the cochlea. Furthermore, high drug concentrations at the application side might damage the highly sensible inner ear cells. In human, intracochlear injection is used only during surgery (18).

Osmotic pumps

Osmotic pumps are used similarly to the microcatheters already described above. Both systems can be used to provide intratympanic or intracochlear drug release. The osmotic pump can be implanted subcutaneously providing flow rates from 0.1 to 10 µl/h from a reservoir containing 0.1 to 2 mL during 1 day up to 6 weeks. Osmotic pressure ensures low but permanent drug delivery rates. A drawback is that the flowrate cannot be adjusted in vivo (85). Those systems can be used to evaluate new therapies in animal models: betamethasone has been administered using an osmotic pump during 14 days following to a damage of the right semicircular canal of guinea pigs. Animals treated with the drug showed better recovery from the induced vestibular illness compared to non-treated animals (101).

Reciprocating perfusion systems

Those systems combine microsystems and microfluidics technologies to create new drug delivery devices that are able to provide drugs to the inner ear more precisely (83). A micropump is infusing and withdrawing inner ear fluids in a cyclic manner nearly simultaneously so that the volume inside the cochlea stays constant (26). This device has been studied in guinea pigs administering 6,7-dinitroquinoxaline-2,3-dione (DNQX), a glutamate receptor blocker. DNQX allowed for following of drug release by recording the Compound Action Potential (CAP) (102). A new version of the reciprocating perfusion system has been presented recently (26).

Cochlear prosthesis-mediated drug delivery

Cochlear implants have been used widely since 35 years to cure hearing loss and consist of an electrode array that is inserted via cochleostomy inside the scala tympani of the cochlea. Different insertion depths are used in practice and in research, ranging from 16 to 31.5 mm (26). The usually drug free electrode is coiled up inside the turns of the cochlea providing a relatively large surface for potential drug delivery. Different strategies are discussed: combining a cochlear implant with a micropump or drug-eluting coatings of the electrode as well as introducing the drug directly into the silicone of the electrode (26). The aim is to reduce damage of the inner ear cells due to the insertion force during surgery. Therefore, dexamethasone-eluting electrodes have been developed and evaluated in vitro and in vivo showing promising results (103–105). Another approach is to deliver the drug (or a dye in this case) via tiny delivery ports that are connected via the implant with a micropump. The distribution of the dye along an artificial cochlea was satisfactory when two outlets served to

release the dye (106). Furthermore, electrodes have been coated with hydroxyl ethyl cellulose to adjust drug release and have been used to deliver neurotrophic factors, e.g., brain-derived neurotrophic factor (BDNF) or neurotrophin-3 (26).

Since silicones are already widely used inside the inner ear, e.g. in the form of cochlear implants, this polymer seems to be advantageous to deliver drugs to the inner ear in a sustained manner. Therefore, the following chapter will be focused on drug release from silicone matrices.

1.4.   Drug release from silicone matrices

The incorporation of drugs within silicone matrices can be very helpful to improve the therapeutic efficacy and safety of a large variety of medical treatments. The basic idea is that the polymeric system accurately controls the resulting drug release rate during pre-programmed periods of time. Examples for promising applications include the local delivery of drugs to sites of action, which are difficult to reach (without causing major side effects in the rest of the human body due to high systemic drug concentrations). This includes for instance the treatment of diseases and disorders of the inner ear (107,108). But also local treatments of the vagina (109), heart (110), eye (111,112) or scars (113) can be very challenging and silicone matrices can be highly beneficial in these cases. Furthermore, silicone matrices offer a great potential for the design of advanced intraperitoneal controlled release implants (114) and central venous catheters (115).

Importantly, the release periods can be very long (e.g. several months or years) and the resulting advantages for the patient long-lasting. For example, Mond and Stokes (110) reported on the benefits of silicone-based, dexamethasone-eluting electrodes in pacemakers, which effectively lower the stimulation threshold at the "electrode-tissue interface". In a double-blind human study over 10 years the mean stimulation thresholds for the drug-eluting devices remained almost constant (exhibiting a narrow standard deviation), whereas the drug-free systems showed an unpredictable increase in the threshold values and wide standard deviations. Interestingly, 20 % of the dexamethasone is estimated to still remain within the silicone matrices even after 10 years implantation in humans (based on the analysis of explanted devices). The authors state that drug release may well continue at sufficient levels for an additional 10 years. This is a very promising clinical evidence for the benefits of silicone-based controlled drug delivery systems. However, the development of such devices is

generally very cumbersome, since often long release periods are targeted and so far very little information is available on the impact of the device design on the resulting system performance (in particular drug release kinetics) in a *quantitative* way. So, highly time-consuming and cost-intensive series of trial-and-error experiments are mandatory.

In order to adjust a desired drug release profile from a silicone matrix, different formulation parameters can be varied. For instance, the type of silicone (e.g. with a particular type of side chains and contents of amorphous silica) can be altered, different types and amounts of additives can be incorporated and/or the initial drug content can be varied. Also, the geometry and dimensions of the system might be changed. Both determine the pathway lengths, which have to be overcome by the drug to be released. Interesting reports are available in literature on the effects of the composition of silicone matrices on the resulting drug release kinetics (116–119). For example, Di Colo and co-workers studied the impact of adding glycerol, ethylene glycol and poly(ethylene glycol) to silicone disks loaded with prednisolone (120,121). Importantly, the presence of these hydrophilic additives effectively increased the resulting drug release rate. It has to be pointed out that silicones are generally hydrophobic and water penetration into the systems is very limited. Furthermore, commonly used silicones do not degrade in the human body. Craig and co-workers (109) published a very interesting study on the importance of the solubility of the drug in silicone matrices for the resulting release kinetics. Clindamycin, 17β-estradiol, 17β-estradiol-3-acetate, 17β-estradiol diacetate, metronidazole, norethisterone, norethisterone acetate and oxybutynin release was studied from intravaginal rings, prepared by injection molding. Also, Liu et al. (105) investigated the impact of the initial drug loading and of the dimensions of differently shaped silicone matrices on dexamethasone release. Waever et al. (122) used dexamethasone loaded silicone rods and discs for controlled local delivery in order to modulate inflammation in islet transplantation, and varied the initial drug loading.

It has to be highlighted that the underlying mass transport mechanisms in polymeric drug delivery systems can be rather complex (123–125). The basic idea is that the presence of the polymer prevents immediate drug release upon contact with aqueous body fluids. Generally, first water penetrates into the system and dissolves the drug (126). Once dissolved (in the form of *individual* molecules), the drug can diffuse through the polymeric system into the surrounding environment. Drug diffusion might take place through an intact polymeric network and/or through water filled pores. The amount of water available for drug dissolution in the system and the drug solubility in the matrix can be decisive (127). In the case of substantial polymer swelling and/or dissolution, important time- and position-dependent

changes in the system's composition might occur over time, altering the conditions for drug transport (128). Furthermore, the homogeneity of the initial drug distribution within the silicone matrix can be of importance (129). More or less complex mathematical theories can be used to quantify the involved mass transport processes and describe drug release from polymeric delivery systems (130–133). Also neural networks can be applied (134,135). Ideally, the mathematical theory should be mechanistically realistic and take all decisive phenomena into account, thus, allowing for the quantitative prediction of the effects of the device design on the resulting drug release kinetics (136). Negligible mass transport phenomena should not be considered, to keep the model as simple as possible. However, yet there is a lack of reliable mathematical theories allowing for such *in-silico* simulations of the impact of formulation parameters on the resulting system performance.

1.5. Objectives

The objective of this thesis was to develop implants capable of releasing the drug in a time controlled manner to the inner ear to treat inner ear diseases. The following steps have been selected to achieve this aim:

- Characterization of dexamethasone loaded silicone matrices *in vitro* to identify easy tools allowing for the adjustment of drug release kinetics from thin films and extrudates. Therefore, different formulation parameters have been varied: the ratio of PEG addition to the silicone, the molecular weight of PEG, the chemical structure of the silicone and the dexamethasone loading. Mathematical modeling helped to elucidate the underlying drug release mechanisms.

- Development of dexamethasone loaded implants using the most promising silicone. Thin films and Ear Cube implants have been prepared and studied *in vitro*. Additionally, the physicochemical properties of Ear Cube implants have been analyzed.

- *In vivo* study with in situ forming dexamethasone loaded implants to examine the feasibility of an implantation of the implant besides the oval window. Additionally, the drug released from the implant has been detected directly inside the explanted gerbil cochlea using Confocal Laser Scanning Microscopy.

2.   Materials and Methods

2.1.   Dexamethasone mobility in thin films

2.1.1. Materials

Kits for the preparation of silicone elastomers: MED-4011, MED-4035, MED-4055, MED-4065, MED-4080, MED-4735, MED-6015, MED-6033, MED-6755, MED50-5438, MED-5440 (NuSil Technology, Carpinteria, CA, USA); LSR OOO-50, LSR 25, LSR 40 (Applied Silicone, Santa Paula, CA, USA); dexamethasone (Discovery Fine Chemicals, Dorset, UK); poly(ethylene glycol) (PEG): PEG 400 (Lutrol E400; BASF, Ludwigshafen, Germany) and PEG 1000 (Polyglycol 1000; Hoechst, Frankfurt, Germany); calcium chloride dihydrate, magnesium sulfate tetrahydrate, potassium chloride, sodium chloride and 4-(2-hydroxyethyl) piperazine-1-ethanesulfonic acid (HEPES) (HEPES Pufferan, Carl Roth, Lauterbourg, France); acetonitrile and tetrahydrofuran (HPLC grade; Fisher Scientific, Illkirch, France).

2.1.2. Preparation of drug loaded films

Thin dexamethasone-loaded films were prepared using different commercially available silicone preparation kits, obtained from 2 suppliers (NuSil Technology and Applied Silicone). All kits consisted of 2 parts, which were mixed to initiate crosslinking and, thus, system hardening. It has to be pointed out that some of these raw materials were pasty (MED-4735, MED-4035, MED-4055, MED-4065, MED-4080), while others were liquid (MED-4011, MED-6015, MED-6033, MED-6755, MED50-5438, MED-5440, LSR OOO-50, LSR 25, LSR 40).

Pasty silicone kits: Equal amounts of Parts A and B (approximately 5 g) of the preparation kits were passed separately 10 times through a two roll mill (Chef Premier KMC 560/AT970A; Kenwood, Havant, UK). To initiate polymer crosslinking, both parts were manually blended and the mixture was passed 10 times through the mill. Subsequently, appropriate amounts of dexamethasone powder (as received) were added and the mixture was passed another 40 times through the mill to obtain a homogenous film. Crosslinking was completed by a thermal treatment in an oven at 60 °C for 24 h.

Liquid silicone kits: Equal amounts of Parts A and B (approximately 5 g) (except for LSR 25, LSR 40, MED-4011, MED-6015, where 10 Parts A were combined with 1 Part B:

approximately 10 g plus 1 g) of the preparation kits were manually blended for 5 min in an ice-cooled mortar (the cooling slowed down polymer crosslinking). Subsequently, dexamethasone powder (as received) was added and the mixture was manually blended for 10 min in the ice-cooled mortar. The obtained mass was placed between two Teflon films and passed 10 times through a two roll mill (Chef Premier KMC 560/AT970A). Crosslinking was completed by a thermal treatment in an oven at 60 °C for 24 h.

Optionally, 5 or 10 % (w:w) PEG 400 or PEG 1000 was added to the formulation (as indicated). In these cases, the PEG was manually blended with the drug in a mortar. The obtained drug-PEG mixture was incorporated into the formulations in the same way as the drug only (as described above).

The thickness of the resulting films was determined with a micrometer gauge (Digimatic Micrometer; Mitutoyo, Tokyo, Japan).

2.1.3. Preparation of drug loaded extrudates

Different types of dexamethasone-loaded extrudates were prepared with pasty silicone preparation kits. Equal amounts of Parts A and Part B (approximately 5 g) of the preparation kits were passed separately 10 times through a two roll mill (Chef Premier KMC 560/AT970A). To initiate polymer crosslinking, both parts were manually blended and the mixture was passed 10 times through the mill. Subsequently, appropriate amounts of dexamethasone powder (as received) were added and the mixture was passed another 40 times through the mill to obtain a homogenous (and easily deformable) film. The latter was transferred into 5 mL polypropylene luer lock syringes (Terumo Europe, Leuven, Belgium) and extruded using a texture analyzer (TAXT plus, Stable Micro Systems, Surrey, UK), equipped with a self-made syringe fixation device. The obtained extrudates were cured on a Teflon sheet (Bytac; Sigma-Aldrich, St. Louis, US) in an oven at 60 °C for 24 h to complete crosslinking, followed by manual cutting to the desired length.

2.1.4. Drug release measurements

Dexamethasone release was measured from thin films and cylindrical extrudates, as described in the following section. Each experiment was performed in triplicate.

Film pieces were placed into amber glass flasks containing 10 mL (if not otherwise stated) artificial perilymph: an aqueous solution of 1.2 mmol calcium chloride dihydrate, 2 mmol magnesium sulfate tetrahydrate, 2.7 mmol potassium chloride, 145 mmol sodium chloride and 5 mmol HEPES Pufferan. The flasks were horizontally shaken in an incubator (80 rpm; GFL 3033; Gesellschaft fuer Labortechnik, Burgwedel, Germany) at 37°C. At predetermined time points, 1 mL samples were withdrawn and replaced with fresh artificial perilymph. The drug concentration in the withdrawn samples was determined by HPLC analysis (Thermo Fisher Scientic Ultimate 3000 Series, equipped with a pump: LPG 3400 SD/RS, an autosampler: WPS-3000 SL, a column compartment: TCC 3000 D/RS and a UV-Vis detector: VWD-3400RS; Thermo Fisher Scientic, Waltham, USA) (lower quantification limit: 6×10^{-7} mg/L; linear range: 0.0001 - 50 mg/L). Samples (100 µL) were injected into a C18 RP column (Gemini 5 µ C18 110 A, 150 mm x 4.6 mm; Phenomenex, Le Pecq, France) (mobile phase = acetonitrile:water 33:67 V:V, flow rate = 1.5 mL/min). Dexamethasone was detected at $\lambda = 254$ nm.

Cylindrical extrudates were placed into silicone tubes (Helix Medical, Carpinteria, CA, USA) containing 1 mL artificial perilymph, which were horizontally shaken at 80 rpm at 37 °C (GFL 3033). At predetermined time points, the release medium was completely renewed and the drug contents in the withdrawn bulk fluid determined by HPLC analysis, as described above.

2.1.5. Scanning electron microscopy

The morphology of thin silicone films was observed using a scanning electron microscope (S-4000; Hitachi High-Technologies Europe, Krefeld, Germany). Samples were fixed on the sample holder with a ribbon carbon double-sided adhesive and covered with a fine carbon layer. Cross-sections were obtained by freezing the films in liquid nitrogen and manual breaking.

2.2. Ear Cube implants for Controlled Drug Delivery to the Inner Ear

2.2.1. Materials

Kits for the preparation of silicone elastomers: LSR 5 (Applied Silicone, Santa Paula, USA); Kwik-Sil (World Precision Instruments, Sarasota, USA); dexamethasone (Discovery Fine Chemicals, Dorset, UK); calcium chloride dihydrate, magnesium sulfate tetrahydrate, potassium chloride, sodium chloride and 4-(2-hydroxyethyl) piperazine-1-ethanesulfonic acid (HEPES, HEPES Pufferan, Carl Roth, Lauterbourg, France); acetonitrile and tetrahydrofuran (HPLC grade; Fisher Scientific, Illkirch, France).

2.2.2. Preparation of drug-loaded silicone matrices

Ten grams of the "Part A" of the silicone preparation kits were manually blended for 5 min with appropriate amounts of dexamethasone powder (as received) in an ice-cooled mortar. Subsequently, 1 g of the "Part B" of the silicone kits was added and the mixture was further manually blended for 10 min in the ice-cooled mortar (to slow down crosslinking). The obtained mass was transferred into a 5 mL polypropylene luer lock syringe (Terumo Europe, Leuven, Belgium) and degassed under vacuum during 60 min to remove air bubbles.

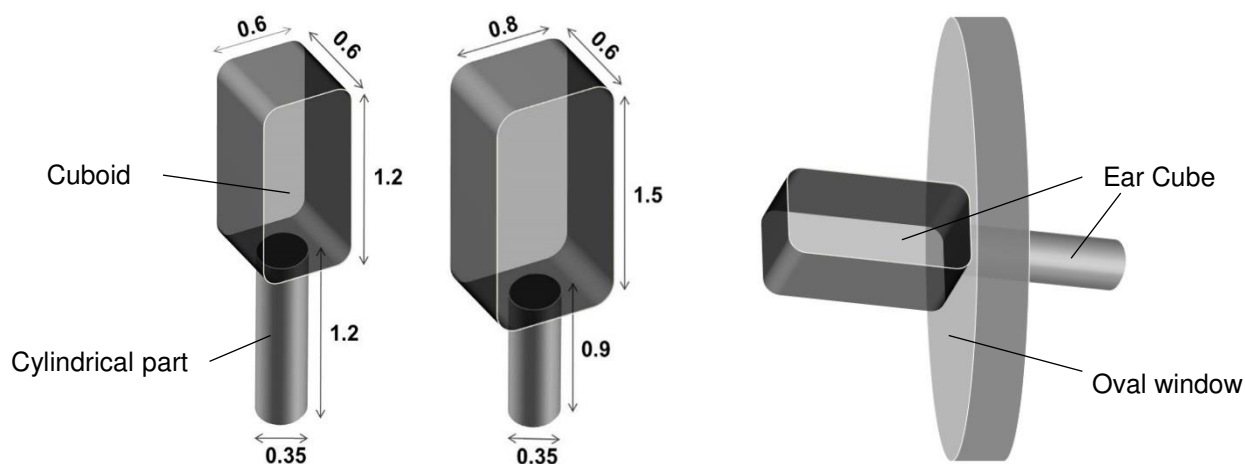**Figure 2.1.** Schematic presentation of the geometries and dimensions (indicated in mm) of a "smaller" and a "larger" Ear Cube. The drawing on the right hand side illustrates how Ear Cubes can be placed into the oval window.

Thin films (Figure 2.2., left hand side) were prepared using a self-made mold, which consisted of a microscope slide covered with 2 layers of a Teflon sheet (Bytac, Sigma

Aldrich, St. Louis, USA). A hole (6 x 1.5 cm) was cut into the upper Teflon sheet. The "silicone kit – drug" mixture was placed into this hole, and a casting knife (Multicator, Erichsen, Hemer, Germany) was used to provide a homogeneous film thickness. Crosslinking was completed by a thermal treatment in an oven at 60 °C for 20 h. The thickness of the films was measured with a micrometer gauge (Digimatic Micrometer, Mitutoyo, Tokyo, Japan). Drug-free films were prepared accordingly, omitting the drug. In these cases, larger glass slides were used instead of microscope slides and the dimensions of the hole were 10 x 13 cm.

Ear Cubes (Figure 2.2., right hand side) were prepared by injecting the "silicone kit – drug" mixture into customized molds (Neurelec, Vallauris, France) using a texture analyzer (TAXT plus, Stable Micro Systems, Surrey, UK). Two types of molds were used to prepare "smaller" and "larger" Ear Cube implants. The geometries and dimensions of the latter are illustrated in Figure 2.1., upon curing for 20 h at 60 °C the implants formed. They were removed from the molds under a microscope.

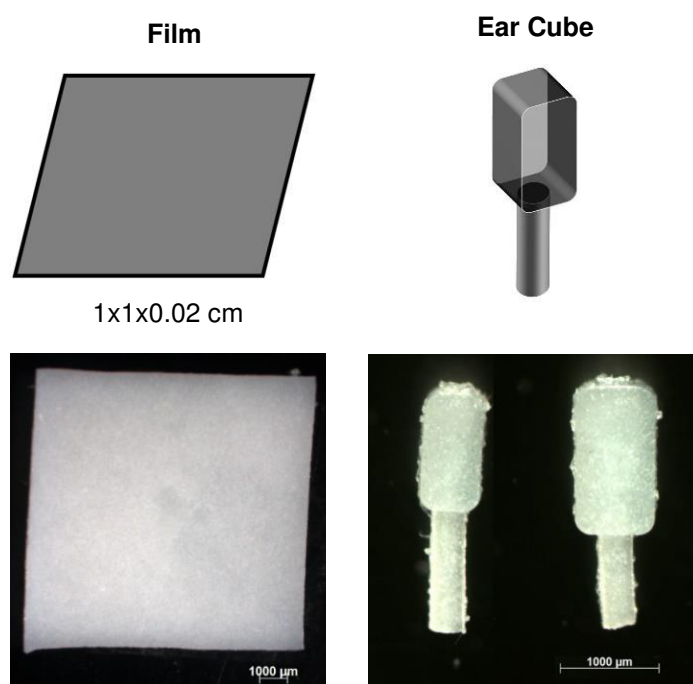**Figure 2.2.** Schematic presentations and macroscopic pictures of the investigated silicone matrices loaded with dexamethasone: Thin films and Ear Cubes. The drug loading was 10 % in all cases.

2.2.3. Drug release measurements

Film pieces (1x1x0.02 cm) were placed into amber glass flasks containing 10 mL artificial perilymph. The flasks were horizontally shaken (80 rpm) in an incubator (GFL 3033,

Gesellschaft fuer Labortechnik, Burgwedel, Germany) at 37 °C. At predetermined time points, 1 mL samples were withdrawn and replaced with fresh artificial perilymph. Each experiment was performed in triplicate.

A hole (diameter 0.04 cm) was drilled into the bottom of an Eppendorf vial (0.2 mL), which had been cut at half height (Figure 2.3.). One Ear Cube was placed into such a hole. The upper part of the Ear Cube was fixed with Kwik-Sil silicone in this Eppendorf vial, which was placed into a second Eppendorf vial (0.2 mL) containing 0.1 mL artificial perilymph. The orifice at the bottom of the first Eppendorf vial was always immersed in the release medium. The system was protected from light and placed in a horizontal shaker at 37 °C (80 rpm, GFL 3033). At predetermined time points, the release medium in the second Eppendorf vial was completely renewed. Each experiment was performed six times.

The drug concentrations in the withdrawn samples was determined by HPLC analysis (Thermo Fisher Scientic Ultimate 3000 Series, equipped with a pump: LPG 3400 SD/RS, an autosampler: WPS-3000 SL, a column compartment: TCC 3000 D/RS and a UV-Vis detector: VWD-3400RS, Thermo Fisher Scientic, Waltham, USA). Samples (100 µL for films, 20 µL for implants) were injected into a C18 RP column (Gemini 5 µm C18 110 A, 150 mm x 4.6 mm, Phenomenex, Le Pecq, France) (mobile phase = acetonitrile:water 33:67 v:v, flow rate = 1.5 mL/min). Dexamethasone was detected at $\lambda = 254$ nm.
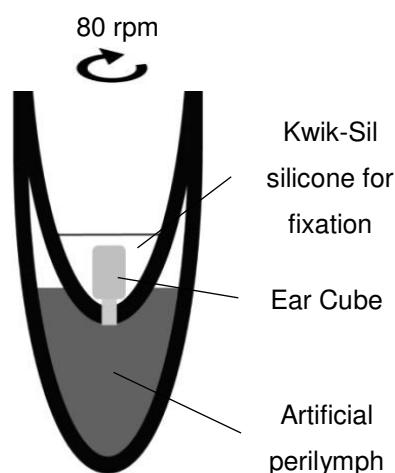

Figure 2.3. Schematic presentation (not up to scale) of the experimental set-up used for drug release measurements from Ear Cubes. Details are given in the text.

2.2.4. Side-by-side diffusion cells

Drug-free silicone films (9x9x0.02 cm) were placed into horizontal side-by-side diffusion cells (2 x 100 mL; Permegear, Hellertown, PA, USA). The donor compartment was filled with artificial perilymph saturated with dexamethasone (an excess of drug was present at the bottom of the chamber, but was not in contact with the silicone film). The acceptor compartment was filled with artificial perilymph. The system was protected from light and placed in a horizontal shaker at 37 °C (80 rpm, GFL 3033). At predetermined time points, 1 mL samples were withdrawn from the acceptor compartment and replaced with fresh medium. The dexamethasone concentrations in the samples were determined by HPLC analysis, as described above. Each experiment was performed in triplicate.

2.2.5. Swelling kinetics of Ear Cubes

The upper parts of Ear Cube implants were fixed using stainless steel wire and a drop of Kwik-Sil silicone at the caps of Eppendorf vials (2 mL), as illustrated in Figure 2.4. The implants were immersed into 2 mL artificial perilymph, and the systems were placed in a horizontal shaker at 37 °C (80 rpm, GFL 3033). To monitor potential Ear Cube swelling, an optical image analysis system (Nikon SMZ-U, Nikon, Tokyo, Japan), equipped with a Zeiss camera (AxioCam ICc 1, Zeiss, Jena, Germany) was used. At predetermined time points, photos were taken and the medium was completely renewed. Each experiment was performed in triplicate.
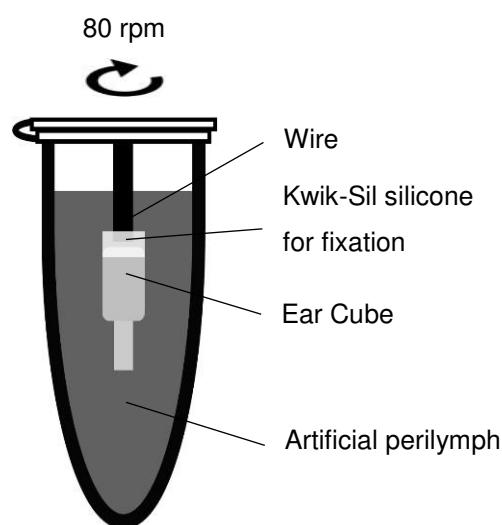

Figure 2.4. Schematic presentation (not up to scale) of the experimental set-up used to monitor the potential swelling of Ear Cubes. Details are given in the text.

2.2.6. Scanning electron microscopy

The morphology of cross-sections of Ear Cubes was studied using a scanning electron microscope (S-4000; Hitachi High-Technologies Europe, Krefeld, Germany). Samples were fixed with a ribbon carbon double-sided adhesive on the sample holder and covered with a fine carbon layer. The cross-sections were obtained by freezing the implants in liquid nitrogen and manual breaking.

2.2.7. Thermal analysis (DSC)

Ear Cubes were placed into open aluminum pans. To avoid ghost peaks, they were cut into two parts: the cylinders and cuboids, which were placed next to each other in the pans. For reasons of comparison, also the pure drug powder (as received) was studied (approximately 2.5 mg). The pans were first cooled to -150 °C and then heated to 280 °C at 10 K min^{-1} (DSC Q10, TA Instruments, Guyancourt, France). The DSC was calibrated using indium.

2.2.8. X-ray diffraction

A Panalytical X'pert Pro diffractometer (PANalytical, Almelo, Netherlands) in transmission mode with incident beam parabolic mirror (λ Cu, Kα = 1.54 Å) was used to record X-ray diffraction patterns. Drug-loaded and drug-free Ear Cubes were cut into two parts (cylinders and cuboids), and only the cuboids were placed inside a Lindemann glass capillary (diameter 1 mm; Hilgenberg, Malsfeld, Germany), which was subsequently fixed on a spinning sample holder. For reasons of comparison, also the pure drug powder (as received) was analyzed.

2.3.   Trans-Oval-Window Implants: Extended Dexamethasone Release

2.3.1. Materials

Kwik-Cast silicone (WPI, Sarasota, FL, USA); dexamethasone (Discovery Fine Chemicals, Dorset, UK); polyethylene glycol (PEG) 400 (Lutrol E400; BASF, Ludwigshafen, Germany); calcium chloride dihydrate, magnesium sulfate tetrahydrate, potassium chloride, sodium chloride, and 4-(2- hydroxyethyl) piperazine-1-ethanesulfonic acid (HEPES Pufferan, Carl Roth, Lauterbourg, France); acetonitrile and tetrahydrofuran (HPLC grade; Fisher Scientific, Illkirch, France); phosphate-buffered saline x 10 solution (PBS; Fisher Scientific); image-iT fx signal enhancer (Life Technologies, Saint Aubin, France); ethylenediamine tetraacetic acid, paraformaldehyde, Teflon films (Bytac), Triton X-100, fetal bovine serum (FBS), ethanol, phalloidin tetramethylrhodamine isothiocyanate, methyl salicylate, benzoate benzyl, 4',6-diamidino-2-phenylindole (DAPI) and fluoroshield (Sigma-Aldrich, St Quentin Fallavier, France); Image-iT fx solution (Molecular Probes, Eugene, OR, USA); rabbit polyclonal dexamethasone antibody (ABCAM, Cambridge, UK); goat anti-rabbit IgG-Alexa 488 (Jackson Immunoresearch Laboratories, West Grove, PA, USA); buprenorphine (Sogeval, York, UK); lidocaine hydrochloride (AstraZeneca, Reims, France); pentobarbital 362.9 mg/mL, injectable solution (TVM, Lempdes, France).

2.3.2. Preparation of drug-loaded Matrices

2.3.2.1.   Thin Films

Thin dexamethasone loaded films based on Kwik-Cast silicone were prepared as follows: PEG 400 and dexamethasone powder (both as received) were blended manually (mass ratio = 1:2) in a mortar. This drug-PEG blend was incorporated separately into Parts A and B of the Kwik-Cast silicone preparation kit in a mortar. The drug-PEG-Part A and drug-PEG-Part B blends were then placed separately into the two chambers of the dual syringe injection system provided by the supplier of Kwik-Cast (WPI). The contents of the two chambers were blended during ejection through the mixer tip (600009, WPI) onto a Teflon sheet. Thin films were subsequently prepared with a casting knife (Multicator 411; Erichsen, Hemer, Germany). Crosslinking completed spontaneously at room temperature within less than 30 min. The thickness of the films was determined with a micrometer gauge (Digimatic

Micrometer; Mitutoyo, Tokyo, Japan). The final percentages of PEG 400 and dexamethasone in the films were 5 and 10 %, respectively.

2.3.2.2.   In-situ forming implants

Implants were prepared using the dual syringe injection system for Kwik-Cast provided by the supplier (WPI). Each chamber contained either Part A or B of the silicone preparation kit, blended with dexamethasone and PEG (the blends were prepared as described in the section Preparation of Drug-loaded Films). The contents of the two chambers were mixed during ejection through the mixer tip (600009, WPI). One drop of this liquid was placed at the bottom of an Eppendorf vial (0.2 mL) into which a hole with a diameter of 0.35mm had been drilled (Figure 2.5., left hand side). The liquid filled the bottom part of the vial including the hole and hardened within a few minutes at room temperature.
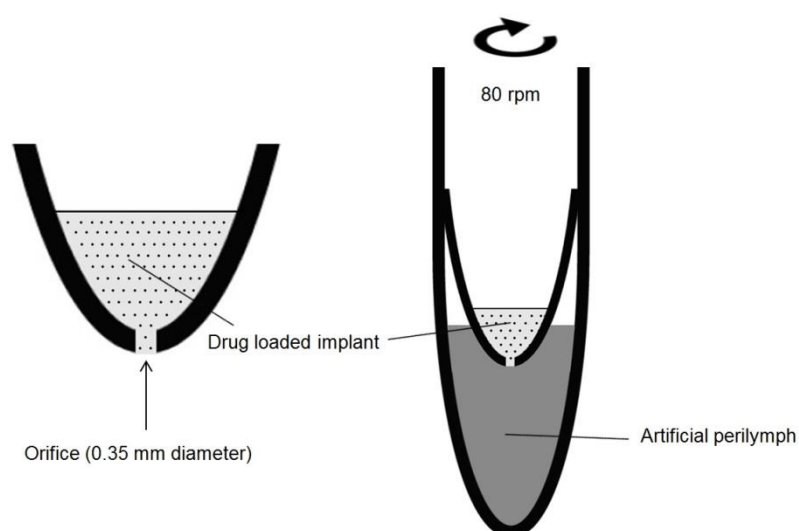
Figure 2.5. Schematic presentation of an implant formed at the bottom of an Eppendorf vial and the set-up used for in vitro drug release measurements (left and right hand side respectively).

2.3.3. Drug Release Measurements

2.3.3.1.   Thin Films

Film pieces (1x1x0.01 cm) were placed into amber glass flasks containing 10 mL artificial perilymph. The flasks were horizontally shaken (80 rpm) in an incubator (GFL 3033, Gesellschaft fuer Labortechnik, Burgwedel, Germany) at 37 °C. At predetermined time

points, 1 mL samples were withdrawn and replaced with fresh artificial perilymph. Each experiment was performed in triplicate.

2.3.3.2.   In-situ forming implants

An Eppendorf vial (0.2 mL) into which a hole (diameter 0.35 mm) had been drilled at the bottom and in which an implant had been formed as described above, was cut at half height (Figure 2.5., right hand side). The bottom part of this first Eppendorf vial was placed into a second Eppendorf vial (0.2 mL), which was (partly) filled with 100 µL artificial perilymph (37 °C). The inner Eppendorf vial was manually fixed within the second Eppendorf vial and its orifice was always immersed in the artificial perilymph. The entire system was protected from light and agitated at 80 rpm in a horizontal shaker at 37 °C (GFL 3033). At predetermined time points, the release medium was completely renewed. Each experiment was performed nine times.

The drug concentrations in the withdrawn samples were determined by high-performance liquid chromatography analysis (Varian Prostar 230, equipped with an autosampler: Prostar 410 and UV-Vis detector: Prostar 325; Varian, Les Ulis, France). Samples (100 µL for films, 20 µL for implants) were injected into a C18 RP column (Gemini 5u C18 110A, 150mm x 4.6 mm; Phenomenex, Le Pecq, France) (mobile phase = acetonitrile:water 33:67 V:V, flow rate = 1.5 mL/min). Dexamethasone was detected at $\lambda = 254$ nm.

2.3.4. Gerbil Study

The animal study received prior approval from the French Ministry of Agriculture and the Ethic Committee for Animal Experimentation (protocol no. 01225.01). Seventeen Mongolian gerbils (Meriones unguiculatus; Charles Rivers, Saint Germain sur l'Arbresle, France), 10 months old (approximately 60 g weight) and of either sex, were divided into three groups (Figure 2.6.):

(1) A verum group (n = 13) that received the trans-oval window implants. After 20 min, 7 and 30 days animals were sacrificed and tissues analyzed.

(2) A control group, which received an intratympanic injection of an 8 % dexamethasone solution on day 0, 1, and 2 (0.1 mL, bilaterally) (n = 2). The animals were sacrificed on day 3 and the tissues analyzed with primary and secondary antibody (positive control group), or secondary antibody only (negative control group).

(3) Gerbils, which received no treatment, were sacrificed after 20 min for tissue analysis (negative control group) (n = 2).
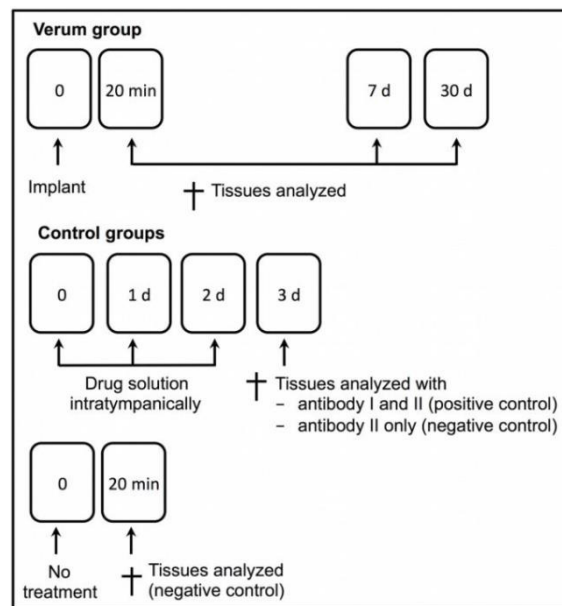
Figure 2.6. Design of the in vivo gerbil study. Details are given in the text.

2.3.5. Implantation Procedure

After anesthetic induction (mixture of 5 % isoflurane and 0.7 L/min oxygen), animals were anaesthetized via an inhalation mask (mixture of 2 % isoflurane and 0.7 L/min oxygen). In addition, 0.20 mL of a 1 % lidocaine solution was subcutaneously injected at the surgical site for local anesthesia.

The stapes area was exposed by a submandibular approach under microscope in sterile conditions. The auditory bulla was opened between two semicircular canals to expose the oval window (Figure 2.7.). A hole (0.35 mm in diameter) was drilled at the medial edge of the oval window using a microdrill handpiece (drill Osseostap, Bien Air, Bien Air France Sarl Surgery, Pantin, France). A drop of a liquid mixture of Parts A and B of the Kwik-Cast

preparation kit, containing 10 % dexamethasone and 5 % PEG 400 (prepared as described in the section Preparation of drug-loaded Matrices) was placed onto the perforation site, next to the stapes' footplate. The implant hardened within a few minutes (Figure 2.7.). Buprenorphine (0.03 mg/kg) was injected intraperitoneally for analgesia after surgery.
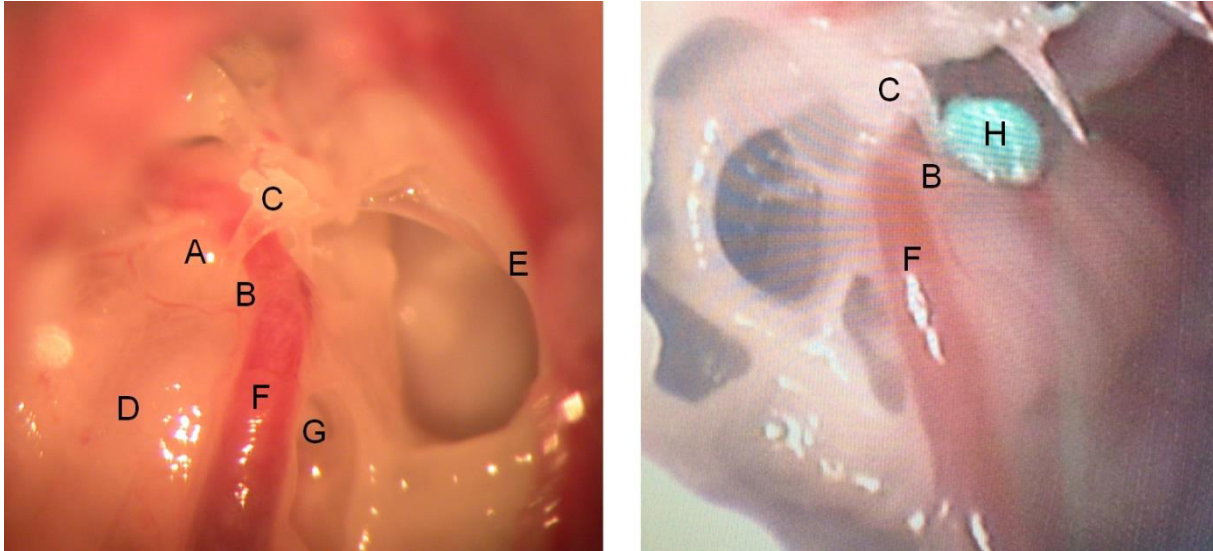
Figure 2.7. Exposition of the middle and inner ear after opening the auditory bulla of gerbil (left hand side: right ear) and Insertion of the implant after micro-shaping on the lateral edge of the oval window (right hand side: left ear): A) surgical implantation site, B) oval window, C) stapes, D) cochlea, E) lateral semicircular canal, F) stapedial artery, G) round window, and H) trans-oval-window implant. To compare these images with a 3D-model of the cochlea please refer to Figure 1.4.

2.3.6. Cochleae Preparation for Further Analysis

At predetermined time points, gerbils were anesthetized (with a mixture of 5 % isoflurane and 0.7 L/min oxygen) and sacrificed by a lethal intraperitoneal injection of sodium pentobarbital (180 mg/kg). The following types of tissue samples were prepared:

(i) The whole cochlea: The auditory bulla was opened to dissect the cochlea and remove it from the otic capsule. A small hole was drilled into both, the apex of the cochlea and the round window with a fine needle. Samples were fixed with paraformaldehyde (4 %) at 4 °C for 24 h. Decalcification was achieved by immersion into a 10 % ethylenediamine tetraacetic acid solution in PBS for 7 days. Specimens were rinsed with 70 % ethanol and stored at 4 °C.

(ii)   Cochlea sections: Upon cochlea dissection, fixation and decalcification [as described in (i), except for ethanol rinsing], cochleae were placed in an aqueous sucrose solution (30 %) for 24 h and then in the embedding medium ''OCT'' (Optimal Cutting Temperature, Cellpath, Newtown, UK). The samples were deep-frozen in liquid nitrogen and stored at -20 °C. Twenty micrometers of sections were prepared with a cryostat (Leica CM3050S; Leica Microsystemes SAS, Nanterre, France) and placed on glass slides (Superfrost plus; Fisher Scientific).

(iii) The organs of Corti: Samples were dissected by removing the bony labyrinth of the whole cochleae and fixed with paraformaldehyde (4 %) at 4 °C for 30 min.

2.3.7. Immunohistochemistry

2.3.7.1.   Silicone Films

Kwik-Cast silicone-based film pieces (0.5x0.5x0.01 cm) loaded with 10 % dexamethasone and containing 5 % PEG 400 were incubated in a blocking solution (0.1 % Triton X-100, 10 % FBS in PBS) at room temperature under gentle agitation for 30 min. Then, an indirect immunolabeling was performed. The film pieces were exposed to a solution of a primary rabbit polyclonal dexamethasone antibody in buffer solution (0.1 % Triton X-100, 20 % FBS in PBS) (1:100) at 4 °C overnight under gentle agitation. Then, the samples were rinsed three times with PBS for 5 min. Afterward, the film pieces were exposed to a solution of AlexaFluor488 secondary antibodies in PBS (1:400) at 4 °C for 4 h, followed by three times rinsing with PBS for 5 min. Finally, the samples were placed on a strip (Ibidi, mSlide, ref. 80826) for confocal microscopy.

2.3.7.2.   Tissue Samples

Whole cochleae were immersed in Image-iT fx solution for 30 min, and subsequently washed three times in PBS containing 0.1 %Triton X-100 for 30 min. The samples were then exposed to a 30 µg/mL phalloidin tetramethylrhodamine isothiocyanate solution in PBS for 30 min and then incubated in a blocking solution (0.1 % Triton X-100, 10 % fetal bovine serum in PBS) at room temperature under gentle agitation for 2 h. The cochleae were exposed to a solution of a primary dexamethasone antibody for 3 days and then to a solution of AlexaFluor488 secondary antibodies for 12 h (as described in the section Silicone Films). The

samples were then incubated in 0.25 µg/mL DAPI solution in PBS for 30 min. Specimens were rinsed three times with PBS, for 15 min each, after each step.

After three consecutive ethanol baths (ethanol 70, 95, and 100 %) for 2 h each, dehydrated cochleae were transferred into a clearing solution of MSBB (mixing of five parts methyl salicylate and threeparts benzoate benzyl) diluted in a solution of 1:1 absolute ethanol. Samples were placed into successive MSBB baths for 2, 4, and 12 h and protected from light at room temperature with gentle agitation.

Cochlea sections and organs of Corti were treated in the same way as whole cochleae, but applying shorter exposure times. These samples were mounted with fluoroshield at the end of these steps.

Samples from nontreated animals were treated in the same way, using primary and secondary antibodies (serving as negative controls). Samples from gerbils receiving dexamethasone solution intratympanically were treated either with primary and secondary antibodies (serving as positive controls), or with secondary antibodies only (serving as another negative control).

2.3.7.3.   Confocal Laser Scanning Microscopy

A Confocal Laser Scanning Microscope, equipped with 10x/0.3, 20x/0.6 objectives and 40x/1.3, 63x/1.4 immercell oil objectives (LSM 710; Carl Zeiss, Jena, Germany) was used. Three lasers were applied: a 405-nm UV diode, a 488-nm argon laser, and a 561-nm DPSS diode contributed to excite DAPI (nuclear labeling), Alexa 488 (dexamethasone labeling) and Phalloidin TRITC (actin cytoskeleton labeling), respectively. Serial sections from the three-dimensional reconstruction were acquired using 2 and 4 µm Z-steps. Snapshot of several regions of the sample were acquired by fast-scanning step. The Z-stack images allowed obtaining maximum projections. Images were acquired and analyzed with the ZEN software.

3. Results and Discussion

3.1. Dexamethasone mobility in thin films

3.1.1. Effects of PEG addition

The diagrams on the left hand side of Figure 3.1 show the absolute amounts of dexamethasone released from thin films with an initial drug loading of 10 % into artificial perilymph. Three types of *liquid* silicone preparation kits were used (MED-4011, MED-6015, MED-6755). Optionally, 5 or 10 % PEG 1000, or 10 % PEG 400 was added (as indicated). The symbols represent the experimentally measured results. Clearly, the addition of different amounts of PEG had a strong effect on the resulting drug release kinetics, whereas the variation of the type of PEG (and of the type of silicone) had a moderate impact on dexamethasone release in the investigated ranges. As it can be seen: (i) Increasing PEG amounts led to increasing drug release rates. (ii) Higher molecular weight PEG led to faster drug release compared to lower molecular weight PEG. (iii) The absolute dexamethasone release rate generally increased in the following rank order: MED-4011 < MED-6015 < MED-6755, irrespective of the presence/absence of PEG.

In order to quantitatively evaluate these results, an analytical solution of Fick's second law of diffusion was used to describe the experimentally measured dexamethasone release kinetics. The model is based on the assumption that drug diffusion within the polymeric films is the dominant mass transport step. Furthermore, the theory considers initially homogeneous distributions of the drug, silicone and PEG within the films, perfect sink conditions and constant drug diffusion coefficients. Importantly, the model does not take into account limited drug solubility effects. Under these conditions, the following equation can be derived and used to quantify dexamethasone release from the investigated silicone films, optionally containing different amounts and types of PEG (137):

$$\frac{M_t}{M_\infty} = 1 - \frac{8}{\pi^2} \sum_{n=0}^{\infty} \frac{1}{(2n+1)^2} \, exp\left(\frac{-D(2n+1)^2 \pi^2 t}{L^2}\right) \tag{1}$$

where M_t and M_∞ denote the absolute cumulative amounts of drug released at time t and infinity, respectively; n is a dummy variable, D the "apparent" diffusion coefficient of the drug within the polymeric system; L represents the thickness of the film.

absolute release   normalized relative release

Figure 3.1. Effects of adding different types and amounts of PEG to thin films prepared with *liquid* silicone preparation kits (MED-4011; MED-6015; MED-6755) on the resulting dexamethasone release kinetics: left hand side – absolute drug release; right hand side - normalized relative drug release (film dimensions: 1x1x0.02 cm; 10 % drug loading). The symbols represent the experimentally measured results, the solid curves the fitted theory (Eq. 1).
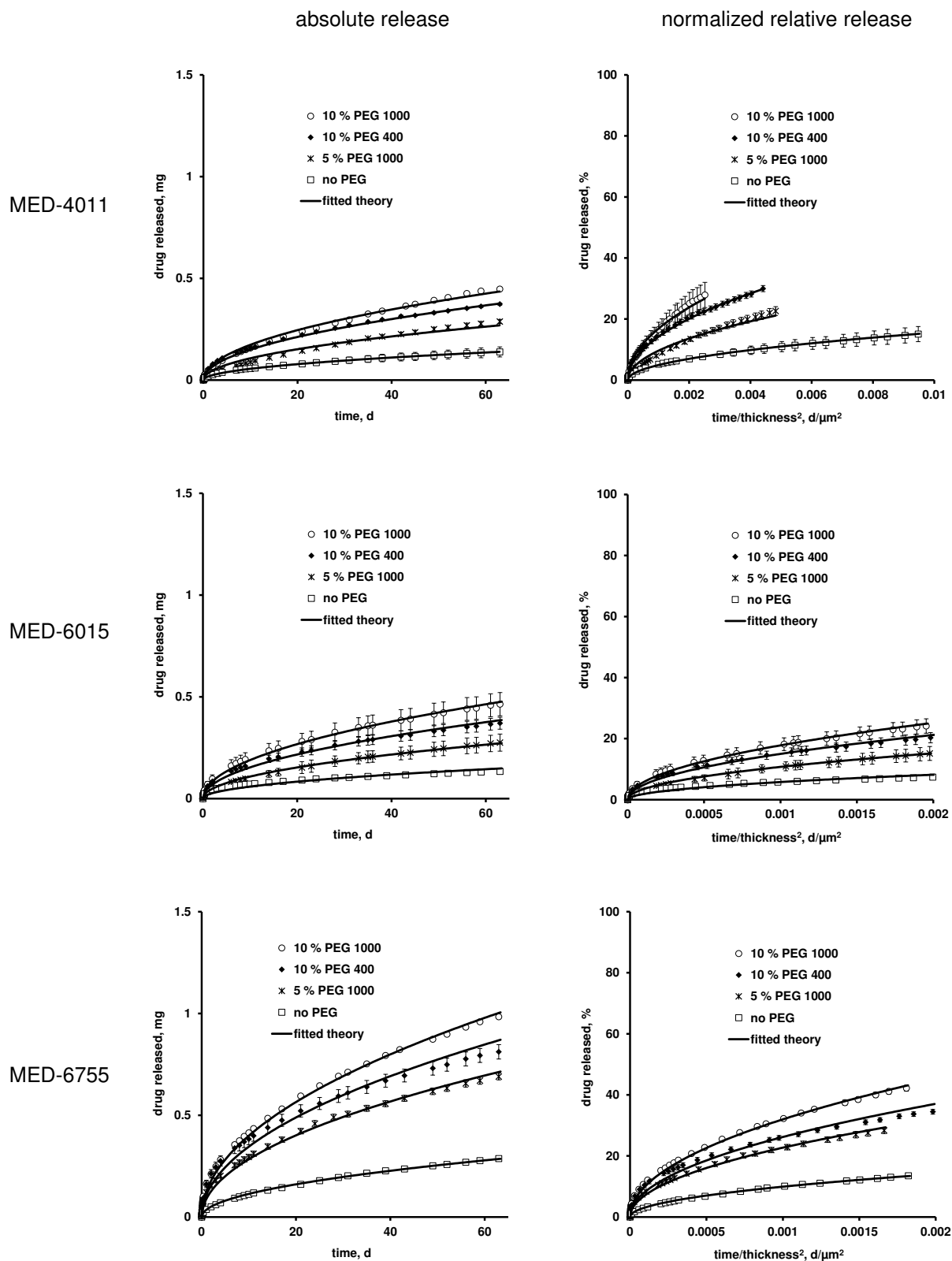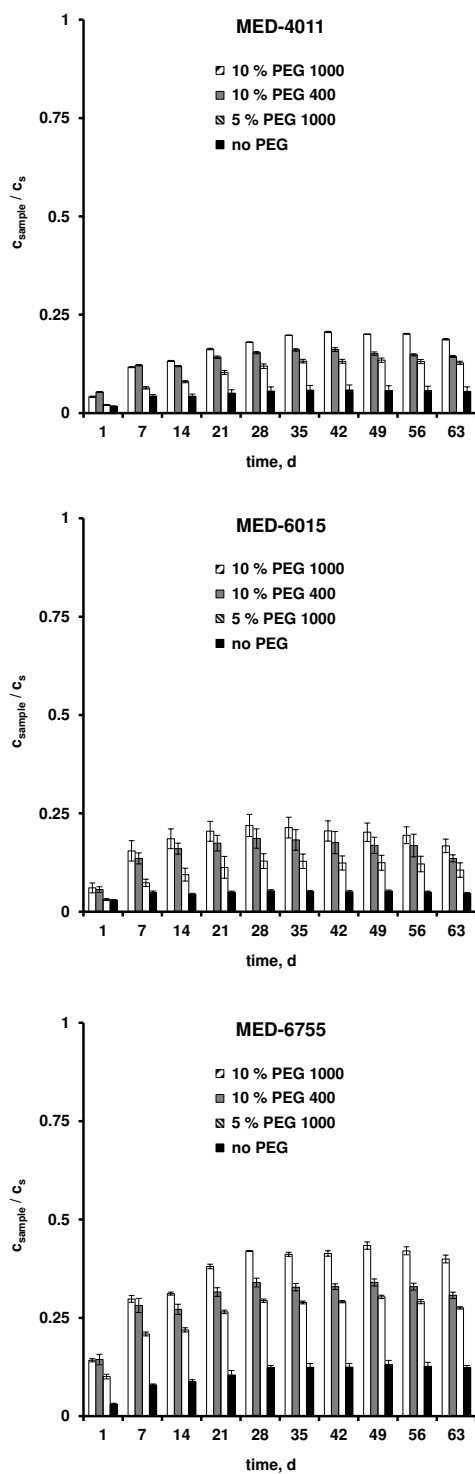
Figure 3.2. Effects of adding different types and amounts of PEG to thin films prepared with *liquid* silicone preparation kits (MED-4011; MED-6015; MED-6755) on the resulting degree of sample saturation (film dimensions: 1x1x0.02 cm; 10 % drug loading).

The curves in Figure 3.1 show the fittings of Eq. 1 to the experimentally determined dexamethasone release kinetics (the correspondent degree of drug saturation for each curve is shown in Figure 3.2). As it can be seen, good agreement between experiment and theory was obtained in all cases, irrespective of the presence/absence of PEG. This can serve as an indication for the fact that drug diffusion indeed plays a major role in the control of drug release from these systems (135). If this is true, the observed drug release kinetics can be normalized with respect to the film thickness (which slightly varied from sample to sample). It has to be pointed out that the film thickness determines the length of the diffusion pathways to be overcome and, hence, affects the drug release rates. Consequently, the observed drug release kinetics shown on the left hand side of Figure 3.1 should be viewed with some caution: Not only the variation of the films' composition impacts drug release, but also unintended variations in the thickness of the film samples. To avoid this bias, the results were normalized according to Eq. 1: Instead of the "time", the "time/thickness²" is plotted on the x-axes in the diagrams on the right hand side of Figure 3.1. In addition, the percentage of drug release is plotted on the y-axes (instead of the absolute amounts). This normalization of the drug release rates allows for a more reliable comparison of the release profiles if the effects of the film composition are to be studied. Unfortunately, sometimes in the literature drug release kinetics from films of different composition and different thickness are compared without normalization, and the impact of the film formulation and the impact of the film thickness are not always appropriately distinguished. As it can be seen on the right hand side of Figure 3.1, the above described general tendencies remained the same, while the relative importance of some effects were altered.

Importantly, based on the fittings in Figure 3.1 (curves), the "apparent" diffusion coefficient of dexamethasone in the investigated silicone films (optionally containing different types and amounts of PEG) could be determined. This parameter can be used as a measure for the mobility of the drug within the polymeric matrices. Figure 3.3 shows its dependence on the type and amount of added PEG for the investigated silicone types, ranging from $D = 5.51 \pm 1.71$ to $64.54 \pm 0.64 \times 10^{-14}$ cm²/s for MED-4011, from $D = 7.59 \pm 0.58$ to $72.04 \pm 17.96 \times 10^{-14}$ cm²/s for MED-6015 and from $D = 22.41 \pm 0.16$ to $232.41 \pm 5.78 \times 10^{-14}$ cm²/s for MED-6755. It has to be pointed out that Eq. 1 does not take limited drug solubility effects into account. Since the amounts of water penetrating into the systems and the solubility of the drug are limited, it can be expected that not all of the drug is rapidly dissolved. SEM pictures revealed that small drug crystals were homogenously distributed throughout the films, irrespective of the type of silicone (also, all films were opaque).
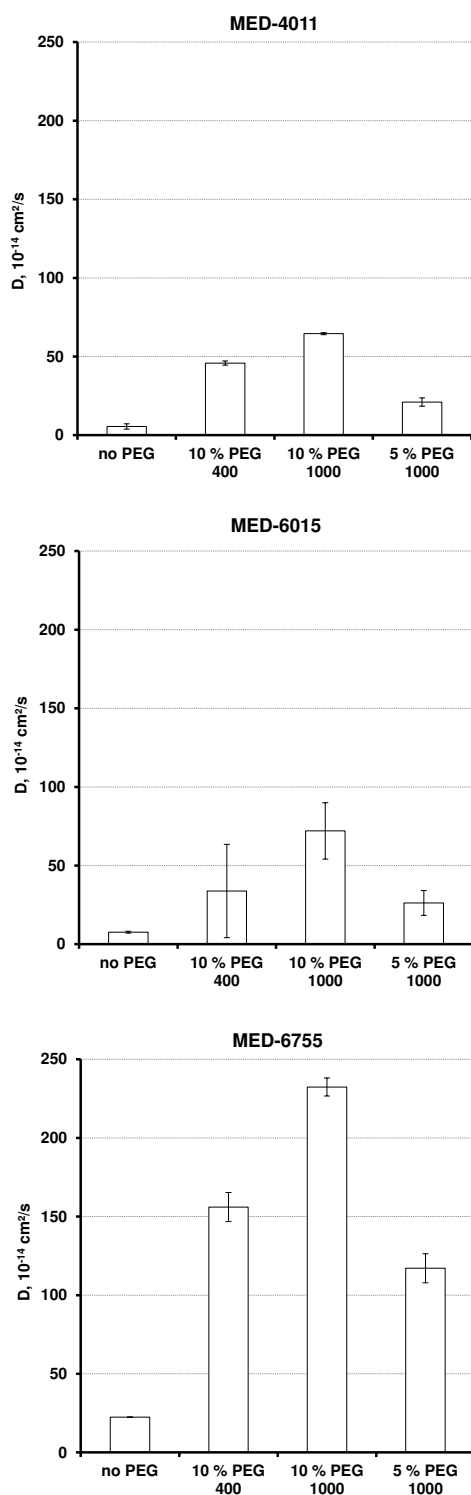
Figure 3.3. Impact of the addition of different types and amounts of PEG to thin silicone films prepared with *liquid* silicone preparation kits (MED-4011; MED-6015; MED-6755) on the resulting "apparent" dexamethasone diffusion coefficient (determined based on the fittings shown in Figure 3.1).

Figure 3.4 shows two examples. Thus, dissolved and non-dissolved dexamethasone are likely to co-exist during prolonged periods of time within the matrices. Importantly, only dissolved drug is available for diffusion. Consequently, the determined drug diffusivities are "biased" or "lumped" values, which is emphasized in this article using the term *"apparent"* drug diffusion coefficient. The real drug diffusivity is likely to be much higher: In reality, the non-dissolved drug is not able to diffuse, but the applied model assumes all drug to be able to diffuse. A much more comprehensive mathematical model is required to more realistically describe the exact mass transport phenomena in the investigated systems (including time- and position-dependent matrix compositions and drug diffusivities). But such a model must be based on a much broader experimental data basis (e.g. including information on structural changes of the films during drug release). Based on the available data, the best parameter to describe the mobility of the drug in the silicone matrices is the "apparent" drug diffusivity discussed above: Importantly, it takes all the practically relevant effects directly or indirectly into account. In particular, this "lumped" parameter is highly useful for the comparison of dexamethasone mobility in the investigated silicone films of different composition.
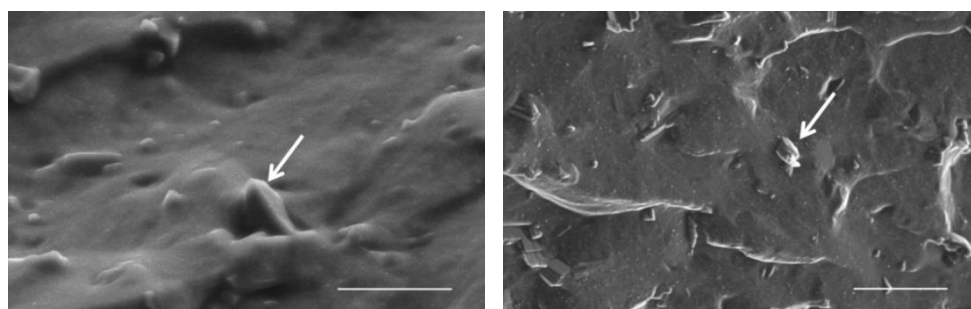
Figure 3.4. Scanning electron microscopy pictures of cross-sections of thin silicone films loaded with 10 % dexamethasone, prepared with: a) MED-5440, b) MED-6755 (scale bar = 5 µm). The arrows indicate drug crystals.

As it can be seen in Figure 3.3, the above described general effects of the addition of different amounts and types of PEG on dexamethasone release are confirmed by the analysis based on the "apparent" drug diffusivity (being a quantitative measure for drug mobility in the silicone matrices): (i) The addition of increasing amounts of PEG to the system leads to higher drug mobility. This can probably be attributed to the fact that PEG is much more hydrophilic than the investigated silicones, thus, the presence of increasing amounts of PEG drives more and more water into the system. Consequently, more drug can dissolve and the permeability of the dissolved drug is increased. This is true for all the investigated silicone

types. (ii) Interestingly, at the same PEG content, the higher molecular weight PEG 1000 leads to faster drug release than the lower molecular weight PEG 400, in all cases. The exact reasons for this phenomenon are not fully understood. Eventually, the PEG distribution in the films is dependent on the PEG molecular weight, resulting for instance in differently structured water-filled channels, through which the drug can diffuse. (iii) The dexamethasone mobility depends on the type of silicone, generally increasing in the following rank order: MED-4011 < MED-6015 < MED-6755. This aspect will be discussed in more detail in the following section.

Note that all the results shown in Figures 3.1, 3.2 and 3.3 were obtained with *liquid* silicone preparation kits. Importantly, also *pasty* kits are available on the market. The difference "pasty-liquid" can be decisive in practice, e.g. strongly affecting the manufacturing procedure of the drug delivery system. The effects of the addition of different amounts and types of PEG on dexamethasone release from films prepared with the pasty silicone preparation kits MED-4065, MED-4080 and MED-4735 are illustrated in Figure 3.5 (note that in the case of MED-4735 and 10 % PEG 400 the resulting films were too sticky to be handled). The correspondent degree of drug saturation for each curve is shown in Figure 3.6. As in the case of liquid silicone preparation kits, the addition of increasing amounts of PEG led to increasing drug release rates. However, in contrast to the investigated liquid kits, the addition of shorter chain PEG 400 led to faster drug release compared to longer chain PEG 1000. This difference in the impact of the molecular weight of the added PEG to liquid versus pasty silicone preparation kits might be explained as follows: PEG 400 is liquid, whereas PEG 1000 is solid. The mixing with the liquid and pasty kits might lead to blends with different degrees of homogeneity, and the PEG affinity to preparation kit compounds might depend on the PEG chain length and type of kit. These differences can lead to different inner film structures, resulting in an altered apparent drug mobility. In the case of pasty silicone preparation kits, films might result, from which shorter chain PEG 400 more easily leaches out into the surrounding bulk fluid than longer chain PEG 1000, and/or the shorter chain PEG 400 might create a higher osmotic pressure and lower viscosity in water-filled pores. Potential differences in the PEG distribution within the silicone matrix might also lead to different degrees of polymer-polymer interactions (e.g. MED-4735-based films containing 10 % PEG 400 were too sticky to be handled, thus, PEG might also act as a plasticizer for the silicones). Such effects might contribute to the observed faster drug release from PEG 400-containing films compared to PEG 1000-containing films prepared with pasty preparation kits.
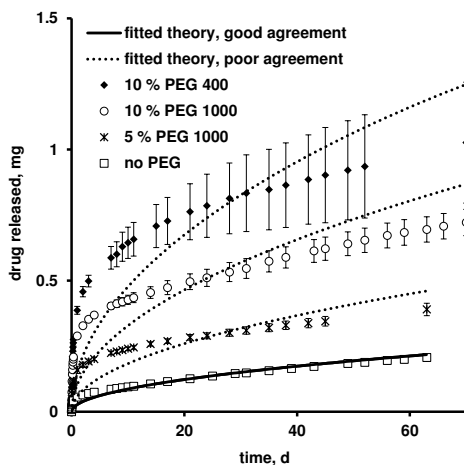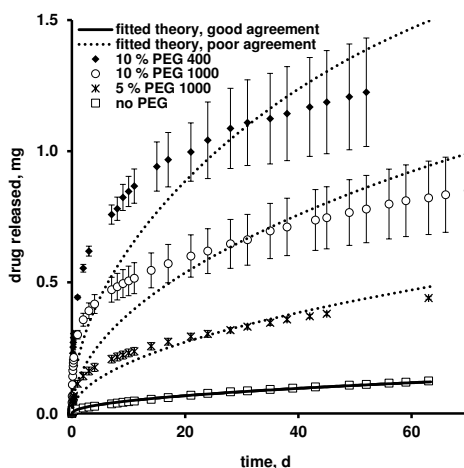
Figure 3.5. Effects of adding different types and amounts of PEG to thin films prepared with *pasty* silicone preparation kits (MED-4065; MED-4080; MED-4735) on the resulting dexamethasone release kinetics (absolute drug release) (film dimensions: 1x1x0.02 cm; 10 % drug loading). The symbols represent the experimentally measured results, the *solid* curves the fitted theory (Eq. 1) in case of good agreement, and the *dotted* curves show the fitted theory (Eq. 1) in case of poor agreement.
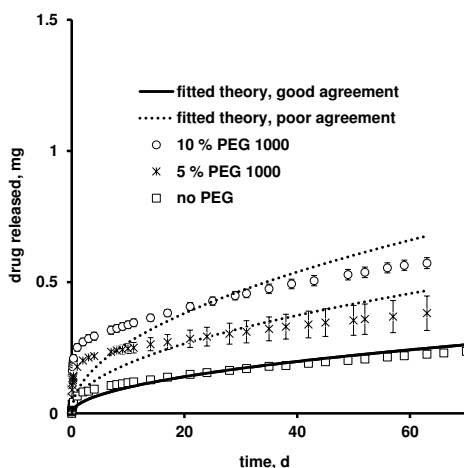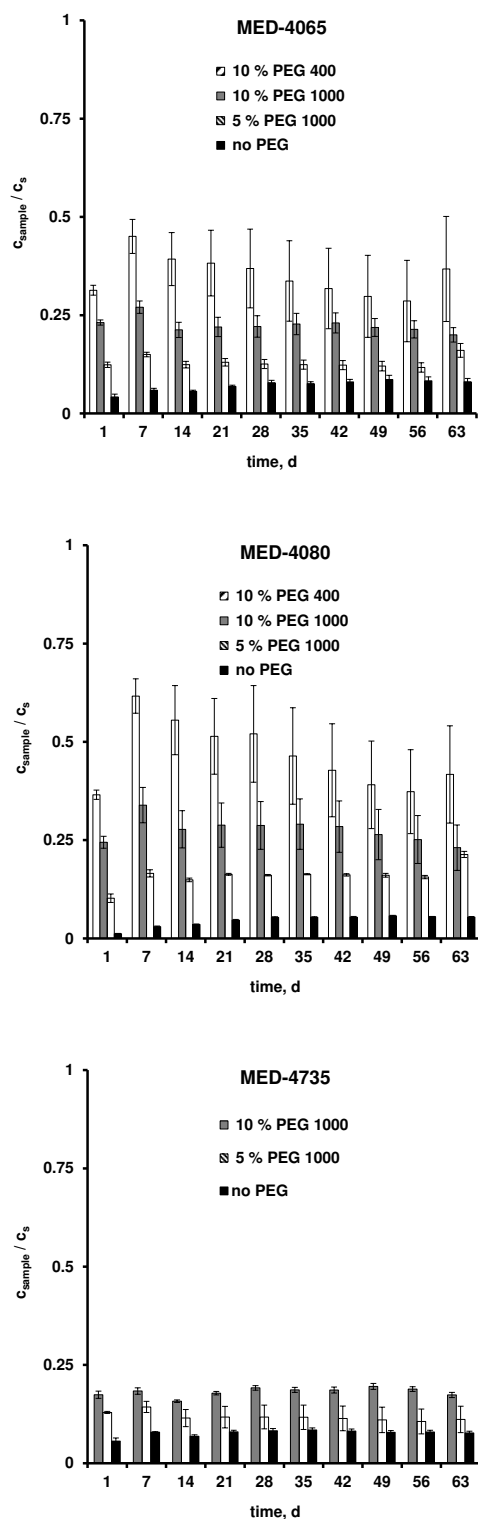
Figure 3.6. Effects of adding different types and amounts of PEG to thin films prepared with *pasty* silicone preparation kits (MED-4065; MED-4080; MED-4735) on the resulting degree of sample saturation (film dimensions: 1x1x0.02 cm; 10 % drug loading).

As in the case of liquid silicone preparation kits, Eq. 1 was fitted to the experimentally determined dexamethasone release kinetics (curves in Figure 3.5). Interestingly, only in the case of PEG-free systems good agreement between theory and experiment was observed (solid curves), indicating that diffusion is likely to play a major role for the control of drug release. In contrast, substantial and systematic deviations were observed between theory (dotted curves) and experiment (symbols) in the case of all PEG-containing films: Drug release was underestimated at early time points and overestimated at later time points. This clearly indicates that not only diffusional mass transport is decisive in these systems. This is why no "apparent" drug diffusivities could be determined for PEG-containing silicone matrices prepared with pasty kits, and the respective drug release kinetics could not be normalized with respect to the film thickness. Thus, the arbitrary variations in the thickness of the film samples referred to in Figure 3.5 partially contribute to the observed differences in drug release. However, since the film thickness variations were of the same order of magnitude as the variations observed with film samples prepared with liquid silicone preparation kits (Figure 3.1), it can be expected that the impact of the investigated film formulation parameters is much more important than the impact of the arbitrary variations in the film thickness.

3.1.2. Effects of the type of silicone

The impact of the type of silicone, including the type of side chains and contents of amorphous silica, on dexamethasone release from thin films into artificial perilymph is shown in Figure 3.7. The films were prepared with the liquid preparation kits MED-6033 and MED-6015 (containing dimethyl-side chains) as well as MED-5440 and MED-50-5438 (containing fluorine-side chains). MED-5440 and MED-50-5438 contained 19 and 20 % amorphous silica, respectively. All films were free of PEG. As it can be seen, the type of silicone had a significant impact on drug release. Note that the films in Figure 3.7 had a larger surface area than those in Figures 3.1 and 3.5. So, a direct comparison of the absolute drug release rates between the three figures should be viewed with some caution. The curves in Figure 3.7 show the fittings of Eq. 1 to the experimentally measured drug release kinetics. As it can be seen, good agreement was obtained in all cases, further confirming that in all PEG-free silicone systems diffusional mass transport seems to be decisive for the control of drug release. Thus, also in these cases, the release rates can be normalized to the film thickness, as shown in Figure 3.7b.

Figure 3.7. Effects of varying the type of silicone on the resulting: a) absolute dexamethasone release, b) normalized relative drug release, c) "apparent" dexamethasone diffusion coefficient from/in thin films, and d) degree of sample saturation (dimensions: 3.5x3.5x0.1 cm; dexamethasone loading 10 %). In a) and b) the symbols show the experimental results and the curves the fitted theory (Eq. 1). The diffusivities illustrated in c) were determined based on the fittings shown in a) and b). MED-6033 and MED-6015 contain dimethyl-side chains, MED-5440 and MED-50-5438 contain fluorine-side chains. All films were free of PEG.

When comparing the dexamethasone release kinetics from the films prepared with the MED-6015 (open triangles; virtually overlapping with the open diamonds of MED-6033) and MED-5440 (filled squares) kits, the importance of the film thickness normalization becomes evident: In Figure 3.7a, MED-5440-based films show faster release than MED-6015-based films, but this difference can be attributed to the difference in film thickness (and not to the different film composition or structure): The average film thicknesses of MED-5440-based films were about 35 % smaller than the average film thicknesses of MED-6015-based films.
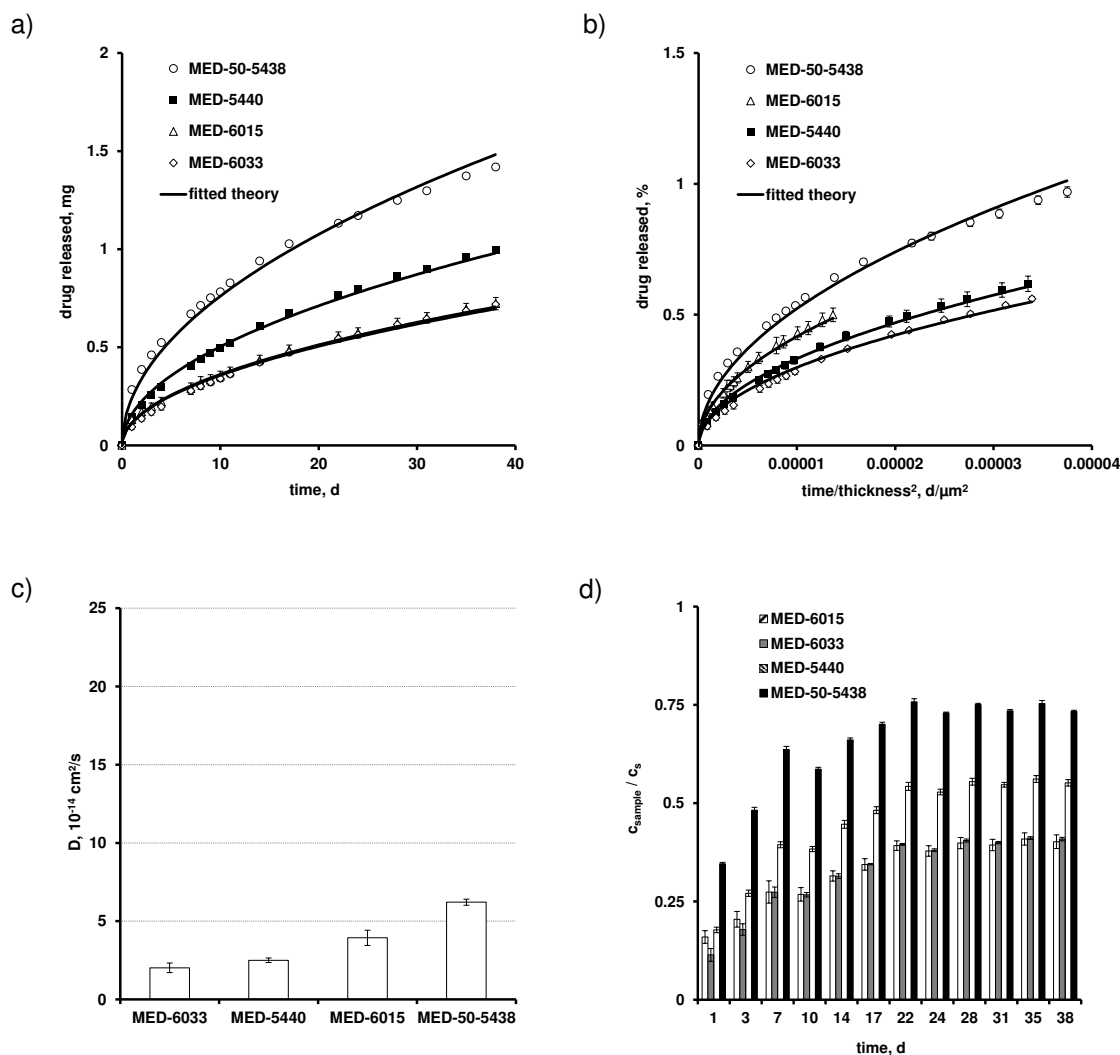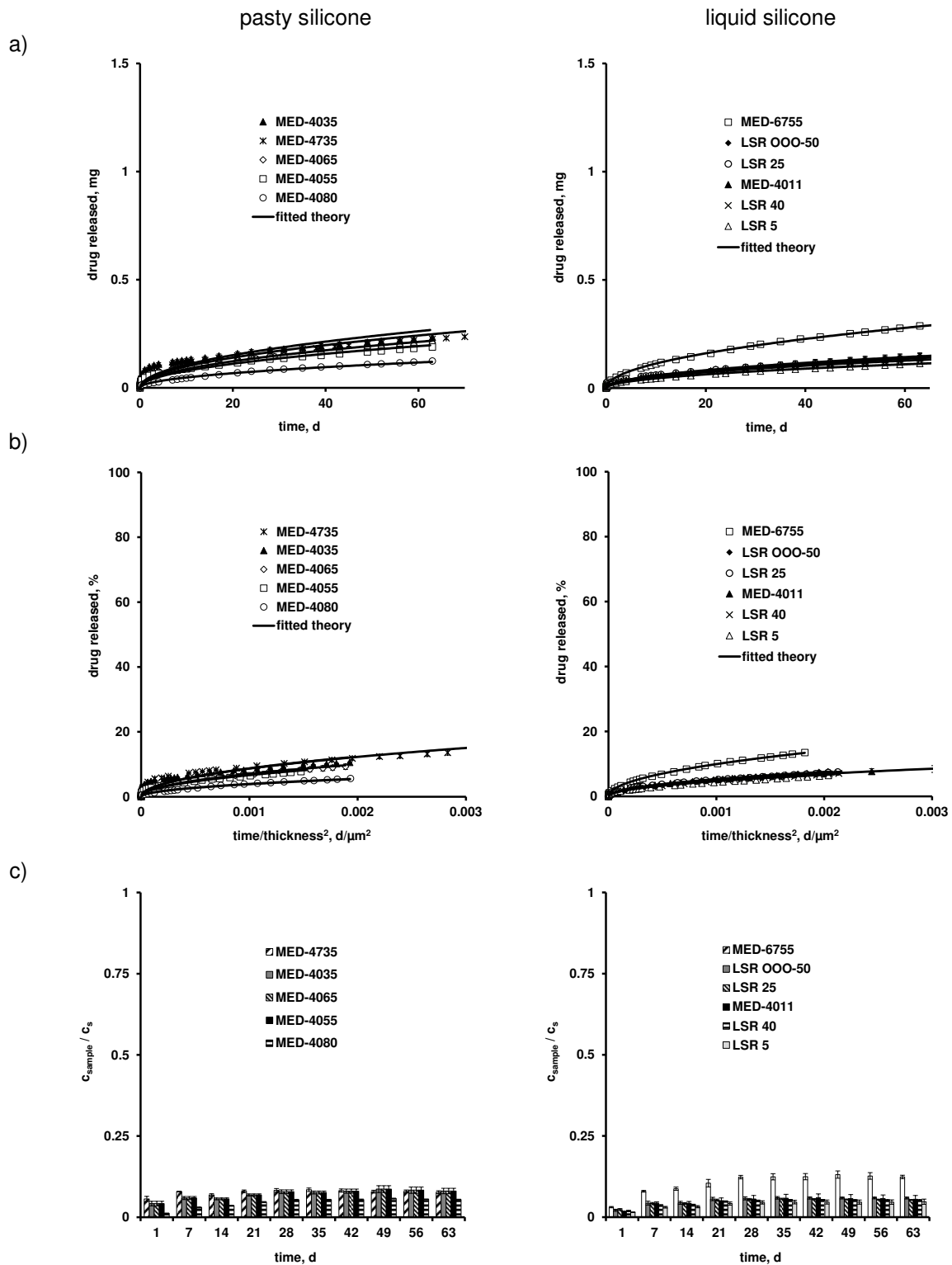
Figure 3.8. Effects of varying the type of silicone on the resulting: a) absolute dexamethasone release, b) normalized relative drug release, and c) degree of sample saturation (dimensions: 1x1x0.02 cm; dexamethasone loading 10 %). The symbols in a) and b) show the experimental results, the curves the fitted theory (Eq. 1). All films were free of PEG.

pasty silicone

liquid silicone
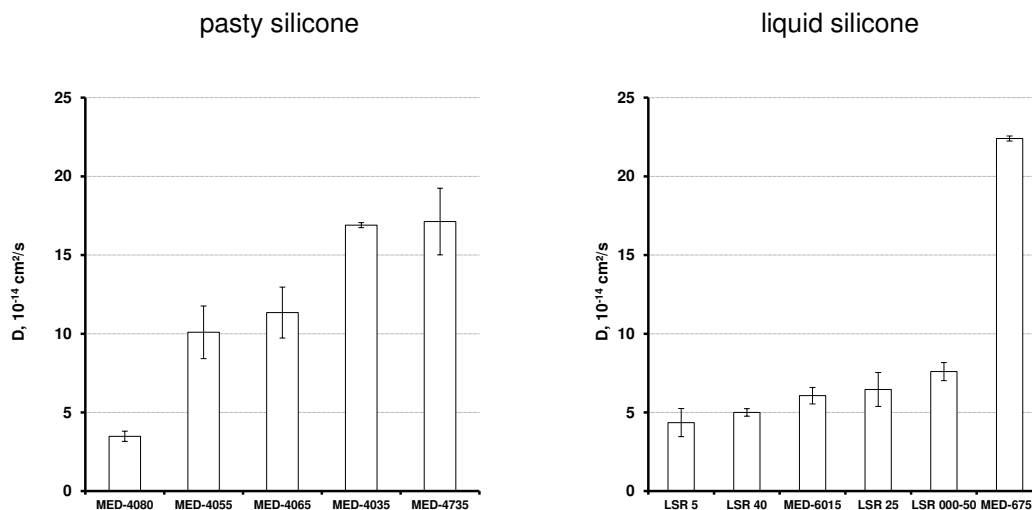
Figure 3.9. Effects of varying the type of silicone on the resulting "apparent" dexamethasone diffusion coefficient from/in thin films (dimensions: 1x1x0.02 cm; dexamethasone loading 10 %). The diffusivities illustrated in Figure 3.9 were determined based on the fittings shown in Figure 3.8a and b. All films were free of PEG.

The shorter diffusion pathways in MED-5440-based films led to faster drug release. Importantly, this "film thickness effect" is avoided upon appropriate normalization of the results: Figure 3.7b shows that the mobility of dexamethasone is higher in MED-6015-based films (open triangles) than in MED-5440-based films (filled squares). Thus, erroneous conclusions can easily be drawn when comparing non-normalized drug release kinetics. Again, based on the fittings of Eq. 1 to the experimental results, the "apparent" dexamethasone diffusion coefficients in the investigated silicone films could be determined: As it can be seen in Figure 3.7c, the type of silicone can effectively be used to adjust a desired dexamethasone mobility in the polymeric matrices. But note that the values remain relatively small ($D = 2.02 \pm 0.31 \times 10^{-14}$ cm^2/s for silicone MED-6033) compared to those of PEG-containing films ($D = 232.41 \pm 5.78 \times 10^{-14}$ cm^2/s for silicone MED-6755 with 10 % PEG 1000) (Figure 3.3, the y-axes being differently scaled).

The absolute dexamethasone release kinetics from films prepared using different types of pasty and liquid silicone preparation kits are shown in Figure 3.8a. Note that the film dimensions were different from those of the films shown in Figure 3.7. Thus, a direct comparison is not straightforward. Fitting Eq. 1 to the experimentally determined drug release kinetics, good agreement between theory and experiment was obtained in all cases (curves and symbols), further confirming the dominant role of diffusional mass transport for the control of drug release from PEG-free silicone films. The respective normalized

54

dexamethasone release kinetics are shown in Figure 3.8b. When comparing the latter to Figure 3.7b, note the different scaling of the x-axes. As it can be seen, the dexamethasone release rate can be varied to a certain extent by varying the type of silicone. Figure 3.9 shows the "apparent" diffusion coefficients of the drug in these systems, determined based on the fittings illustrated in Figures 3.8a and b. Roughly, a desired dexamethasone diffusivity can be adjusted in the range of 3.5 and 22.4 x 10^{-14} cm²/s using these silicone preparation kits.

3.1.3. Impact of the initial drug loading

Another formulation parameter, which can potentially be altered in order to adjust a desired drug mobility within silicone matrices (and, hence, desired drug release profiles), is the initial drug loading of the system. The symbols in Figure 3.10a show the experimentally measured absolute amounts of dexamethasone released from films with an initial drug content of 10, 30, 40 and 50 %, respectively. All films were prepared with the MED-4011 silicone kit, and were free of PEG. Note that intentionally a higher volume of release medium was used in these cases (900 ml instead of 10 mL) in order to avoid potential drug saturation effects in the surrounding bulk fluid. Clearly, the absolute drug release rate increased with increasing initial drug loading. This can at least partially be explained by the increasing porosity of the polymeric matrix upon drug exhaust, resulting in an increased mobility for the remaining drug. The respective *relative* amounts of dexamethasone released from the films as a function of time are illustrated in Figure 3.10b. Interestingly, the relative release rates were very similar for the drug loadings 10, 30 and 40 % (but some caution should be paid, since these curves are not normalized to the films' thicknesses). Again, fitting Eq. 1 to the experimental results led to good agreement in all cases (curves and symbols in Figure 3.10). Thus, irrespective of the initial drug content, diffusional mass transport seems to play a dominant role in all PEG-free silicone matrices investigated in this study.

Importantly, this fact allows normalizing the observed drug release kinetics with respect to the films' thicknesses. As it can be seen in Figure 3.10c, the relative normalized drug release rates are virtually overlapping for films loaded with 10 and 30 % dexamethasone.
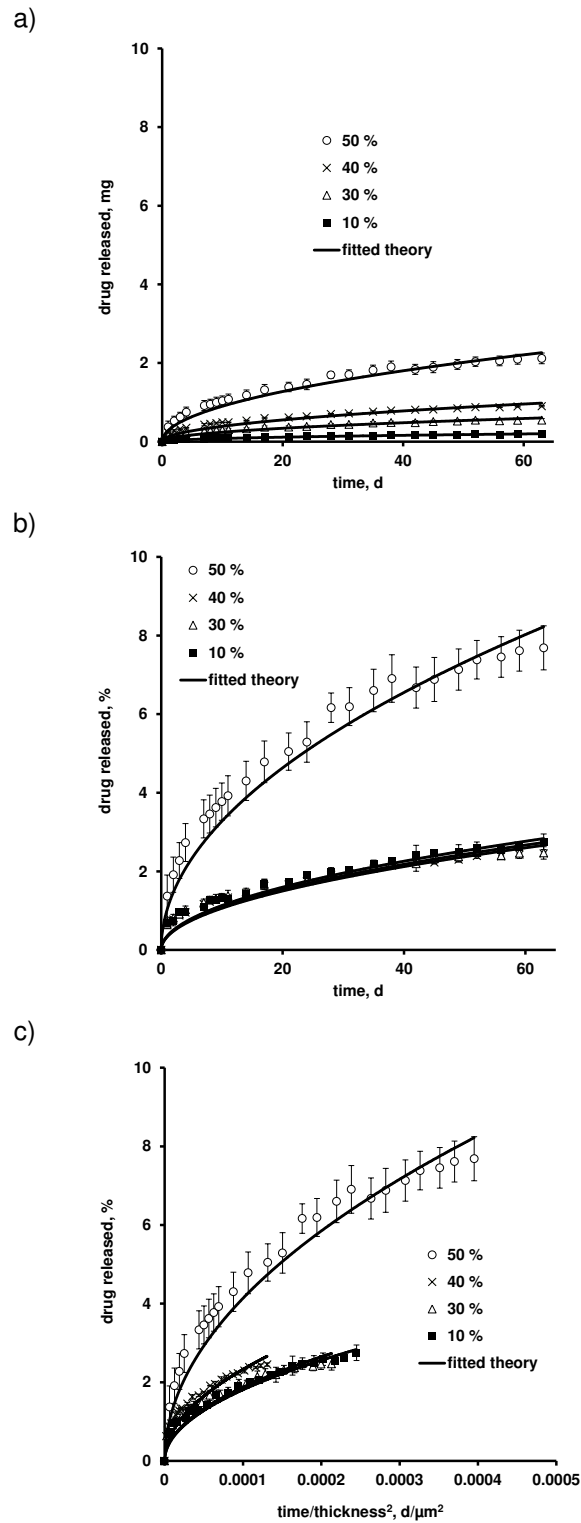
Figure 3.10. Impact of the initial drug loading (indicated in the diagrams) on dexamethasone release from thin films in 900 mL artificial perilymph: a) absolute drug release, b) relative drug release, and c) normalized relative drug release. All films (dimensions 1x1x0.05 cm) were based on MED-4011 and free of PEG. The symbols represent the experimentally measured results, the solid curves the fitted theory (Eq. 1).

Somewhat faster drug release was observed at an initial drug loading of 40 %, and substantially faster drug release at 50 % initial dexamethasone content. The reason for this phenomenon might at least partially be related to the percolation theory: Above a certain, critical threshold value for the drug loading, a continuous 3-dimensional network of drug particles is created (as shown previously, dexamethasone is likely to be dispersed in the silicone matrix in the form of small particles (135)). Thus, water can more easily penetrate into the system upon drug dissolution, and the remaining drug can more rapidly leach out into the surrounding bulk fluid (through water filled pores, and not through an intact silicone network).

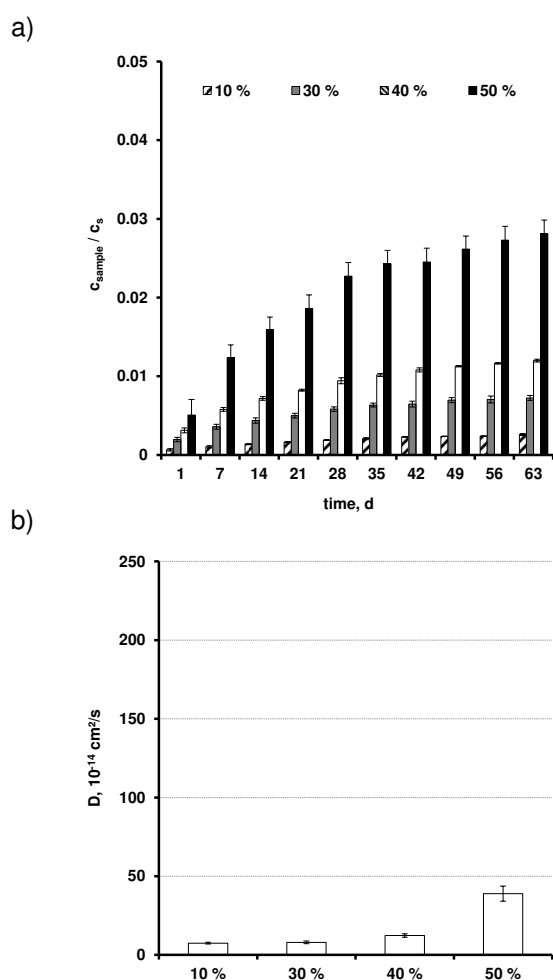**Figure 3.11.** Impact of the initial drug loading (indicated in the diagrams) on the: a) degree of sample saturation, and b) "apparent" drug diffusion coefficient of dexamethasone in thin silicone films (determined via the fittings shown in Figure 3.10). The films (dimensions 1x1x0.05 cm) were based on MED-4011 and free of PEG. The release medium was 900 mL artificial perilymph.

Figure 3.11a shows that perfect sink conditions were provided throughout the duration of the experiments (the solubility of dexamethasone in the release medium at 37 °C is 82.3 ± 1.7 mg/L (104)). Even at an initial drug content of 50 %, the degree of bulk fluid saturation (with dexamethasone) did not exceed 3 % (note that this is the degree of drug saturation in the release medium *outside* of the films, not *within* the films). Importantly, the fittings shown in Figure 3.10, again, allowed the determination of the respective "apparent" dexamethasone diffusion coefficients in the investigated silicone matrices, now as a function of the initial drug content. As it can be seen in Figure 3.11b, the drug mobility in the polymeric systems could be substantially increased when increasing the initial drug content (from D = 7.45 ± 0.53 to 38.89 ± 4.81 x 10^{-14} cm^2/s for silicone loaded with 10 and 50 % drug respectively). However, the obtained *D* values were still much lower than those observed upon addition of different types and amounts of PEG (Figure 3.3). This can at least partially be explained by the higher water-solubility of PEG compared to dexamethasone.

It has to be pointed out that these "apparent" diffusion coefficients do not depend on the system geometry and dimensions and can, thus, be directly compared between films, cylinders, spheres and any other geometry of a drug delivery system, and this for arbitrary dimensions.

3.1.4. Theoretical predictions for cylindrical extrudates

Importantly, the knowledge of the dependence of the "apparent" drug diffusion coefficient of dexamethasone on the type of silicone, type and amount of optionally added PEG and initial drug loading can be used to *theoretically predict* the impact of the systems' composition on the resulting drug release kinetics from arbitrarily sized and shaped silicone matrices. For instance, the diffusion coefficients of the drug determined with polymeric films (*D*) can be used to predict drug release from cylinders of varying dimensions. The dashed curves in Figure 3.12 show some examples for this type of *in-silico* simulations. In these cases, dexamethasone release from cylindrical extrudates based on different types of silicones, optionally exhibiting different dimensions, was theoretically predicted. In all cases, the drug loading was 10 % and the systems were PEG-free. The extrudates in Figures 3.12a and b were 0.24 cm in diameter and 2.3 cm in length. They were based on MED-4735 (a) or MED-4055 (b), respectively. The extrudates in Figures 3.12c were 0.20 cm in diameter and 3.2 cm in length, and based on MED-4065. The respective analytical solution of Fick's

second law of diffusion for cylindrical geometry (considering the same initial and boundary conditions as those described above for the derivation of Eq. 1, which is valid for thin films) is as follows (136,138):

$$\frac{M_t}{M_\infty} = 1 - \frac{32}{\pi^2} \cdot \sum_{n=1}^{\infty} \frac{1}{q_n^2} \cdot \exp\left(-\frac{q_n^2}{R^2} \cdot D \cdot t\right) \cdot \sum_{p=0}^{\infty} \frac{1}{(2 \cdot p + 1)^2} \cdot \exp\left(-\frac{(2 \cdot p + 1)^2 \cdot \pi^2}{H^2} \cdot D \cdot t\right) \quad (2)$$

where M_t and M_∞ represent the absolute cumulative amounts of dexamethasone released at time t and infinite time, respectively; q_n are the roots of the Bessel function of the first kind of zero order $[J_0(q_n)=0]$; R and H denote the radius and height of the cylinder.
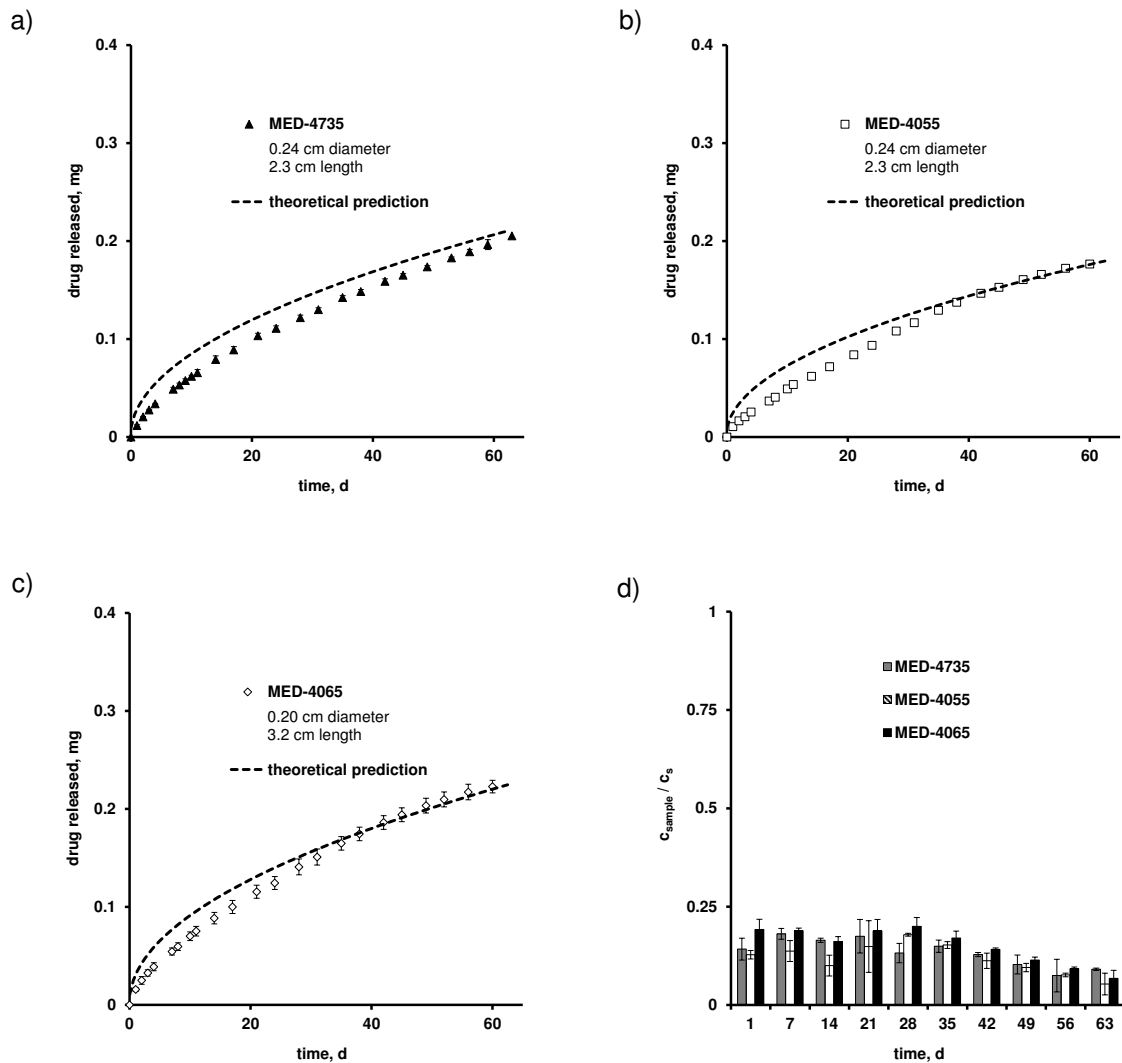

Figure 3.12. Theoretical predictions (dashed curves, Eq. 2) and independent experiments (symbols): Dexamethasone release from cylindrical extrudates (10 % drug loading, no PEG) based on: a) MED-4735, b) MED-4055, c) MED-4065, and d) degree of sample saturation. The systems' dimensions are indicated in the diagrams.

The dashed curves in Figure 3.12 show the theoretical predictions made with Eq. 2, using the "apparent" dexamethasone diffusion coefficients determined with thin films. As it can be seen, the impact of the variations in the extrudates' dimensions and type of silicone on drug release was only minor. This is very interesting information when optimizing this type of controlled release dosage forms: Instead of performing long lasting release experiments, this knowledge becomes available within a few seconds (using a standard personal computer). In order to evaluate the reliability of these theoretical predictions, the respective cylinders were prepared in reality and the resulting dexamethasone release kinetics measured in practice (symbols in Figure 3.12). As it can be seen, good agreement between the *theoretical predictions* and *independent experiments* was observed in all cases. This demonstrates: (i) the reliability of the theoretical predictions, (ii) the potential practical benefit of such *in-silico* simulations to facilitate product optimization (which can for example avoid series of time-consuming and cost-intensive trial-and-error studies), and (iii) the fact that diffusional mass transport seems to be also the dominant mass transport mechanism in cylindrical extrudates of the same composition.

The knowledge presented in this chapter was used to adjust the drug release from liquid silicone rubber to prepare miniaturized Ear Cube implants that will be presented in the next section. The silicone LSR 5 was chosen to prepare those implants because of its relatively low viscosity and, thus, good injectability even at higher drug loadings (compared to the other silicones that were discussed in the present chapter). This plays a decisive role because the silicone - drug mixture has to be injected into customized molds. Furthermore, the workability time of silicone LSR 5 is sufficient to prepare the implant: The slow curing at room temperature does not interfere with the mixing, degassing and injection into the mold. Additionally, the drug release rate can easily be adjusted by changing the drug content of the silicone: The absolute drug release rate is increased with higher drug loadings. Overall, silicone LSR 5 provides ideal properties to prepare miniaturized Ear Cube implants loaded with dexamethasone.

3.2.   Ear Cube implants for Controlled Drug Delivery to the Inner Ear

Figure 2.1 shows schematically the design of the novel Ear Cube implants: On the left hand side, a "smaller" Ear Cube is shown, in the middle a "larger" one. The dimensions are indicated in mm. The cartoon on the right hand side illustrates how an Ear Cube can be placed into a hole drilled into (or close to) the oval window. The *cylindrical part* of the Ear Cube assures its fixation in (or close to) the oval window and is partially surrounded by perilymph. The *cuboid* is located in the middle ear. Importantly, the administration of such Ear Cubes is less invasive compared to the placement of intracochlear implants (which are entirely placed into the inner ear). At the same time, they allow for reliable controlled release into the inner ear (since they are fixed at or close to the oval window, in contrast to semi-solid formulations, which are placed without reliable fixation in the middle ear). If needed, a supplementary drop of spontaneously hardening silicone might be added onto the cuboid *in vivo*, to further assure its durable fixation on (or close to) the oval window. Drug transport into the cochlea is expected to occur: 1) through the cylindrical part of the Ear Cube, and 2) upon partitioning from the cuboid into the oval window, followed by diffusion through this membrane.

3.2.1. Physico-chemical key properties of the Ear Cubes

Macroscopic pictures of a "smaller" and a "larger" Ear Cube (loaded with 10 % dexamethasone) are shown in Figure 2.2 (at the bottom on the right hand side). As it can be seen, both implants appear to be homogeneous. The white color can serve as a first indication for the fact that the drug is not molecularly dispersed within the silicone (which is transparent without drug). Scanning electron microscopy pictures of cross-sections of an Ear Cube are shown in Figure 3.13. The scheme on the left hand side illustrates where the cross-sections were made: In the cylindrical parts of the implants. Clearly, tiny crystals are distributed throughout the silicone matrix.

Figure 3.14 shows the DSC thermograms and X-ray diffraction patterns of a drug-free and a drug-loaded Ear Cube (10 % dexamethasone). For reasons of comparison, also dexamethasone powder (as received) was studied. As it can be seen, the latter was crystalline, exhibiting a melting peak at 263 °C and various sharp diffraction peaks. In contrast, drug-free Ear Cubes were X-ray amorphous and did not show any melting peak at 263 °C. Importantly, Ear Cubes loaded with 10 % dexamethasone showed a melting peak at that temperature and X-ray diffraction peaks at the same angles as the reference drug powder. Thus, the tiny crystals visible in the SEM pictures in Figure 3.13 are dexamethasone crystals. Interestingly,

the surfaces below the melting peaks in the DSC thermograms in Figure 3.14a allowed estimating that virtually the entire drug amount in the Ear Cubes is in the crystalline state. Thus, the presence of amorphous dexamethasone or dexamethasone dissolved in the silicone matrix is likely to be negligible. This is consistent with the fact that the glass transition temperature (Tg) of the silicone was not significantly altered upon drug incorporation (being in the range of -120 to -117 °C in drug-free and drug-loaded Ear Cubes).

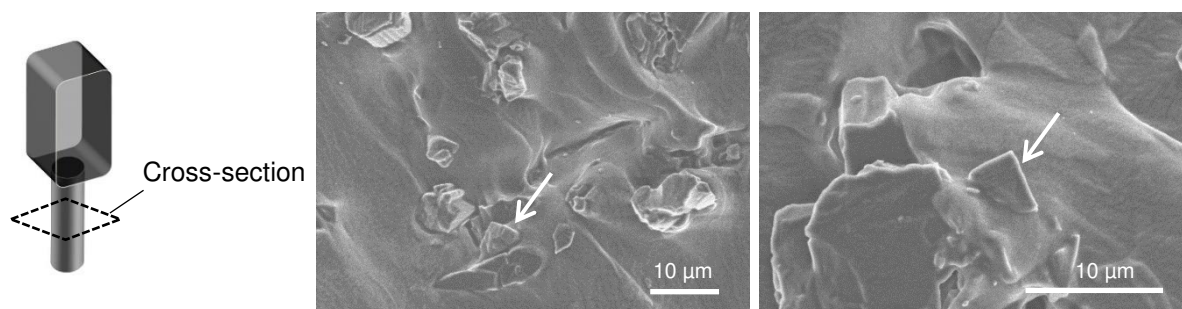**Figure 3.13.** SEM pictures of cross-sections of an Ear Cube implant: The scheme on the left hand side illustrates where the cross-sections were made. The arrows mark tiny crystals. The drug loading was 10 %.
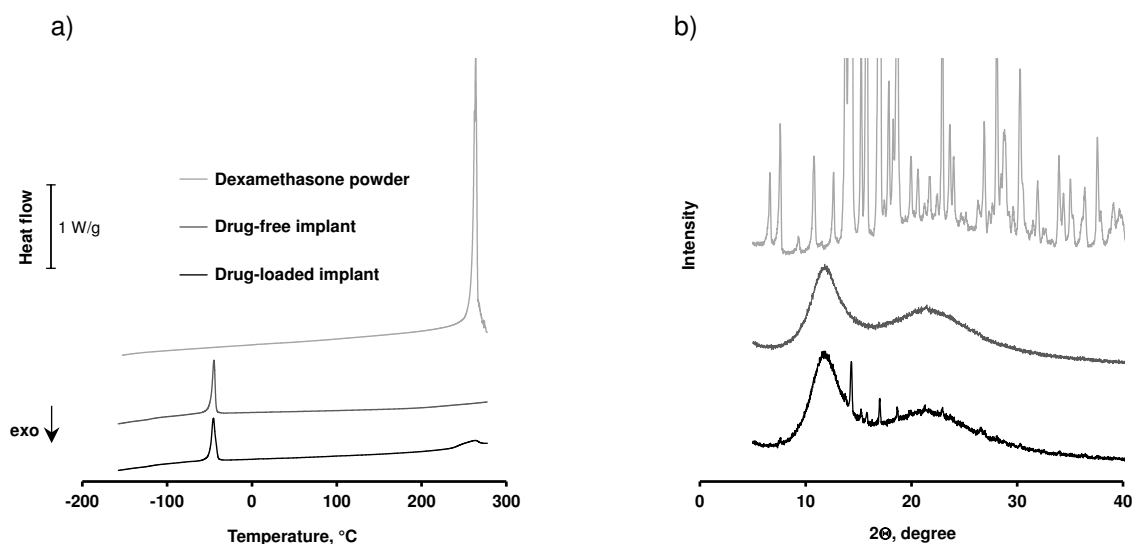

Figure 3.14. a) DSC thermograms, and b) X-ray diffraction patterns of dexamethasone powder (as received), of a drug-free and of a drug-loaded Ear Cube implant (10 % dexamethasone).

3.2.2. Characterization of thin films of identical composition

In order to determine the mobility of the drug in the investigated silicone matrices, thin films based on the same type of silicone (LSR 5) and loaded with different amounts of dexamethasone (10 to 40 %) were prepared and characterized. Also in these cases (and independent of the drug loading), the drug was virtually completely dispersed in the form of tiny crystals within the polymeric matrices, as evidenced for instance by the white (and homogeneous) color of the films (see for instance the picture on the left hand side at the bottom in Figure 2.2). The symbols Figure 3.15a show the experimentally measured release kinetics of dexamethasone (absolute amounts) from the thin silicone films into artificial perilymph at 37 °C. As it can be seen, the absolute release rate increased with increasing drug loading. Based on the hypothesis that dexamethasone diffusion through the polymeric matrix is the dominant mass transport step controlling drug release, the following analytical solution of Fick's second law can be used to quantitatively describe the drug release kinetics (137):

$$\frac{M_t}{M_\infty} = 1 - \frac{8}{\pi^2} \sum_{n=0}^{\infty} \frac{1}{(2n+1)^2} \, exp\left(\frac{-D(2n+1)^2 \pi^2 t}{L^2}\right)$$

(1)

where M_t and M_∞ denote the absolute cumulative amounts of drug released at time t and infinity, respectively; n is a dummy variable, D the "apparent" diffusion coefficient of the drug within the polymeric system; L represents the thickness of the film.

It has to be pointed out that the silicone films did not swell or dissolve/erode to a noteworthy extend during the observation period. This is taken into account by Equation 1 (as well as a homogeneous initial drug distribution and sink conditions in the surrounding bulk fluid). In contrast, the model does not consider potential limited drug solubility effects *within* the silicone matrices. Since dexamethasone is distributed in the form of tiny crystals in the polymer and the amounts of water penetrating into the system upon exposure to the release medium are limited, it can be expected that not all the drug is rapidly dissolved in the matrix. Thus, dissolved and non-dissolved dexamethasone co-exist. Importantly, only dissolved drug is available for diffusion. Hence, when using Equation 1 to describe drug release from the investigated films, the diffusion coefficient (D) is likely to be a "lumped" parameter: It is not the "real" drug diffusivity in the investigated silicone matrices, but the "apparent" diffusion coefficient, which is biased by limited drug solubility effects (121).
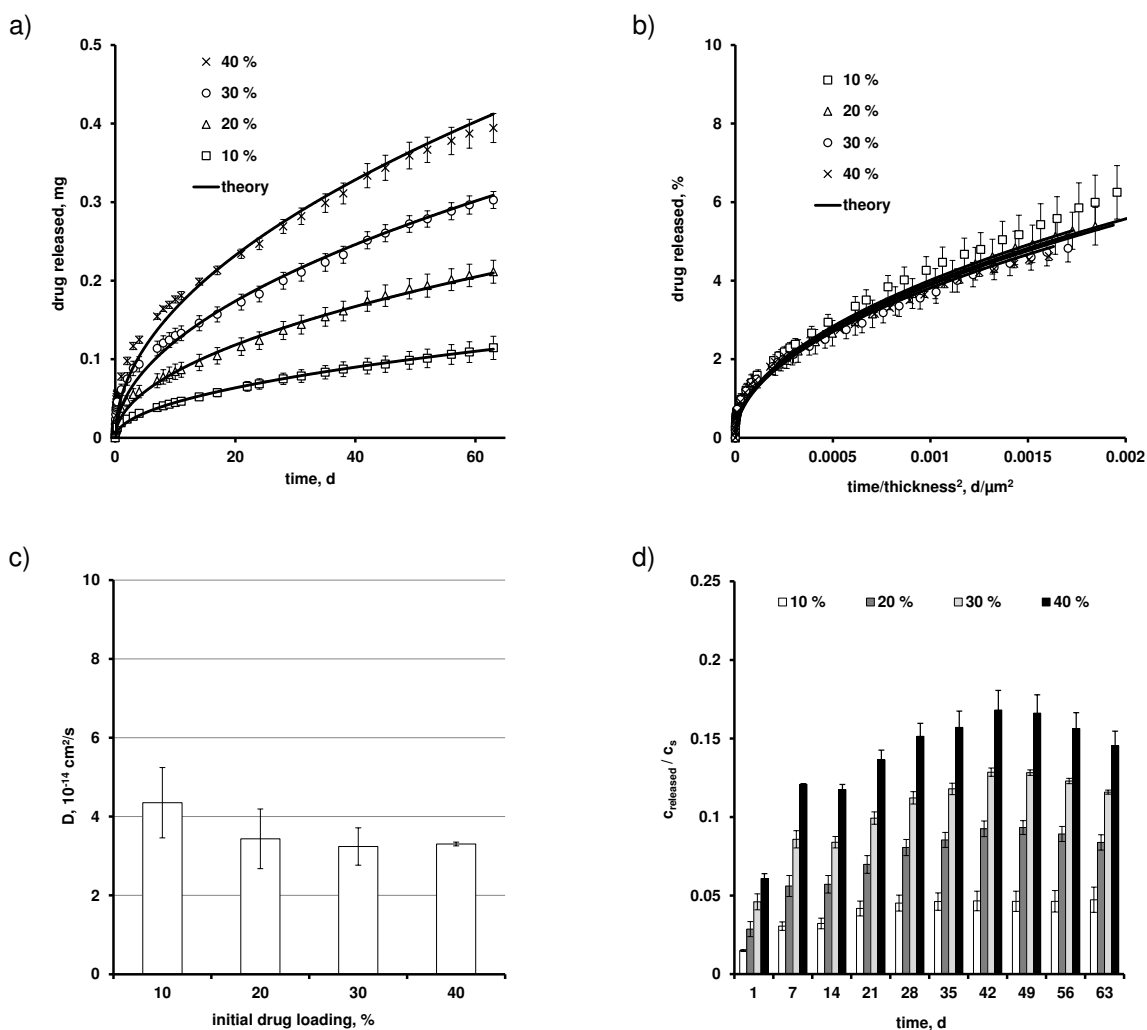
Figure 3.15. Thin films: Impact of the drug loading (indicated in the diagrams) on the: a) absolute drug release rate, b) normalized relative drug release rate, c) "apparent" drug diffusion coefficient in the silicone matrix, and d) degree of saturation of the withdrawn samples. In a) and b), the symbols represent the experimental results, and the curves the fitted theory (Equation 1).

Fitting Equation 1 to the experimentally determined dexamethasone release kinetics from thin silicone films loaded with 10 to 40 % drug resulted in good agreement in all cases (curves and symbols in Figure 3.15a). Thus, drug diffusion through the polymeric matrix seems to play an important role for the control of drug release. This knowledge allows normalizing drug release to the films' thicknesses: It has to be pointed out that arbitrary variations in the films' thickness can affect the resulting drug release kinetics (determining the lengths of the diffusion pathways, which need to be overcome). Consequently, some caution should be paid when comparing the results shown in Figure 3.15a: Not only the variation in the initial drug

loading might affect the release rates, but also unintended variations in the film thickness. Figure 3.15b shows the drug release kinetics, which were normalized to the films' thicknesses (and the total drug amounts). As it can be seen, the *normalized relative* drug release rates were rather similar in all cases (at least in the investigated observation periods): The relative release rate only slightly decreased with increasing initial drug loading (but caution should be paid, since the standard deviations were overlapping).

Based on the fittings shown in Figures 3.15a and 3.15b, the "apparent" diffusion coefficient of dexamethasone in LSR 5 silicone could be determined in a quantitative way for the different drug loadings. As it can be seen in Figure 3.15c, the "apparent" D-values slightly decreased with increasing drug content (again, please note that the standard deviations are overlapping). This can serve as a further indication for the fact that limited drug solubility effects are playing a role in the investigated systems and that the D-values are lumped parameters. Note that *outside* of the silicone matrices (in the well stirred release medium surrounding the films) sink conditions were provided throughout the experiments, as illustrated in Figure 3.15d: The ratios "drug concentration in the withdrawn samples/drug solubility" are plotted as a function of time for the different initial drug loadings.

To be able to determine the diffusion coefficient of dexamethasone in the investigated silicone without the bias of limited drug solubility effects within the polymeric matrix, another type of experiments was conducted: Thin, *drug-free* LSR 5 silicone films were prepared and dexamethasone diffusion through these films was measured in horizontal side-by-side diffusion cells. The donor compartment was filled with artificial perilymph, which was saturated with the drug (and contained undissolved drug excess), whereas the acceptor compartment contained (initially) drug-free perilymph. Sink conditions were provided in the acceptor compartment throughout the experiment. The side-by-side diffusion cells were placed in a horizontal shaker (80 rpm) and kept at 37 °C. Figure 3.16 shows the experimentally determined cumulative amounts of drug that reached the acceptor compartment as a function of time (the blow-up zooms on early time points). As it can be seen, a straight line was observed (after a short lag time), indicating that steady state conditions were rapidly reached: The donor compartment remained saturated, the acceptor compartment provided sink conditions, and the films did not swell or dissolve/erode to a noteworthy extent.

Under these conditions, the following equation can be used to describe drug transport through the silicone films:

$$M_t = \frac{A \cdot D \cdot K \cdot C_s}{L} \cdot t \tag{3}$$

where M_t is the cumulative amount of drug transported at time t; A is the surface area of film available for diffusion in the diffusion cell; D is the diffusion coefficient of the drug within the film; K is the partition coefficient of the drug between the film and the bulk fluid; c_s denotes the solubility of the drug in the bulk fluid, and L the thickness of the film.

Importantly, the slope of the straight line in Figure 3.16 allows determining the product "drug diffusivity x partition coefficient". In the present case, D x $K = 2.3 \pm 0.2$ x 10^{-10} was found.
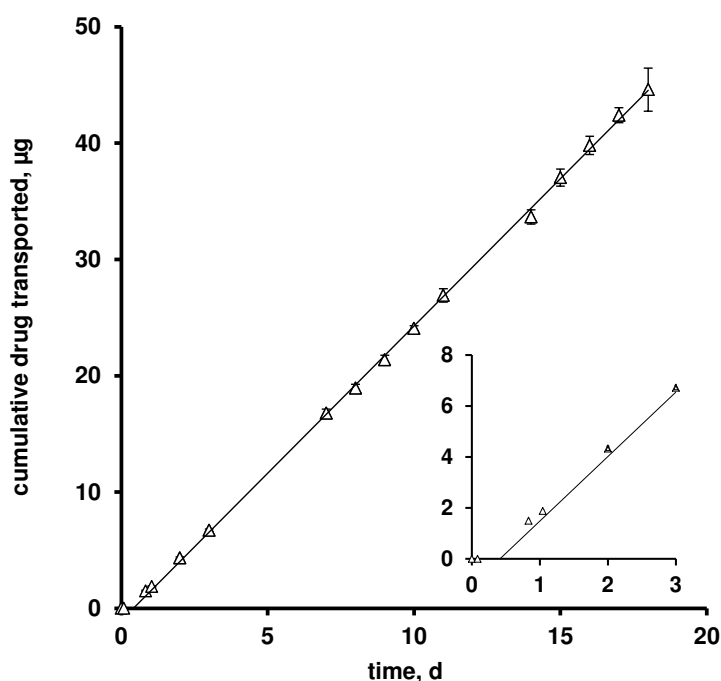

Figure 3.16. Side-by-side diffusion cells: Dexamethasone transport through thin (initially drug-free) silicone films. The blow-up zooms on early time points.

Furthermore, the prolongation of the straight line allowed determining its intersection with the time-axis, which was found to be at $t = 0.41$ d.

Importantly, this value (together with the film's thickness) allows calculating the diffusion coefficient of the drug in the polymeric matrix without the bias of limited drug solubility effects, as follows:

$$D = \frac{L^2}{6 \cdot t_{lag}} \qquad (4)$$

where D is the diffusion coefficient of the drug within the film; L is the thickness of the film, and t_{lag} is the lag time.

In the present case, the diffusivity of dexamethasone in LSR 5 silicone was found to be equal to $1.9 \pm 0.1 \times 10^{-9}$ cm²/s. This is a significantly higher value compared to the "lumped" drug diffusivities determined by fitting Equation 1 to the experimentally determined drug release kinetics from thin films (Figure 3.15). The difference can mainly be attributed to the limited amounts of water present in the silicone films and the limited solubility of the drug. This should be kept in mind when using such "lumped" parameters. On the other hand, the determined "lumped" diffusivities much better take into the account the conditions in drug-loaded silicone matrices (e.g., implants) compared to the "more realistic" drug diffusion coefficient determined with drug-free films: For instance, the impact of the initial drug loading on the "apparent" drug mobility in the polymeric matrix is not considered when conducting side-by-side diffusion cell experiments with drug-free films. Ideally, both types of experiments and appropriate theories should be conducted/applied (or the drug solubility *within* the silicone matrix *during* drug release should be known). In any case, all assumptions a specific mathematical model is based on, should be considered. And caution should be paid, if certain processes are "lumped", or not taken into account. From a practical point of view, it might not harm if "lumped" parameters are used to estimate the impact of formulation parameters on drug release. In contrast, it might reduce the workload, since the knowledge of certain parameters (e.g. the drug solubility *within* the polymeric matrix *during* drug release) is not mandatory.

3.2.3. Drug release from Ear Cubes

Importantly, knowing the "apparent" drug diffusion coefficient of dexamethasone in the investigated silicone matrices, the resulting drug release rates from Ear Cubes can be

theoretically predicted. In the present case, the "apparent" dexamethasone diffusivity in LSR 5 silicone matrices containing 10 to 30 % drug was used to predict the release rates from "smaller" and "larger" Ear Cubes (Figure 2.1) (note that implants loaded with 40 % dexamethasone were difficult to prepare, due to the high viscosity of the "drug-silicone preparation kit" blend). Since only the very early drug release phases were experimentally measured in this study (< 1 % of the total drug amount was released during the first 2 months), the applied theory only considered dexamethasone release from the *cylindrical parts* of the Ear Cubes (highlighted in the schemes in Figure 3.17). Two different equations were applied:

1) An analytical solution of Fick's law of diffusion considering dexamethasone release through all surfaces of the cylinders (scheme on the left hand side of Figure 3.17) (137):

$$\frac{M_t}{M_\infty} = 1 - \frac{32}{\pi^2} \cdot \sum_{n=1}^{\infty} \frac{1}{q_n^2} \cdot \exp\left(-\frac{q_n^2}{R^2} \cdot D \cdot t\right) \cdot \sum_{p=0}^{\infty} \frac{1}{(2 \cdot p + 1)^2} \cdot \exp\left(-\frac{(2 \cdot p + 1)^2 \cdot \pi^2}{H^2} \cdot D \cdot t\right) \tag{2}$$

where M_t and M_∞ represent the absolute cumulative amounts of dexamethasone released at time t and infinite time, respectively; n and q denote dummy variables; q_n are the roots of the Bessel function of the first kind of zero order [$J0(q_n)=0$]; R and H denote the radius and height of the cylinder.

2) An analytical solution of Fick's law of diffusion considering dexamethasone release only through the circular surface at the bottom the cylinders (scheme on the right hand side of Figure 3.17) (137):

$$\frac{M_t}{M_\infty} = 1 - \sum_{n=0}^{\infty} \frac{8}{(2 \cdot n + 1)^2 \cdot \pi^2} \cdot \exp\left(-\frac{(2 \cdot n + 1)^2 \cdot \pi^2}{4 \cdot H^2} \cdot D \cdot t\right) \tag{5}$$

where M_t and M_∞ represent the absolute cumulative amounts of drug released at time t, and infinite time, respectively; n is a dummy variable, and H the height of the cylinder.

Equation 2 likely *over*estimates drug release, because the upper circular surface of the cylinders is not available for drug release and it is uncertain whether all the other cylinder surfaces are fully wetted and available for drug release. On the other hand side, Equation 5 likely *under*estimates dexamethasone release, since drug release is probably not fully

restricted to only the bottom circular surface of the cylinders. A more comprehensive mathematical model could be used to more precisely quantify drug release from the given geometries, but the reliability of such predictions remains questionable, because of the uncertainty which parts of the surfaces are effectively wetted. In this study, the aim was only to roughly estimate the amounts of drug released from the Ear Cubes at "very early" time points.
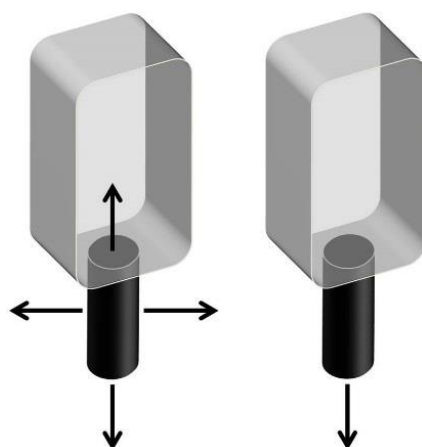
Figure 3.17. Schematic presentation of the geometries and directions of drug diffusion considered in Equation 2 (left hand side) and Equation 5 (right hand side) in order to estimate dexamethasone release from Ear Cubes at very early time points. Details are given in the text.

The curves in Figure 3.18 show the theoretically predicted dexamethasone release kinetics from a "smaller" and a "larger" Ear Cube, loaded with 10 to 30 % drug. The green/orange/red colors correspond to implants loaded with 10/20/30 % dexamethasone, respectively. The solid curves were calculated using Equation 2 and likely overestimate drug release, while the dashed curves were calculated using Equation 5 and likely underestimate drug release (for the reasons discussed above). The left column shows the relative drug release rates, the middle column the absolute release rates. As it can be seen, the predicted *relative* drug release rates decrease with increasing initial dexamethasone loading, whereas the predicted *absolute* drug release rates increase with increasing initial drug content. The first tendency can be explained by the decrease in the "apparent" drug diffusivity with increasing dexamethasone loading (Figure 3.15c) (due to the increasing importance of limited drug solubility effects). The second tendency is due to the increasing drug concentration gradients (since all drug is considered to be rapidly dissolved upon exposure to the release medium), and the increasing matrix porosity upon drug exhaust with increasing initial drug content. If these rough estimations are correct, the cumulative amounts of dexamethasone released from the Ear Cubes should be in the range of 0.06 to 1.45 %, or 0.046 to 2.35 µg after 2 months.

Thus, drug release can be expected to be controlled during several years *in vivo* (which can be highly desirable, avoiding additional surgeries). When comparing the "smaller" and "larger" Ear Cubes (top versus bottom row in Figure 3.18), it becomes evident that the (relative and absolute) dexamethasone release rates are expected to be higher from "smaller" Ear Cubes, irrespective of the initial drug loading. This is due to the fact that the "smaller" Ear Cubes have a longer cylindrical part than the "larger" Ear Cubes (Figure 2.1), and that drug release at these early time points is considered to be limited to this part of the implants.
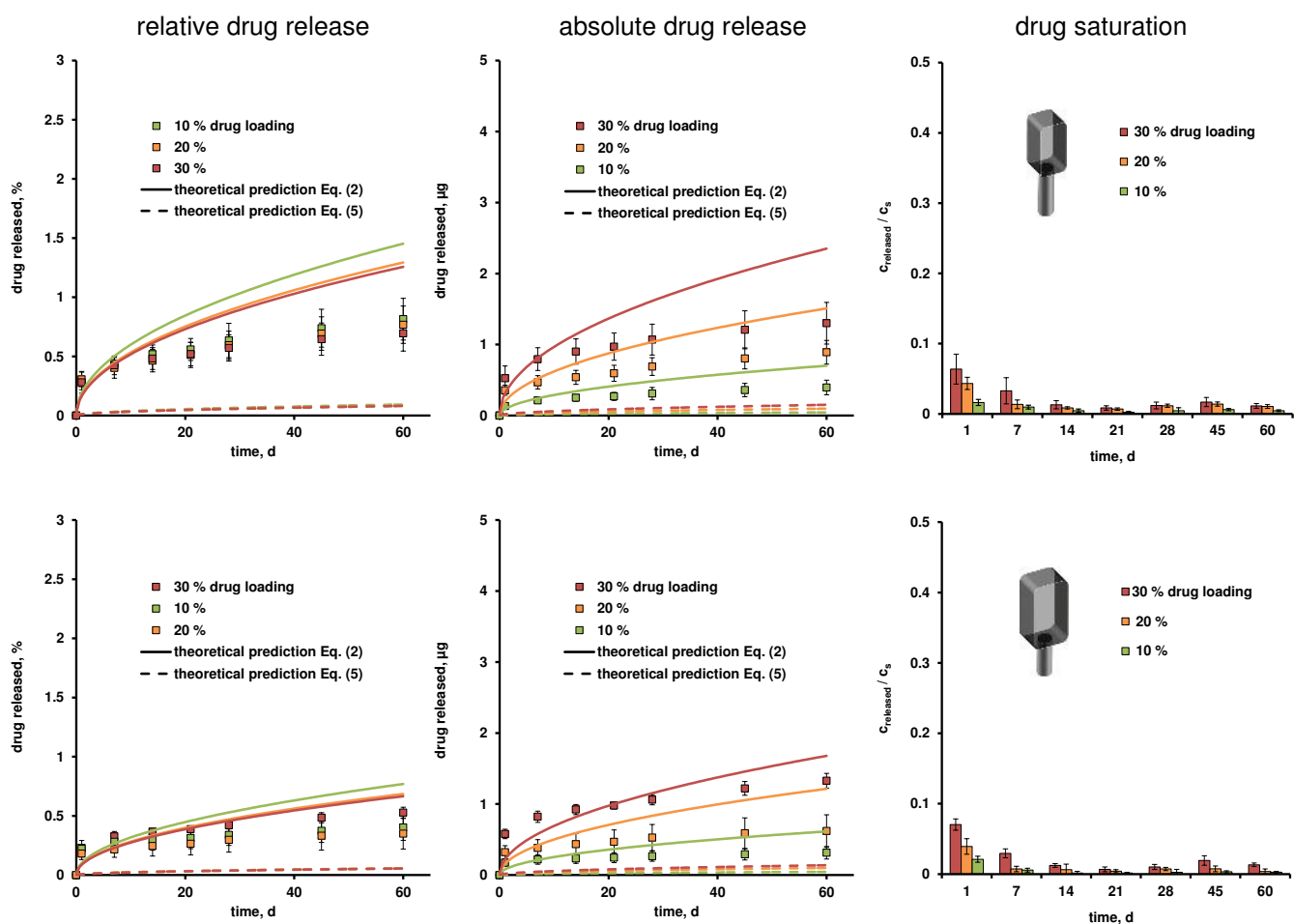
Figure 3.18. Dexamethasone release from Ear Cubes (top row: smaller Ear Cubes, bottom row: larger Ear Cubes): Impact of the initial drug loading (indicated in the diagrams). The relative and absolute release rates as well as the degree of saturation of the withdrawn samples are illustrated (left, middle and right column). The symbols represent the experimental results. The solid curves indicate the theoretically predicted drug release kinetics using Equation 2, while the dashed curves represent the theoretically predicted release kinetics using Equation 5. The drug loading was 10, 20 and 30 % (corresponding to green, orange and red symbols, curves and bars).

In order to evaluate the reliability of the theoretical predictions, "smaller" and "larger" Ear Cubes loaded with 10 to 30 % dexamethasone were prepared in reality and drug release was measured using the experimental setup illustrated in Figure 2.3. The green, orange and red symbols in Figure 3.18 show the respective experimental results. As it can be seen, most of the independent experimental results were located within the theoretically predicted ranges. Thus, the basic hypothesis that dexamethasone release is predominantly controlled by diffusion through the silicone matrices (and limited drug solubility effects) seems to be realistic. The expected impact of the initial drug loading on the resulting *absolute* drug release rates was confirmed for both types of Ear Cubes, while the differences with respect to the *relative* drug release rates were within the orders of magnitude of the experimental errors. It has to be pointed out that *in vivo* the drug can also be expected to diffuse from the cuboid into the oval window and cross this membrane. This mass transport way was not simulated in the experimental set-up. Thus, *in vivo* drug release is likely to be somewhat faster, but is still likely to be sustained during several years. The right column in Figure 3.18 shows the experimentally measured degree of drug saturation in the withdrawn samples, as a function of time and initial drug loading. As it can be seen, sink conditions were provided, irrespective of the initial drug loading, sampling time point and type of Ear Cube.

3.2.4. Absence of Ear Cube swelling

Another very important practical aspect for the newly proposed Ear Cubes is their swelling behavior upon exposure to aqueous media. Significant swelling could cause tissue irritation/damage due to the tiny dimensions of the cochlea, oval window and middle ear. In addition, the anchorage in (or close to) the oval window might be compromised. For these reasons, potential changes in the Ear Cubes' dimensions were monitored upon exposure to artificial perilymph at 37 °C. Figure 3.19 shows macroscopic pictures of a "smaller" (top row) and a "larger" (bottom row) Ear Cube before exposure to the release medium and after 14 and 60 d, respectively. Also, the two diagrams at the bottom of Figure 3.19 illustrate the dynamic changes in the Ear Cubes' dimensions as a function of time. Clearly, the geometries and sizes of the Ear Cubes remained about constant: No noteworthy swelling was observed. This is very important from a practical point of view.
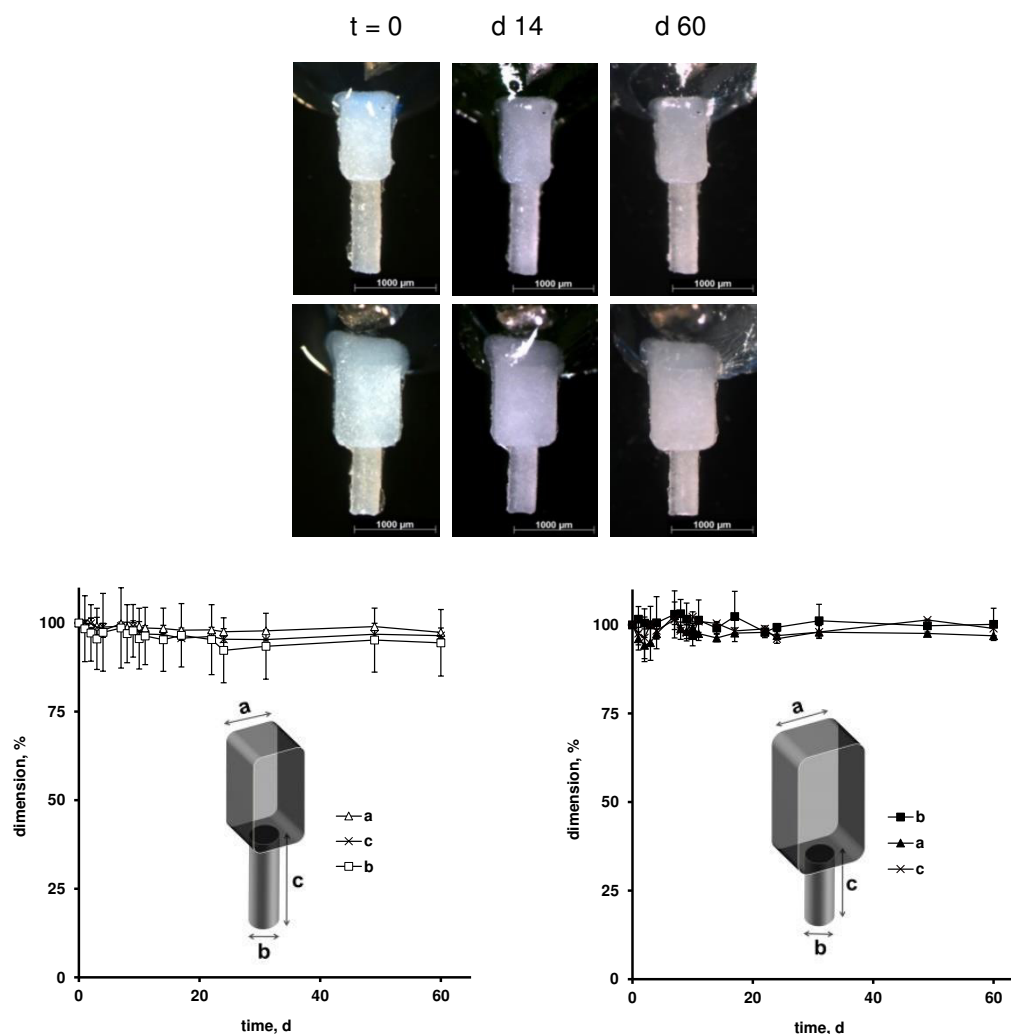
Figure 3.19. Absence of Ear Cube swelling: Macroscopic pictures (top row: "smaller" Ear Cubes, bottom row: "larger" Ear Cubes), and "dimensions versus time" plots. The initial drug loading was 10 %. Details are given in the text.

In the next chapter, a new type of in situ forming implant releasing dexamethasone beside the stapes' footplate will be presented. This in situ formed implant is inspired by in situ forming gels that are already used in clinical trials to deliver drugs to the inner ear (as described in section 1.3.2.1 Intratympanic drug delivery). The system of an in situ forming silicone-based implant is promising because it can easily be injected into the middle ear cavity and is curing directly in vivo. Another advantage is that the shape of the implant adapts perfectly to the patient's individual anatomy. Patients could benefit from this adaptable system since the anatomy of the middle ear cavity can differ to a big extend from one patient to another.

To prepare this new in situ forming implant, another type of silicone has to be tested. The silicone should be easily injectable on one hand. On the other hand, the polymer has to cure relatively fast in vivo because otherwise it could be eliminated through the Eustachian tube. To increase the drug release from the implant, the hydrophilic excipient PEG 400 was added to the formulation.

.

3.3.   Trans-Oval-Window Implants: Extended Dexamethasone Release

3.3.1. Results

3.3.1.1.   In vitro studies

Dexamethasone Release From Silicone-based Films

As it can be seen (Figure 3.20), the drug release rate decreased with time from thin films based on Kwik-Cast silicone. Drug release was prolonged and continuous during the observation period (30 days). Importantly, drug saturation effects were not affecting dexamethasone release to a noteworthy extent.
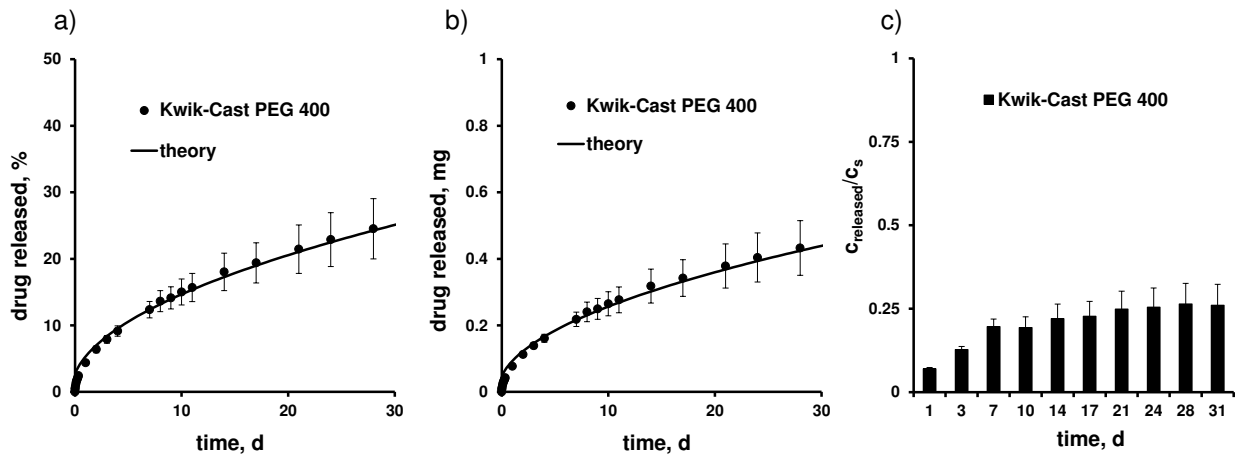
Figure 3.20. Dexamethasone release from thin films based on Kwik-Cast silicone, loaded with 10 % drug and 5 % PEG 400 in 10 mL artificial perilymph: a) relative drug release, b) absolute drug release, and c) degree of drug saturation of the withdrawn samples. The symbols represent the experimental results, the curves the fitted theory (Equation 1).

Fitting the following analytical solution of Fick's second law of diffusion (137) to the experimental results resulted in good agreement between theory (curves) and experiments (symbols) (Figure 3.20a and b):

$$\frac{M_t}{M_\infty} = 1 - \frac{8}{\pi^2} \sum_{n=0}^{\infty} \frac{1}{(2n+1)^2} \, exp\left(\frac{-D(2n+1)^2 \pi^2 t}{L^2} \right) \tag{1}$$

where M_t and M_∞ denote the absolute cumulative amounts of drug released at time t and infinity, respectively; n is a dummy variable, D the "apparent" diffusion coefficient of the drug within the polymeric system; L represents the thickness of the film.

Thus, drug diffusion through the polymeric matrix seems to play a major role for the control of dexamethasone release. Based on these calculations, the following apparent dexamethasone diffusion coefficient in the investigated Kwik-Cast silicone-PEG matrix could be determined: $D = 1.2 \times 10^{-11}$ cm^2/s.

Dexamethasone Release From Silicone-based Implants

As in the case of the thin films, the drug release rate from Silicone-based implants decreased with time and sink conditions were maintained during the observation period (Figure 3.21). It has to be pointed out that dexamethasone release was much slower from the implants compared to the films (Figure 3.21 vs. Figure 3.20). This can at least partially be attributed to the much lower surface area exposed to the release medium in relation to the total system's volume.
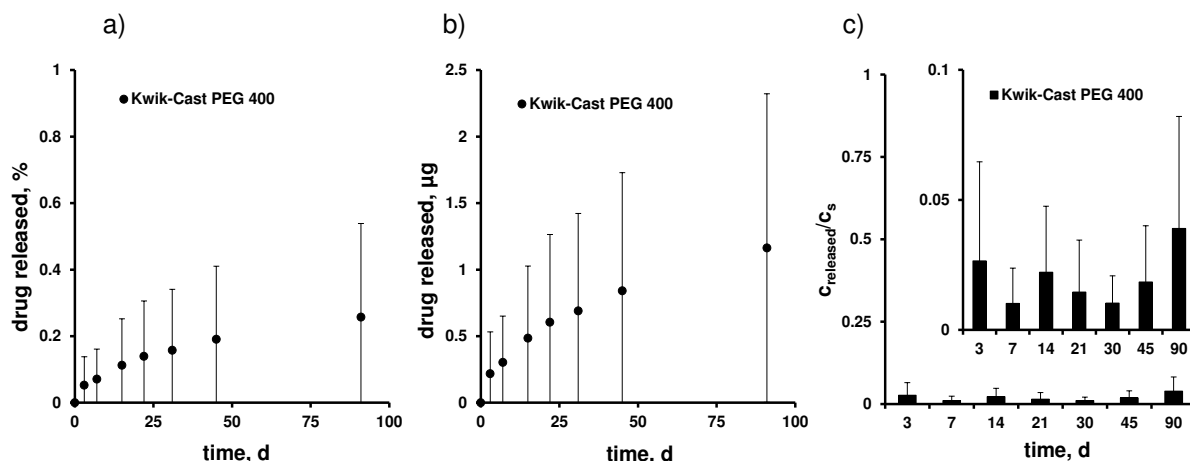
Figure 3.21. Dexamethasone release from miniaturized implants loaded with 10 % drug and 5 % PEG 400 into 100 mL artificial perilymph: a) Relative drug release, b) absolute drug release, and c) degree of drug saturation of the withdrawn samples.

3.3.1.2. In vivo studies

Implantation

The chosen silicone for implantation was Kwik-Cast, loaded with 10 % dexamethasone and 5 % PEG 400. Drug crystals can be observed by Confocal Laser Scanning Microscopy (CLSM). The drug was dispersed in the form of small particles in the matrix and was not completely dissolved (Figure 3.22). Twelve gerbils were implanted bilaterally by a submandibular approach.
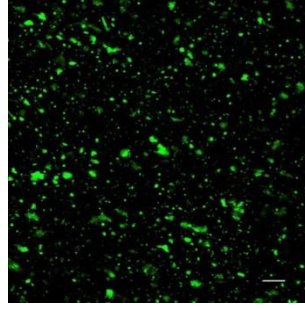
Figure 3.22. Thin silicone film loaded with 10% dexamethasone and 5% PEG 400 observed with CLSM (scale bar =100 µm).

Confocal Microscopy

Confocal imaging allowed a morphometric and threedimensional analysis of the whole cochlea. DAPI and Phalloidin enabled a fluorescent labeling of the nucleus and the cytoskeleton of the cell, respectively.

Because the structure of the cochlea has been preserved during the immunohistochemical treatment, the entire architecture with the three turns of the cochlea can be clearly seen (Figure 3.23A).
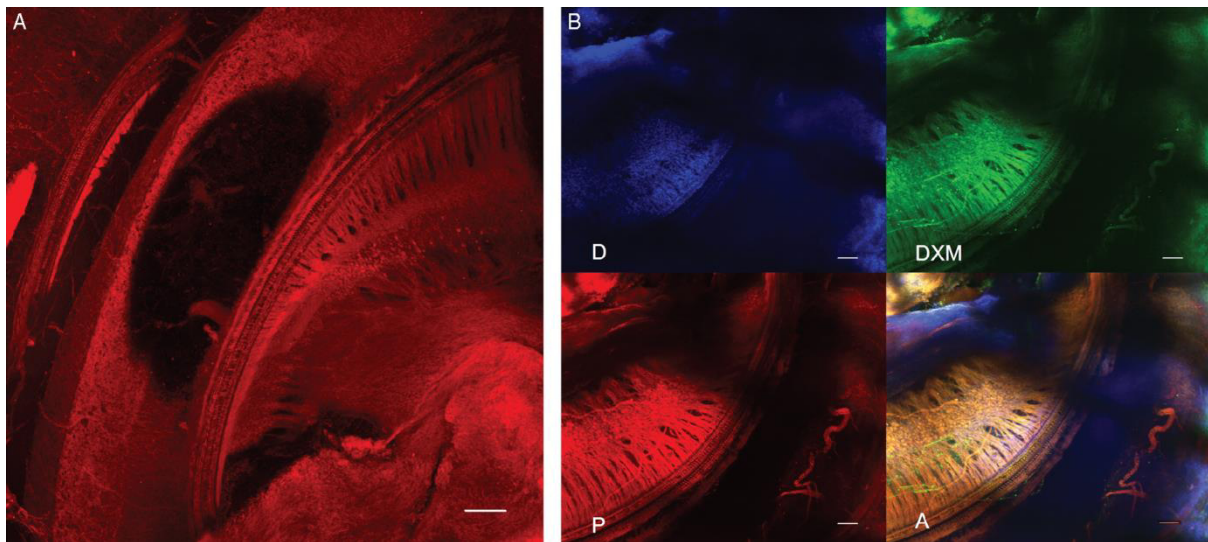
Figure 3.23. A) Maximum intensity projection of a whole cochlea after implantation with CLSM: Maximum intensity projection of a medial view upon treatment with Phalloidin (for actin cytoskeleton labeling). Three turns of the cochlea can be seen: the apical, middle, and basal turn (scale bar = 50 µm, objective x 10). B) Maximum intensity projections of cochlea of gerbils receiving the novel implant: Transapical views of the middle turn of the whole cochlea of animals sacrificed on day 7 by CLSM (objective x 10, scale bar = 50 µm). Labeling of cell nuclei with DAPI (D), actin cytoskeleton with phalloidin (P), dexamethasone (DXM). All three labelings are superposed in the fourth picture of each series (A).

By turning the image during the three-dimensional acquisition, the middle turn of cochlea with the three rows of outer hair cells and one row of inner hair cells seemed to be intact after implantation (Figure 3.24).
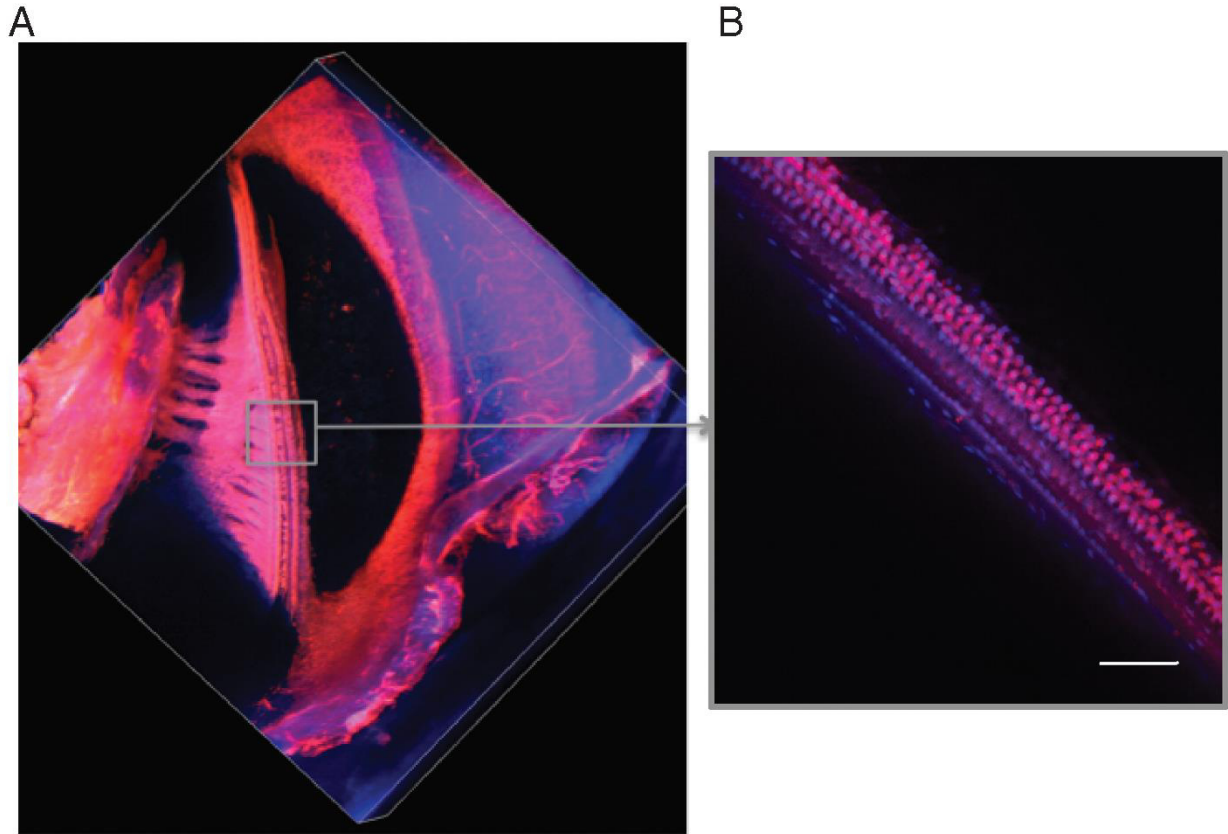
Figure 3.24. Maximum intensity projections. A) Middle turn of a whole cochlea after implantation (medial three-dimensional view) (objective x 10). B) Three rows of outer hair cells and one row of inner hair cells in the middle turn of the cochlea with CLSM (scale bar = 20 µm, objective x 20). The red labeling (with phalloidin) visualizes actin cytoskeleton, the blue labeling (with DAPI) cell nuclei.

Confocal imaging of cochlea sections enabled to validate the specificity of anti-dexamethasone immunolabeling compared with controls wherein the green fluorescence was absent (Figure 3.25).
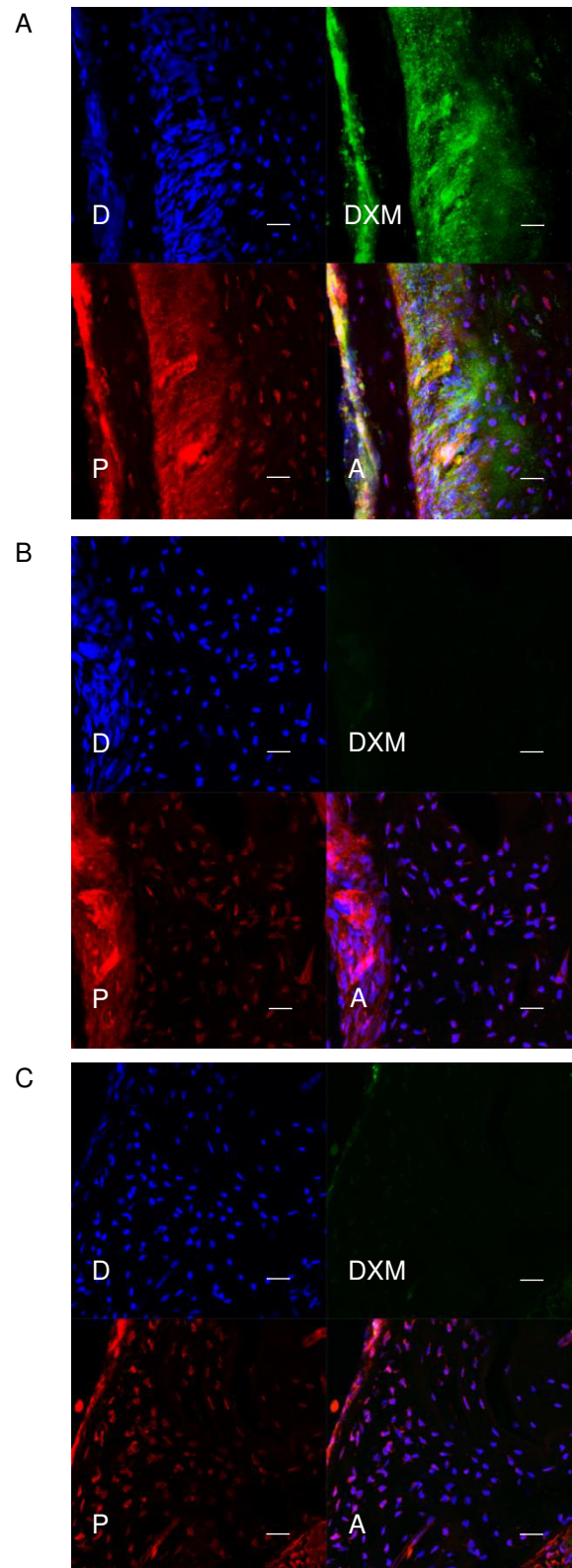
Figure 3.25. Cochlea sections taken A) after intratympanic injection of a solution of dexamethasone, immunolabeling with primary and secondary antibodies, B) after intratympanic injection of a solution of dexamethasone, immunolabeling with secondary antibody only, and C) on untreated ear, immunolabeling with primary and secondary antibodies (scale bar = 20 µm, objective x 10). Labeling of cell nuclei with DAPI (D), actin cytoskeleton with phalloidin (P), dexamethasone (DXM). All three labelings are superposed in the fourth picture of each series (A).

Imaging of the whole cochlea, confirmed the absence of autofluorescence or nonspecific staining (Figure 3.26).
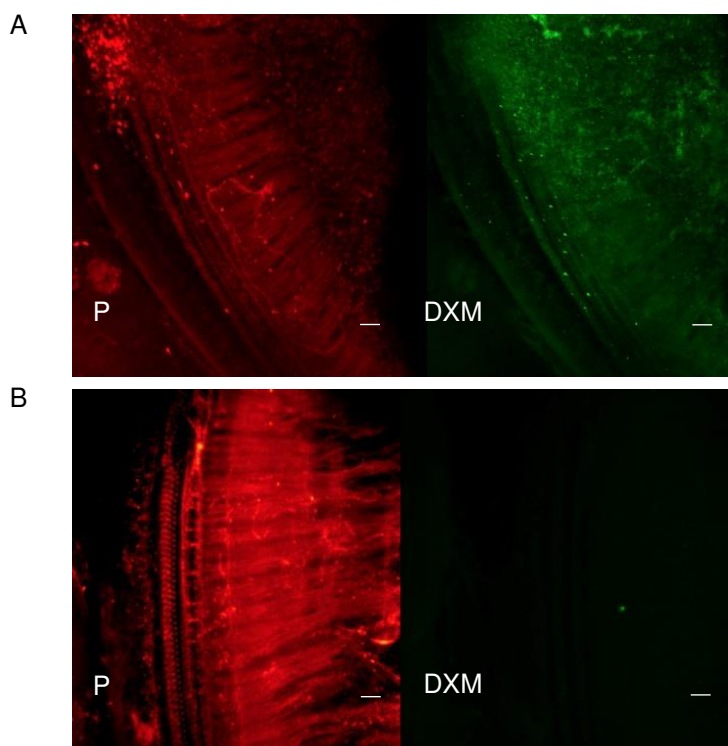
Figure 3.26. Transapical view of the middle turn of the cochlea in CLSM. A) Cochlea after intratympanic injection of a solution, and B) Untreated cochlea. In both cases labeling with primary and secondary antibodies (scale bar = 20 µm, objective x 10). Labeling of actin cytoskeleton with phalloidin (P) and dexamethasone (DXM).

Images of whole cochleae also allowed the detection of specific anti-dexamethasone fluorescence in the hair cells. Interestingly, this immunolabeling was detected in hair cells of all implanted cochleae (protocol as described in the section Immunohistochemistry). The staining intensity reached a climax for the cochlea collected at day 7 postimplantation (Figures 3.23B and 3.27B). For these experiments, the same parameters for the laser intensity and the voltage of the detector were used to compare intensity between the different conditions.

Surprisingly, the anti-dexamethasone labeling could be already detected inside the hair cells 20 min postimplantation and even at day 30 the labeling was still observed (Figure 3.27). The detection at very early time points might be attributable to rapid dexamethasone release from the (still liquid) formulations right upon injection and/or drug diffusion occurring during sample preparation.

Specific fluorescence imaging of the organ of Corti allowed to localize the immunostaining directly inside the hair cells (Figure 3.28A–C). Anti-dexamethasone labeling was present mainly in the cell body and not in the cell nucleus (Figure 3.28C–E).
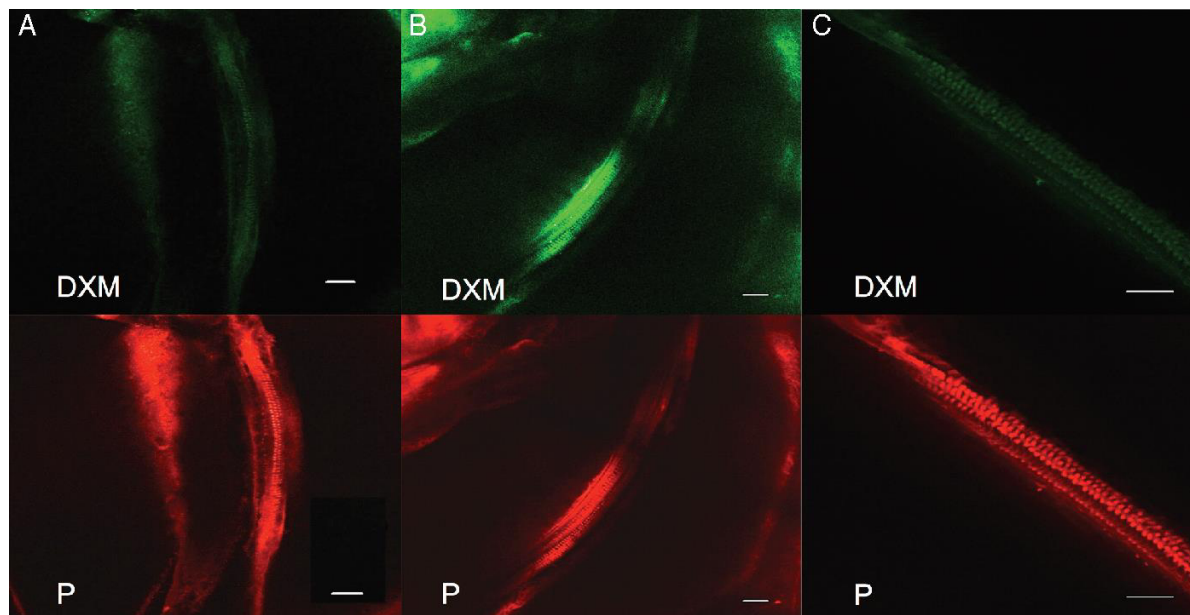
Figure 3.27. Snapshot of a transapical view of the middle turn of the whole cochlea by CLSM. Cochlea collected at A) day 0, B) day 7, and C) day 30, after implantation (scale bar = 50 µm, objective x 10). Labeling of dexamethasone (DXM) with anti-dexamethasone antibodies and actin cytoskeleton with phalloidin (P).

3.3.2. Discussion

Silicone was chosen as a polymer for its properties of biocompatibility, biodurability, chemical-thermal stability and lack of toxicity. It is already used in many medical applications (139) in humans. Cochlear implantation was especially established as a safe and effective method for the rehabilitation of patients with profound hearing loss (140). Recently, the development of an electrode array, from MED-4735 silicone, with prolonged release of dexamethasone was reported as part of preservation of residual hearing after cochlear implantation (103,104).

Several researchers are interested in the use of resorbable biopolymers for drug release in the round window: gelatin (141), polylactide-co-glycolide (142), chitosan glycerol phosphate (96). The main disadvantage of these polymers is the limited amount of drug that could be incorporated into the matrix and formed to a particular shape (143). In adition, the quick

release and degradation of these matrixes are not suitable for the treatment of chronic pathologies.
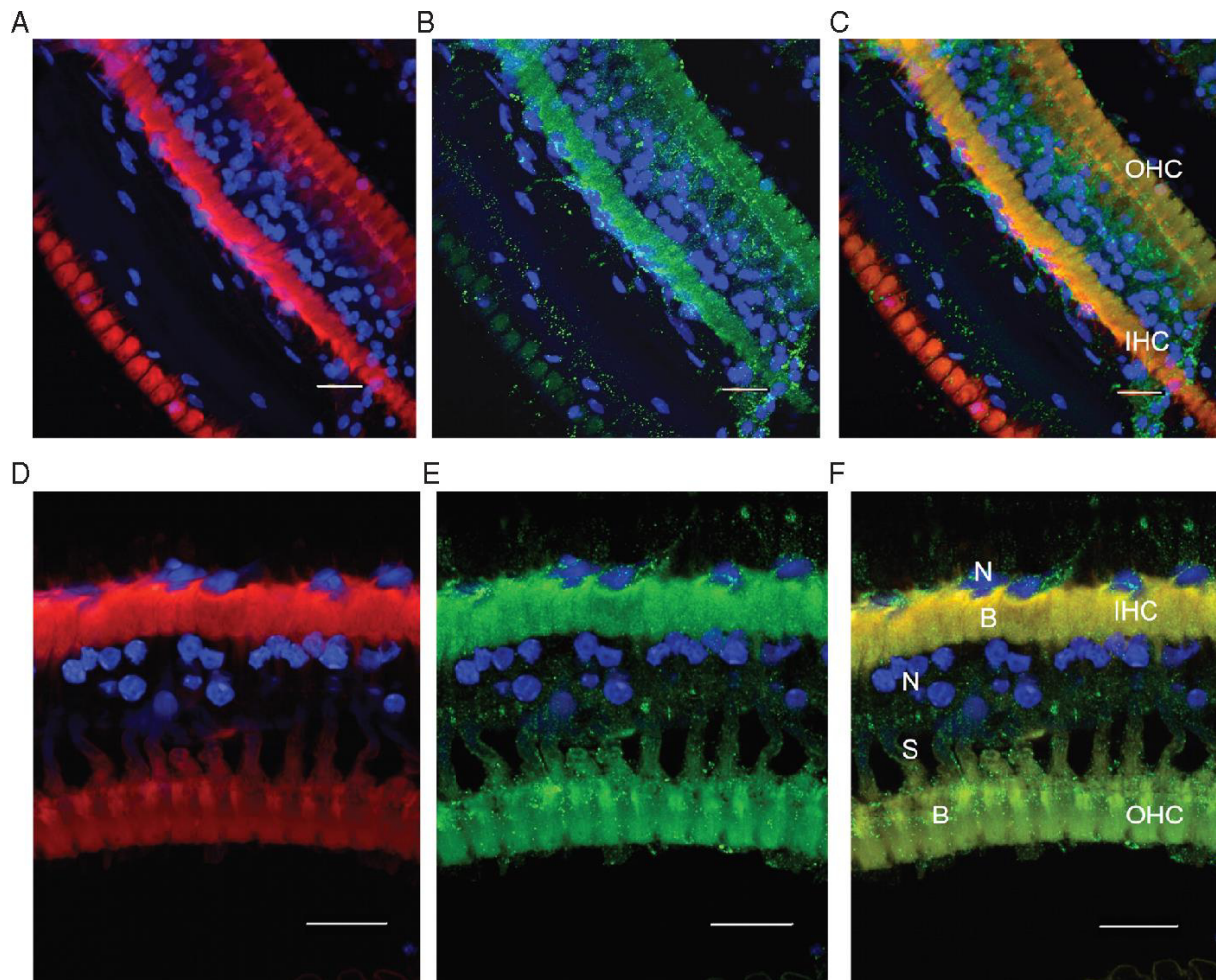
Figure 3.28. Maximum intensity projection of organ of Corti after implantation. View of three rows of outer hair cells (layered) and one row of inner hair cells by CLSM (A, B, C). Location of specific labeling in inner hair cells and outer hair cells (scale bar = 20 µm, objective x 20). Snapshot of organ of Corti after implantation (D, E, F). View of one row of outer hair cells and one row of inner hair cells with CLSM (D, E, F). Visualization of cell bodies, cell nuclei, and stereocils. Location of specific labeling (green) in cell body (scale bar = 20 µm, objective x 63). A and D, Labeling with phalloidin (red) and DAPI (blue); B and E, labeling with anti-DXM antibodies (green) and DAPI (blue); C and F, labeling with phalloidin (red), DAPI (blue), and anti-dexamethasone antibodies (green). N = cell nucleus; B = cell body; S = stereocil; OHC = outer hair cell; IHC = inner hair cell.

The Mongolian gerbil was chosen as experimental model because this animal, commonly used in otologic research, has a superficial auditory bulla and an auditory spectrum similar to humans (144). Indeed, several experimental studies focused on preservation of residual hearing after cochlear implantation (103,145).

Surgery had to be cautious since the stapedial artery passes between the crus of the stapes. One gerbil died from massive bleeding after a stapedial artery injury. In humans, the stapedial artery is an embryonic artery that atrophies normally around the 10th week in utero. Unlike humans, it persists in many animals, particularly rodents including gerbils (146). Given these anatomical animal characteristics, the site of implantation in this study, originally planned on the footplate of stapes, was changed for the lateral side of the oval window.

Carrying out acquisitions of a gerbil cochlea in confocal microscopy was very challenging due to their geometry and complex architecture, the superposition of the structures, the inhomogeneity of the tissues, and the time consuming process of cochlea clarification (147).

The cochlea is one of the densest organs in the human body. The protocol of clarification that has been used (148) turned the entire cochlea transparent. Seven days were required to decalcify the cochlea of the gerbils entirely, versus only 4 days required for the cochlea of mice (147).

Many studies were performed on sectional tissues (149) or on mounted organs of Corti (150). This strategy reduces or suppresses the time needed for clarification but does not allow to preserve the overall cochlear architecture.

In a recent study, the intensity of immunostaining reached a maximum at 1 h, then decreased at 6 and 12 h after corticosteroid intratympanic injection. Additionally, there was a more important uptake of the dexamethasone by the inner hair cells compared to outer hair cells (149).

In this study, the specific dexamethasone labeling was detected in the inner ear at day 0, day 7, and day 30 postimplantation. The labeling was more intense at day 7, this could be in connection with the initially higher release rate of dexamethasone observed in vitro at early time points. The affinity for dexamethasone seemed to be the same for inner hair cells and outer hair cells and there was a main uptake of drug by cell bodies of hair cells.

In the short term, we would like to optimize the creation of implants to make their size reproducible. We will also use acoustic trauma experimental model and auditory brainstem response to evaluate effectiveness of our implants on hearing preservation. In the long term, this new strategy of local treatment could be useful, in humans, in sudden sensorineural hearing loss, tinnitus, autoimmune disease, and ototoxic hearing loss.

4.   Conclusion

Today, the therapy of hearing loss is a challenge due to the vast variety of etiologies that in most of the cases remain unknown. Different therapies are currently under development mainly focusing on local controlled drug delivery to the inner ear. The major difficulties are the small dimensions of the system as well as the sensibility of the inner ear hair cells. Miniaturized implants might provide a suitable therapy for patients suffering from hearing loss. In this thesis, two different types of silicone-based implants, releasing dexamethasone for a prolonged period that can be implanted at the stapes' footplate have been developed and characterized.

In the introduction, the anatomy and physiology of the inner ear as well as its barriers were summarized, including an explanation on the function of the auditory perception and the sense of balance. Subsequently, diseases of the inner ear have been described focusing on hearing loss. Furthermore, different strategies for the treatment of hearing loss have been reviewed describing intratympanic and intracochlear drug delivery approaches.

In the first section of the results, it has been proofed that different formulation parameters, such as the type of silicone, addition of varying amounts and types of PEG as well as the initial drug loading can be used to adjust desired drug mobility in controlled release silicone matrices. Importantly, often diffusional mass transport is decisive for the control of drug release. Thus, the "apparent" diffusion coefficient of the drug within the system can be used to: (i) quantify the effects of the formulation parameters, and (ii) theoretically predict drug release from dosage forms of arbitrary geometry and dimensions. Hence, time-consuming and cost-intensive series of trial-and-error experiments can be replaced by *in-silico* simulations. This is particularly helpful, if long-term drug release (e.g. during several weeks, months or years) is targeted.

This knowledge has been used to prepare silicone-based implants described in the second section: The newly proposed Ear Cubes offer an interesting potential for local controlled drug delivery to the inner ear: They can control drug release during long periods of time, can be securely fixed at (or close to) the oval window and their placement is less invasive compared to intracochlear implants. They could also be placed into tiny holes drilled into the round window.

A second type of silicone-based implants is presented in the third part: A new in situ forming device for local drug delivery to the inner ear using a non-degradable polymeric silicone matrix has been developed. The in vitro study of dexamethasone demonstrated a

continuous and prolonged release from dexamethasone-loaded implants for at least 90 days. After implantation of gerbils near the stapes' footplate, corticosteroid detection inside the hair cells by cochlear confocal microscopy proves the effectiveness of dexamethasone-loaded implants as a targeted strategy for controlled release to the inner ear. This type of implant could also be used as carrier for other therapies.

Future studies should address the *in vivo* efficacy (e.g., reduction of hearing loss due to acoustic trauma) and suitability to delivery other types of drugs than dexamethasone (e.g., gentamicin, adenovirus, eukaryotic vectors).

References

1. WHO | Deafness and hearing loss. 2015 [Internet] [cited-2015-Sep-10]. *http://www.who.int/mediacentre/factsheets/fs300/en/*

2. Blackwell D, Lucas J, Clarke T. Summary health statistics for U.S. adults: National Health Interview Survey, 2012. National Center for Health Statistics, 2014.

3. Vohr B. Overview: Infants and children with hearing loss—part I. Ment. Retard. Dev. Disabil. Res. Rev. 9(2), 62–64, 2003.

4. Zahnert T. The Differential Diagnosis of Hearing Loss. Dtsch. Ärztebl. Int. 108(25), 433–444, 2011.

5. Helfer TM, Jordan NN, Lee RB, Pietrusiak P, Cave K, Schairer K. Noise-Induced Hearing Injury and Comorbidities Among Postdeployment U.S. Army Soldiers: April 2003–June 2009. Am. J. Audiol. 20(1), 1-33, 2011.

6. Ylikoski ME, Ylikoski JS. Hearing loss and handicap of professional soldiers exposed to gunfire noise. Scand J. Work Environ. Health. 20(2), 93–100, 1994.

7. CDC | Severe hearing impairment among military veterans--United States, 2010. MMWR Morb. Mortal Wkly. Rep. 60(28), 955–958, 2011.

8. CDC | Occupationally-Induced Hearing Loss. 2010. NIOSH Publications and Products. [Internet] [cited-2015-Sep-11]. *http://www.cdc.gov/niosh/docs/2010-136/*

9. CDC | Table 6. Incidence rates and numbers of nonfatal occupational illnesses by major industry sector, category of illness, and ownership. 2013 [Internet] [cited-2015-Sep-11]. *http://www.bls.gov/news.release/osh.t06.htm*

10. WHO | 1.1 billion people at risk of hearing loss. 2015. [Internet] [cited-2015-Sep-10]. *http://www.who.int/mediacentre/news/releases/2015/ear-care/en/*

11. Derebery MJ, Vermiglio A, Berliner KI, Potthoff M, Holguin K. Facing the music: pre- and postconcert assessment of hearing in teenagers. Otol. Neurotol. 33(7), 1136–1141, 2012.

12. Olusanya BO, Neumann KJ, Saunders JE. The global burden of disabling hearing impairment: a call to action. Bull. World Health Organ. 92(5), 367–373, 2014.

13. Kochkin S. The impact of untreated hearing loss on household income. Better Hear Inst. 1–10, 2005.

14. Adedeji TO, Tobih JE, Sogebi OA, Daniel AD. Management challenges of congenital and early onset childhood hearing loss in a sub-Saharan African country. Int. J. Pediatr. Otorhinolaryngol. 79(10), 1625–1629, 2015.

15. Lee KJ. Essential Otolaryngology. McGraw-Hill Education / Medical 10th Ed., 2012.

16. Hoth S. Audiometry. Springer Handbook of Medical Technology, 2011.

17. Robles L, Ruggero MA. Mechanics of the Mammalian Cochlea. Physiol. Rev. 81(3), 1305–1352, 2001.

18. El Kechai N, Agnely F, Mamelle E, Nguyen Y, Ferrary E, Bochot A. Recent advances in local drug delivery to the inner ear. Int. J. Pharm. 494(1), 83–101, 2015.

19. Thorne M, Salt AN, DeMott JE, Henson MM, Henson OW, Gewalt SL. Cochlear Fluid Space Dimensions for Six Species Derived From Reconstructions of Three-Dimensional Magnetic Resonance Images. The Laryngoscope 109(10), 1661–1668, 1999.

20. Hain T, Helminsky J. Anatomy and Physiology of the normal Vestibular System. Vestibular Rehabilitation F.A. Davis Company 3, 2–18, 2007.

21. Khan S, Chang R. Anatomy of the vestibular system: a review. NeuroRehabilitation 32, 437–443, 2013.

22. Halmagyi M, Curthoys I, Bronstein A. Oxford Textbook of Vertigo and Imbalance. Oxford, 2013.

23. Ohyama K, Salt AN, Thalmann R. Volume flow rate of perilymph in the guinea-pig cochlea. Hear Res. 35(2–3), 119–129, 1988.

24. Juhn SK, Rybak LP, Fowlks WL. Transport characteristics of the blood—Perilymph barrier. Am. J. Otolaryngol. 3(6), 392–396, 1982.

25. Swan EEL, Mescher MJ, Sewell WF, Tao SL, Borenstein JT. Inner ear drug delivery for auditory applications. Adv. Drug. Deliv. Rev. 60(15), 1583–1599, 2008.

26. Ayoob AM, Borenstein JT. The role of intracochlear drug delivery devices in the management of inner ear disease. Expert Opin. Drug Deliv. 12(3), 465–479, 2015.

27. Saito T, Zhang Z-J, Tokuriki M, Ohtsubo T, Noda I, Shibamori Y, Yamamoto T, Saito H. Expression of multidrug resistance protein 1 (MRP1) in the rat cochlea with special reference to the blood–inner ear barrier. Brain Res. 895(1–2), 253–257, 2001.

28. Saito T, Zhang ZJ, Tokuriki M, Ohtsubo T, Noda I, Shibamori Y, Yamamoto T, Saito H. Expression of p-glycoprotein is associated with that of multidrug resistance protein 1 (MRP1) in the vestibular labyrinth and endolymphatic sac of the guinea pig. Neurosci. Lett. 303(3), 189–192, 2001.

29. Chandrasekhar SS, Rubinstein RY, Kwartler JA, Gatz M, Connelly PE, Huang E, Baredes S. Dexamethasone pharmacokinetics in the inner ear: Comparison of route of administration and use of facilitating agents. Otolaryngol. -- Head Neck Surg. 122(4), 521–528, 2000.

30. Volandri G, Di Puccio F, Forte P, Carmignani C. Biomechanics of the tympanic membrane. J. Biomech. 44(7), 1219–1236, 2011.

31. Salt AN, King EB, Hartsock JJ, Gill RM, O'Leary SJ. Marker entry into vestibular perilymph via the stapes following applications to the round window niche of guinea pigs. Hear Res. 283(1–2), 14–23, 2012.

32. Mikulec AA, Plontke SK, Hartsock JJ, Salt AN. Entry of substances into perilymph through the bone of the otic capsule following intratympanic applicatons in guinea pigs: Implications for local drug delivery in humans. Otol. Neurotol. 30(2), 131–138, 2009.

33. Thomson S, Madani G. The windows of the inner ear. Clin. Radiol. 69(3), 146–152, 2014.

34. Rask-Andersen H, Liu W, Erixon E, Kinnefors A, Pfaller K, Schrott-Fischer A, Glueckert R. Human Cochlea: Anatomical Characteristics and their Relevance for Cochlear Implantation. Anat. Rec. Adv. Integr. Anat. Evol. Biol. 295(11), 1791–1811, 2012.

35. Alzamil KS, Linthicum FH. Extraneous round Window Membranes and Plugs: Possible Effect on Intratympanic Therapy. Ann. Otol. Rhinol. Laryngol. 109(1), 30–32, 2000.

36. Gan RZ, Feng B, Sun Q. Three-Dimensional Finite Element Modeling of Human Ear for Sound Transmission. Ann. Biomed. Eng. 32(6), 847–859, 2004.

37. King EB, Salt AN, Kel GE, Eastwood HT, O'Leary SJ. Gentamicin administration on the stapes footplate causes greater hearing loss and vestibulotoxicity than round window administration in guinea pigs. Hear Res. 304, 159–66, 2013.

38. Bergin M, Vlajkovic S, Bird P, Thorne P. Systematic review of animal models of middle ear surgery. World J. Otorhinolaryngol. 3(3), 71–88, 2013.

39. human ear | anatomy. Encyclopedia Britannica. [Internet] [cited-2015-Sep-18]. *http://global.britannica.com/science/ear*

40. Peng AW, Salles FT, Pan B, Ricci AJ. Integrating the biophysical and molecular mechanisms of auditory hair cell mechanotransduction. Nat. Commun. 2, 523, 2011.

41. Kingma H, Janssen M, Bronstein A. Oxford Textbook of Vertigo and Imbalance. Oxford, 2013.

42. Goodall AF, Siddiq MA. Current understanding of the pathogenesis of autoimmune inner ear disease: a review. Clin. Otolaryngol. 40(5), 412–419, 2015.

43. Lobo DR, García-Berrocal JR, Ramírez-Camacho R. New prospects in the diagnosis and treatment of immune-mediated inner ear disease. World J. Methodol. 4(2), 91–98, 2014.

44. Phillips JS, McFerran D. Tinnitus Retraining Therapy (TRT) for tinnitus. Cochrane Database Syst. Rev. 3, 2010.

45. Hoare DJ, Kowalkowski VL, Kang S, Hall DA. Systematic review and meta-analyses of randomized controlled trials examining tinnitus management. The Laryngoscope 121(7), 1555–1564, 2011.

46. Kaltenbach JA. Tinnitus: Models and mechanisms. Hear Res. 276(1–2), 52–60, 2011.

47. Hobson J, Chisholm E, El Refaie A. Sound therapy (masking) in the management of tinnitus in adults. Cochrane Database of Systematic Reviews 11, 2012.

48. Greco A, Gallo A, Fusconi M, Marinelli C, Macri GF, de Vincentiis M. Meniere's disease might be an autoimmune condition? Autoimmun. Rev. 11(10), 731–738, 2012.

49. Pullens B, van Benthem PP. Intratympanic gentamicin for Ménière's disease or syndrome. 2011. Cochrane Database of Systematic Reviews 3, 2011.

50. Phillips JS, Westerberg B. Intratympanic steroids for Ménière's disease or syndrome. Cochrane Database of Systematic Reviews 7, 2011.

51. Schacht J, Talaska AE, Rybak LP. Cisplatin and Aminoglycoside Antibiotics: Hearing Loss and Its Prevention. Anat. Rec. Adv. Integr. Anat. Evol. Biol. 295(11), 1837–1850, 2012.

52. O'Leary SJ, Klis SFL, de Groot JCMJ, Hamers FPT, Smoorenburg GF. Perilymphatic application of cisplatin over several days in albino guinea pigs: dose-dependency of electrophysiological and morphological effects. Hear Res. 154(1–2), 135–145, 2001.

53. van As JW, van den Berg H, van Dalen EC. Medical interventions for the prevention of platinum-induced hearing loss in children with cancer. Cochrane Database of Systematic Reviews 7, 2014.

54. Awad Z, Huins C, Pothier DD. Antivirals for idiopathic sudden sensorineural hearing loss. Cochrane Database of Systematic Reviews 8, 2012.

55. WHO | Grades of hearing impairment. [Internet] [cited-2015-Sep-11]. *http://www.who.int/pbd/deafness/hearing_impairment_grades/en/*

56. Smith RJ, Shearer AE, Hildebrand MS, Van Camp G. Deafness and Hereditary Hearing Loss Overview. 2014. GeneReviews(®). [Internet] [cited-2015-Oct-1]. *http://www.ncbi.nlm.nih.gov/books/NBK1434/*

57. Kuhn M, Heman-Ackah SE, Shaikh JA, Roehm PC. Sudden Sensorineural Hearing Loss: A Review of Diagnosis, Treatment, and Prognosis. Trends Amplif. 15(3), 91–105, 2011.

58. Lin C, Lin S-W, Weng S-F, Lin Y-S. Risk of Sudden Sensorineural Hearing Loss in Patients with Systemic Lupus Erythematosus: A Population-Based Cohort Study. Audiol. Neurotol. 18(2), 95–100, 2013.

59. Carlson ML, Jacob JT, Pollock BE, Neff BA, Tombers NM, Driscoll CLW, Link MJ. Long-term hearing outcomes following stereotactic radiosurgery for vestibular schwannoma: patterns of hearing loss and variables influencing audiometric decline. J. Neurosurg. 118(3), 579–587, 2012.

60. Hellmann MA, Steiner I, Mosberg-Galili R. Sudden sensorineural hearing loss in multiple sclerosis: clinical course and possible pathogenesis. Acta. Neurol. Scand. 124(4), 245–249, 2011.

61. Mosnier I, Stepanian A, Baron G, Bodenez C, Robier A, Meyer B, Fraysse B, Defay F, Ameziane N, Ferrary E, Sterkers O, De Prost D. Cardiovascular and Thromboembolic Risk Factors in Idiopathic Sudden Sensorineural Hearing Loss: A Case-Control Study. Audiol. Neurotol. 16(1), 55–66, 2011.

62. Nguyen KD, Lopez I, Ishiyama G, Ishiyama A. Review of Opioid-Associated Hearing Loss and Possible Mechanism of Opioid-Mediated Endothelin-1-Dependent Cochlear Vasoconstriction. J. Otol. Rhinol. 3:2, 2014.

63. Cannizzaro E, Cannizzaro C, Plescia F, Martines F, Soleo L, Pira E, Coco DL. Exposure to ototoxic agents and hearing loss: A review of current knowledge. Hear Balance Commun. 12(4), 166–175, 2014.

64. Schimmang T, Maconochie M. Gene expression profiling of the inner ear. J. Anat., 2015.

65. Roth TN, Hanebuth D, Probst R. Prevalence of age-related hearing loss in Europe: a review. Eur. Arch. Otorhinolaryngol. 268(8), 1101–1107, 2011.

66. Stachler RJ, Chandrasekhar SS, Archer SM, Rosenfeld RM, Schwartz SR, Barrs DM, Brown S, Fife T, Ford P, Ganiats TG. Clinical Practice Guideline Sudden Hearing Loss. Otolaryngol. -- Head Neck Surg. 146(3), 1–35, 2012.

67. Ealy M, Smith RJH. Otosclerosis. Adv. Otorhinolaryngol. 70, 122–129, 2011.

68. Agarwal L, Pothier DD. Vasodilators and vasoactive substances for idiopathic sudden sensorineural hearing loss. Cochrane Database of Systematic Reviews 4, 2009.

69. Wei BP, Stathopoulos D, O'Leary S. Steroids for idiopathic sudden sensorineural hearing loss. Cochrane Database of Systematic Reviews 7, 2013.

70. Wilson WR, Byl FM, Laird N. The efficacy of steroids in the treatment of idiopathic sudden hearing loss: A double-blind clinical study. Arch. Otolaryngol. 106(12), 772–776, 1980.

71. Nosrati-Zarenoe R, Hultcrantz E. Corticosteroid treatment of Idiopathic Sudden Sensorineural Hearing Loss. Part 1 : a randomized triple-blind placebo controlled trial. 2011.

72. Cinamon U, Bendet E, Kronenberg J. Steroids, carbogen or placebo for sudden hearing loss: a prospective double-blind study. Eur. Arch. Otorhinolaryngol. 258(9), 477–480, 2001.

73. R. J. Stokroos EMT F. W. J. Albers. Antiviral Treatment of Idiopathic Sudden Sensorineural Hearing Loss: A Prospective, Randomized, Double-blind Clinical Trial. Acta. Otolaryngol. 118(4), 488–495, 1998.

74. Westerlaken BO, Stokroos RJ, Wit HP, Dhooge IJM, Albers FWJ. Treatment of Idiopathic Sudden Sensorineural Hearing Loss with Antiviral Therapy: A Prospective, Randomized, Double-Blind Clinical Trial. Ann. Otol. Rhinol. Laryngol. 112(11), 993–1000, 2003.

75. Tucci DL, Farmer JCJ, Kitch RD, Witsell DL. Treatment of Sudden Sensorineural Hearing Loss with Systemic Steroids and Valacyclovir. Otol. Neurotol. 23(3), 301–308, 2002.

76. Uri N, Doweck I, Cohen-Kerem R, Greenberg E. Acyclovir in the treatment of idiopathic sudden sensorineural hearing loss. Otolaryngol Head Neck Surg. 128(4), 544–549, 2003.

77. Ni Y, Zhao X. Carbogen combined with drugs in the treatment of sudden deafness. J. Clin. Otorhinolaryngol. 18(7), 414–415, 2004.

78. Ogawa K, Takei S, Inoue Y, Kanzaki J. Effect of Prostaglandin E1 on Idiopathic Sudden Sensorineural Hearing Loss: A Bouble-Blinded Clinical Study. Otol. Neurotol. 23(5), 665–668, 2002.

79. Poser R, Hirche H. Randomized double-blind study of therapy of sudden deafness. Low molecular weight dextran + naftidrofuryl vs. low molecular weight dextran + placebo. HNO. 40(10), 396–399, 1992.

80. Salt AN, Plontke SK. Principles of Local Drug Delivery to the Inner Ear. Audiol. Neurotol. 14(6), 350–360, 2009.

81. Cochlear Fluids Simulator Page [Internet] [cited-2015-Dec-2] *http://oto2.wustl.edu/cochlea/model3.html*

82. Liu H, Hao J, Li KS. Current strategies for drug delivery to the inner ear. Acta. Pharm. Sin. B 3(2), 86–96, 2013.

83. McCall AA, Leary Swan EE, Borenstein JT, Sewell WF, Kujawa SG, McKenna MJ. Drug Delivery for Treatment of Inner Ear Disease: Current State of Knowledge. Ear Hear 31(2), 156–165, 2010.

84. Pyykkö I, Zou J, Zhang W, Zhang Y. Nanoparticle-based delivery for the treatment of inner ear disorders. Curr. Opin. Otolaryngol. Head Neck Surg. 19(5), 388–396, 2011.

85. Leary Pararas EE, Borkholder DA, Borenstein JT. Microsystems Technologies for Drug Delivery to the Inner Ear. Adv. Drug Deliv. Rev. 64(14), 1650–1660, 2010.

86. Ng JH, Ho RCM, Cheong CSJ, Ng A, Yuen HW, Ngo RYS. Intratympanic steroids as a salvage treatment for sudden sensorineural hearing loss? A meta-analysis. Eur. Arch. Otorhinolaryngol 272(10), 2777–2782, 2014.

87. El Kechai N, Bochot A, Huang N, Nguyen Y, Ferrary E, Agnely F. Effect of liposomes on rheological and syringeability properties of hyaluronic acid hydrogels intended for local injection of drugs. Int. J. Pharm. 487(1–2), 187–196, 2015.

88. Hill SL, Digges ENB, Silverstein H. Long-term follow-up after gentamicin application via the Silverstein MicroWick in the treatment of Ménière's disease. ENT. Ear, Nose & Throat Journal 85 (8), 494-498, 2006.

89. Barriat S, van Wijck F, Staecker H, Lefebvre PP. Intratympanic Steroid Therapy Using the Silverstein Microwick™ for Refractory Sudden Sensorineural Hearing Loss Increases Speech Intelligibility. Audiol. Neurotol. 17(2), 105–111, 2012.

90. Li L, Ren J, Yin T, Liu W. Intratympanic dexamethasone perfusion versus injection for treatment of refractory sudden sensorineural hearing loss. Eur. Arch. Otorhinolaryngol. 270(3), 861–867, 2012.

91. Kanzaki S, Saito H, Inoue Y, Ogawa K. A new device for delivering drugs into the inner ear: Otoendoscope with microcatheter. Auris. Nasus. Larynx. 39(2), 208–211, 2012.

92. Havenith S, Versnel H, Agterberg MJH, de Groot JCMJ, Sedee R-J, Grolman W, Klis SFL. Spiral ganglion cell survival after round window membrane application of brain-derived neurotrophic factor using gelfoam as carrier. Hear Res. 272(1–2), 168–177, 2011.

93. Silverstein H, Arruda J, Rosenberg SI, Deems D, Hester TO. Direct Round Window Membrane Application of Gentamicin in the Treatment of Meniere's Disease. Otolaryngol -- Head Neck Surg. 120(5), 649–655, 1999.

94. James DP, Eastwood H, Richardson RT, O'Leary SJ. Effects of round window dexamethasone on residual hearing in a Guinea pig model of cochlear implantation. Audiol. Neurotol. 13(2), 86–96, 2008.

95. Eastwood H, Chang A, Kel G, Sly D, Richardson R, O'Leary SJ. Round window delivery of dexamethasone ameliorates local and remote hearing loss produced by cochlear implantation into the second turn of the guinea pig cochlea. Hear Res. 265(1–2), 25–29, 2010.

96. Paulson DP, Abuzeid W, Jiang H, Oe T, O'Malley BW, Li D. A Novel Controlled Local Drug Delivery System for Inner Ear Disease. The Laryngoscope 118(4), 706–711, 2008.

97. Lee KY, Nakagawa T, Okano T, Hori R, Ono K, Tabata Y, Lee SH, Ito J. Novel Therapy for Hearing Loss: Delivery of Insulin-Like Growth Factor 1 to the Cochlea Using Gelatin Hydrogel. Otol. Neurotol. 28(7), 976–981, 2007.

98. Salt AN, Hartsock J, Plontke S, LeBel C, Piu F. Distribution of Dexamethasone and Preservation of Inner Ear Function following Intratympanic Delivery of a Gel-Based Formulation. Audiol. Neurotol. 16(5), 323–335, 2011.

99. Lambert PR, Nguyen S, Maxwell KS, Tucci DL, Lustig LR, Fletcher M, Bear M, LeBel C. A Randomized, Double-Blind, Placebo-Controlled Clinical Study to Assess Safety and Clinical Activity of OTO-104 Given as a Single Intratympanic Injection in Patients With Unilateral Ménière's Disease. Otol. Neurotol. 33(7), 1257–1265, 2012.

100. Du X, Chen K, Kuriyavar S, Kopke RD, Grady BP, Bourne DH, Li W, Dormer K. Magnetic Targeted Delivery of Dexamethasone Acetate across the Round Window Membrane in Guinea Pigs. Otol. Neurotol. 34(1), 41–47, 2013.

101. Shimogori H, Yamashita H. Efficacy of intracochlear administration of betamethasone on peripheral vestibular disorder in the guinea pig. Neurosci. Lett. 294(1), 21–24, 2000.

102. Sewell WF, Borenstein JT, Chen Z, Fiering J, Handzel O, Holmboe M, Kim ES, Kujawa SG, McKenna MJ, Mescher MM, Murphy B, Leary Swan EE, Peppi M, Tao S. Development of a Microfluidics-Based Intracochlear Drug Delivery Device. Audiol. Neurotol. 14(6), 411–422, 2009.

103. Douchement D, Terranti A, Lamblin J, Salleron J, Siepmann F, Siepmann J, Vincent C. Dexamethasone eluting electrodes for cochlear implantation: Effect on residual hearing. Cochlear Implants Int. 16(4), 195–200, 2014.

104. Krenzlin S, Vincent C, Munzke L, Gnansia D, Siepmann J, Siepmann F. Predictability of drug release from cochlear implants. J. Controlled Release 159(1), 60–68, 2012.

105. Liu Y, Jolly C, Braun S, Stark T, Scherer E, Plontke SK, Kiefer J. In vitro and in vivo pharmacokinetic study of a dexamethasone-releasing silicone for cochlear implants. Eur. Arch. Otorhinolaryngol. 1–9, 2015.

106. Paasche G, Bögel L, Leinung M, Lenarz T, Stöver T. Substance distribution in a cochlea model using different pump rates for cochlear implant drug delivery electrode prototypes. Hear Res. 212(1–2), 74–82, 2006.

107. Takumi Y, Nishio S, Mugridge K, Oguchi T, Hashimoto S, Suzuki N, Iwasaki S, Jolly C, Usami S. Gene Expression Pattern after Insertion of Dexamethasone-Eluting Electrode into the Guinea Pig Cochlea. PLoS ONE. 9(10), 2014.

108. Farahmand Ghavi F, Mirzadeh H, Imani M, Jolly C, Farhadi M. Corticosteroid-releasing cochlear implant: A novel hybrid of biomaterial and drug delivery system. J. Biomed. Mater. Res. B. Appl. Biomater. 94(2), 388–398, 2010.

109. Malcolm K, Woolfson D, Russell J, Tallon P, McAuley L, Craig D. Influence of silicone elastomer solubility and diffusivity on the in vitro release of drugs from intravaginal rings. J. Controlled Release 90(2), 217–225, 2003.

110. Mond HG, Stokes KB. The Steroid-Eluting Electrode: A 10-Year Experience. Pacing Clin. Electrophysiol. 19(7), 1016–1020, 1996.

111. Kim J, Peng C-C, Chauhan A. Extended release of dexamethasone from silicone-hydrogel contact lenses containing vitamin E. J. Controlled Release 148(1), 110–116, 2010.

112. Hsu K-H, Gause S, Chauhan A. Review of ophthalmic drug delivery by contact lenses. J. Drug Deliv. Sci. Technol. 24(2), 123–135, 2014.

113. Mojsiewicz-Pieńkowska K, Jamrógiewicz M, Żebrowska M, Mikolaszek B, Sznitowska M. Double layer adhesive silicone dressing as a potential dermal drug delivery film in scar treatment. Int. J. Pharm. 481(1–2), 18–26, 2015.

114. Krier F, Riva R, Defrère S, Mestdagt M, Van Langendonckt A, Drion P, Dehoux J-P, Donnez J, Foidart J-M, Jérome C, Evrard B. Device-based controlled local delivery of anastrozol into peritoneal cavity: in vitro and in vivo evaluation. J. Drug Deliv. Sci. Technol. 24(2), 198–204, 2014.

115. Daneshpour N, Collighan R, Perrie Y, Lambert P, Rathbone D, Lowry D, Griffin M. Indwelling catheters and medical implants with FXIIIa inhibitors: A novel approach to the treatment of catheter and medical device-related infections. Eur. J. Pharm. Biopharm. 83(1), 106–113, 2013.

116. Soulas DN, Sanopoulou M, Papadokostaki KG. Proxyphylline release kinetics from symmetrical three-layer silicone rubber matrices: Effect of different excipients in the outer rate-controlling layers. Int. J. Pharm. 427(2), 192–200, 2012.

117. Soulas DN, Sanopoulou M, Papadokostaki KG. Hydrophilic modification of silicone elastomer films: Thermal, mechanical and theophylline permeability properties. Mater. Sci. Eng. C 33(4), 2122–2130, 2013.

118. Brook MA, Holloway AC, Ng KK, Hrynyk M, Moore C, Lall R. Using a drug to structure its release matrix and release profile. Int. J. Pharm. 358(1–2), 121–127, 2008.

119. Schulze Nahrup J, Gao ZM, Mark JE, Sakr A. Poly(dimethylsiloxane) coatings for controlled drug release—polymer modifications. Int. J. Pharm. 270(1–2), 199–208, 2004.

120. Carelli V, Di Colo G. Effect of different water-soluble additives on water sorption into silicone rubber. J. Pharm. Sci. 72(3), 316–317, 1983.

121. Di Colo G, Carelli V, Nannipieri E, Serafini MF, Vitale D. Effect of water-soluble additives on drug release from silicone rubber matrices. II. Sustained release of prednisolone from non-swelling devices. Int. J. Pharm. 30(1), 1–7, 1986.

122. Weaver JD, Song Y, Yang EY, Ricordi C, Pileggi A, Buchwald P, Stabler CL. Controlled Release of Dexamethasone from Organosilicone Constructs for Local Modulation of Inflammation in Islet Transplantation. Tissue Eng. Part A 21(15-16), 2250–2261, 2015.

123. Siepmann J, Peppas NA. Modeling of drug release from delivery systems based on hydroxypropyl methylcellulose (HPMC). Adv. Drug Deliv. Rev. 64, 163–174, 2012.

124. Siepmann J, Göpferich A. Mathematical modeling of bioerodible, polymeric drug delivery systems. Adv. Drug Deliv. Rev. 48(2–3), 229–247, 2001.

125. Siepmann J, Siepmann F, Florence AT. Local controlled drug delivery to the brain: Mathematical modeling of the underlying mass transport mechanisms. Int. J. Pharm. 314(2), 101–119, 2006.

126. Siepmann J, Siepmann F. Mathematical modeling of drug dissolution. Int. J. Pharm. 453(1), 12–24, 2013.

127. Siepmann J, Karrout Y, Gehrke M, Penz FK, Siepmann F. Predicting drug release from HPMC/lactose tablets. Int. J. Pharm. 441(1–2), 826–834, 2013.

128. Siepmann J, Siepmann F. Mathematical modeling of drug delivery. Int. J. Pharm. 364(2), 328–43, 2008.

129. Karami S, Imani M, Farahmandghavi F. A novel image analysis approach for evaluation of mixing uniformity in drug-filled silicone rubber matrix. Int. J. Pharm. 460(1–2), 158–164, 2014.

130. Snorradóttir BS, Jónsdóttir F, Sigurdsson ST, Thorsteinsson F, Másson M. Numerical modelling and experimental investigation of drug release from layered silicone matrix systems. Eur. J. Pharm. Sci. 49(4), 671–678, 2013.

131. Kaunisto E, Marucci M, Borgquist P, Axelsson A. Mechanistic modelling of drug release from polymer-coated and swelling and dissolving polymer matrix systems. Int. J. Pharm. 418(1), 54–77, 2011.

132. Grassi M, Colombo I, Lapasin R. Experimental determination of the theophylline diffusion coefficient in swollen sodium-alginate membranes. J. Controlled Release 76(1–2), 93–105, 2001.

133. Semmling B, Nagel S, Sternberg K, Weitschies W, Seidlitz A. Impact of different tissue-simulating hydrogel compartments on in vitro release and distribution from drug-eluting stents. Eur. J. Pharm. Biopharm. 87(3), 570–578, 2014.

134. Nemati P, Imani M, Farahmandghavi F, Mirzadeh H, Marzban-Rad E, Nasrabadi AM. Dexamethasone-releasing cochlear implant coatings: application of artificial neural networks for modelling of formulation parameters and drug release profile. J. Pharm. Pharmacol. 65(8), 1145–1157, 2013.

135. Nemati P, Imani M, Farahmandghavi F, Mirzadeh H, Marzban-Rad E, Nasrabadi AM. Artificial neural networks for bilateral prediction of formulation parameters and drug release profiles from cochlear implant coatings fabricated as porous monolithic devices based on silicone rubber. J. Pharm. Pharmacol. 66(5), 624–638, 2014.

136. Siepmann J. In-silico simulations of advanced drug delivery systems: What will the future offer? Int. J. Pharm. 454(1), 512–516, 2013.

137. Crank J. The Mathematics of Diffusion. Clarendon Press 2, 1975

138. Siepmann J, Siepmann F. Modeling of diffusion controlled drug delivery. J. Controlled Release 161(2), 351–362, 2012.

139. Ratner BD, Hoffman AS, Schoen FJ, Lemons JE. Biomaterials Science: An Introduction to Materials in Medicine. Academic Press 879, 2004

140. Berrettini S, Baggiani A. Systematic review of the literature on the clinical effectiveness of the cochlear implant procedure in adult patients. Acta. Otorhinolaryngol. 31(5), 299–310, 2011.

141. Endo T, Nakagawa T, Kita T, Iguchi F, Kim T-S, Tamura T, Iwai K, Tabata Y, Ito J. Novel Strategy for Treatment of Inner Ears using a Biodegradable Gel. The Laryngoscope 115, 2016–2020, 2005.

142. Tamura T, Kita T, Nakagawa T, Endo T, Kim T-S, Ishihara T, Mizushima Y, Higaki M, Ito J. Drug Delivery to the Cochlea Using PLGA Nanoparticles. The Laryngoscope 115(11), 2000–2005, 2005.

143. Salt AN, Plontke SKR. Local inner-ear drug delivery and pharmacokinetics. Drug Discov. Today 10(19), 1299–1306, 2005.

144. Müller M. The cochlear place-frequency map of the adult and developing mongolian gerbil. Hear Res. 94(1–2), 148–156, 1996.

145. Choudhury B, Adunka OF, DeMason CE, Ahmad FI, Buchman CA, Fitzpatrick DC. Detection of Intracochlear Damage with Cochlear Implantation in a Gerbil Model of Hearing Loss. Otol. Neurotol. 32(8), 1370–1378, 2011.

146. Jan ANB, Wasil HMS, Manual D. Realistic 3D Computer Model of the Gerbil Middle Ear, Featuring Accurate Morphology of Bone and Soft Tissue Structures Journal of the Association for Research in Otolaryngology 12(6), 681-696, 2011.

147. Hardie NA, MacDonald G, Rubel EW. A new method for imaging and 3D reconstruction of mammalian cochlea by fluorescent confocal microscopy. Brain Res. 1000(1–2), 200–210, 2004.

148. MacDonald GH, Rubel EW. Three-dimensional imaging of the intact mouse cochlea by fluorescent laser scanning confocal microscopy. Hear Res. 243(1–2), 1–10, 2008.

149. Grewal AS, Nedzelski JM, Chen JM, Lin VY. Dexamethasone uptake in the murine organ of Corti with transtympanic versus systemic administration. J. Otolaryngol. - Head Neck Surg. 42(19), 1-7, 2013.

150. Zhang Y, Zhang X, Li L, Sun Y, Sun J. Apoptosis Progression in the Hair Cells in the Organ of Corti of GJB2 Conditional Knockout Mice. Clin. Exp. Otorhinolaryngol. 5(3), 132, 2012.

Résumé

1. Sujet de recherche et son contexte scientifique

L'oreille interne est l'organe responsable de la perception auditive et le maintien de l'équilibre. L'OMS estime que 360 millions personnes dans le monde (plus que 5 % de la population) souffrent d'une perte auditive handicapante, soit 40 dB dans l'oreille qui entend le mieux. L'impact sur la vie personnelle ainsi que professionnelle est considérable : Dans certaines sociétés les patients sont stigmatisés ou partiellement exclus du système éducatif. Ils ont beaucoup plus de mal à accéder au monde du travail et, par conséquence, cela impacte leur niveau de pauvreté.

L'anatomie et physiologie de l'oreille

Afin de comprendre les différentes stratégies permettant de traiter la surdité et les autres maladies de l'oreille interne, l'anatomie et la physiologie de l'oreille vont brièvement être présentées.

L'oreille peut être divisée en trois parties : (i) l'oreille externe avec l'auricule et le conduit auditif externe. Le tympan sépare cette partie de (ii) l'oreille moyenne qui contient la chaîne ossiculaire (le marteau, l'enclume et l'étrier) et le trompe d'eustache qui lie l'oreille moyenne au rhinopharynx et sert à équilibrer les différences de pression. La fenêtre ovale et la fenêtre ronde sont des membranes semi-perméables qui lient l'oreille moyenne avec l'oreille interne. (iii) L'oreille interne consiste de deux parties : la cochlée et le système vestibulaire.

Dans la cochlée saine, une onde sonore est transformée en signaux mécaniques. La perception auditive se fait en plusieurs étapes : Le son arrive à l'auricule de l'oreille externe et est canalisé et transmis pour faire vibrer le tympan. Cette vibration est amplifiée par la chaîne ossiculaire qui fait vibrer la fenêtre ovale. Par conséquence, les différents espaces liquidiens de l'oreille interne sont déplacés. Ces signaux font balancer des cellules ciliées en fonction de la fréquence et de l'amplitude du signal original. Le mouvement des cellules ciliées induit un signal électrique qui est transformé en perception sensorielle dans le cerveau.

La perception de la position de la tête et de son accélération est la fonction principale du système vestibulaire de l'oreille interne. Le mouvement de la tête induit un déplacement de liquide dans les canaux semi-circulaires dans la direction opposée. Par conséquent, les cellules ciliées du système vestibulaire balancent. Ce signal est ensuite traduit en signal électrique et transmis au cerveau pour assurer l'équilibre du corps.

Quand ces systèmes de perception sont perturbés ou endommagés, différentes maladies de l'oreille interne peuvent se manifester, ex : la surdité, les acouphènes, les réactions auto-immunes de l'oreille interne et la maladie de Menière. Souvent, en clinique un mélange des différentes maladies est observé.

La surdité

La surdité est une maladie qui peut être très effrayante pour le patient, particulièrement quand elle apparaît brusquement. En plus de la surdité, les patients peuvent ressentir un épisode d'acouphènes, de vertiges ou autres symptômes.

La surdité peut se présenter sous une forme périnatale ou elle peut être acquise au cours de la vie. Les causes qui mènent à la surdité sont diverses : On différencie les réactions auto-immunes, physiques et chimiques. Les effets physiques peuvent être le résultat d'une exposition à un bruit aigu ou régulier (traumatisme sonore), l'irradiation de la gorge et de la tête lors d'une radiothérapie ou un traumatisme au cours d'une intervention chirurgicale. Les effets chimiques à l'origine d'une surdité, peuvent quant à eux être provoqués par des antibiotiques ototoxiques ainsi qu'une chimiothérapie anticancéreuse. De plus, une infection virale ou un évènement vasculaire peuvent être à l'origine de surdités brusques. La surdité peut aussi résulter d'une réaction auto-immune déficitaire. Par conséquent, les cellules ciliées peuvent être endommagées, une dégénération de la stria vascularis ou une perte de cellules du ganglion spiral peut se produire. La dimension et la réversibilité de la maladie dépendent fortement de la cause de la surdité. Malheureusement, dans la majorité des cas, la cause de la maladie reste incertaine.

Le traitement est aussi relié à la cause de la maladie. Si celle-ci est connue, le patient est traité en conséquence. Sinon, le patient reçoit souvent des stéroïdes par voie orale ou

intra-tympaniques. Ces stéroïdes sont utilisés pour prévenir les inflammations ou œdèmes pouvant endommager les très sensibles cellules ciliées de l'oreille interne. D'autres stratégies incluent l'administration orale de principes actifs antiviraux, de diurétiques, de vasodilatateurs, d'antioxydants, un traitement avec de l'oxygène hyperbare ou des traitements chirurgicaux de l'oreille. L'application d'un appareil auditif tel que l'implantation d'un implant cochléaire peut être nécessaire si la surdité persiste. Un implant cochléaire transforme de la même façon que les cellules ciliées un son en signal électrique qui peut être retraduit en perception auditive dans le cerveau. L'électrode est reliée à un amplificateur implanté derrière l'oreille du patient. L'implantation d'une électrode dans la scala tympani de l'oreille interne peut alors aider à reconstituer la perception sensorielle.

Libération de principes actifs à l'oreille interne

L'administration d'un principe actif dans l'oreille interne constitue un véritable challenge de par la barrière hémato-cochléaire qui est comparable à la barrière hémato-encéphalique et protège l'oreille de substances toxiques. L'administration d'un principe actif par les voies classiques (orale, intraveineuse, intramusculaire) ne permet pas d'atteindre des concentrations suffisantes au niveau de l'oreille interne pour traiter une maladie. Les jonctions serrées de la barrière hémato-cochléaire peuvent être contournées par un dosage systémique très élevé du principe actif. Une dose élevée de dexaméthasone peut par exemple être une bonne prévention contre la perte de perception auditive lors de l'insertion d'un implant cochléaire. Cependant, un dosage systémique élevé peut mener à des effets secondaires très graves. De la même façon, l'injection locale dans l'oreille interne d'un principe actif ne semble pas favorable car la solution peut s'écouler par le canal d'injection. De plus, pour le traitement d'une maladie chronique plusieurs injections sont nécessaires, augmentant le risque d'infection. La cochlée, est relativement étanche et extrêmement sensible aux changements mineurs de pression et représente donc un espace assez délicat avec un volume très faible.

C'est pourquoi, une administration locale et unique peut fournir de grands avantages. Plusieurs possibilités pour une administration prolongée ont été décrites. L'application d'un hydrogel semi-solide sur la fenêtre ronde peut créer une matrice qui libère le principe actif d'une manière prolongée. Par contre, le gel ne pouvant pas être fixé in vivo, il risque d'être

éliminé très rapidement. En outre, le temps d'exposition et l'anatomie de la fenêtre ronde peut varier d'un patient à l'autre. De plus, la périlymphe (fluide principal dans la cochlée) peut être considérée comme un fluide non-agité avec un transport de masse négligeable. Par conséquent, un principe actif administré dans l'oreille moyenne risque de ne pas être distribué de manière homogène dans la périlymphe de l'oreille interne. D'un point de vue clinique, un autre obstacle doit être surmonté: la taille minuscule de la cochlée et sa difficulté anatomique d'accès.

Pour un traitement à long terme une libération à partir d'implants miniaturisés semble prometteuse : Créer des implants cubiques avec un cylindre peut donc aider à franchir toutes les restrictions mentionnées ci-dessus. L'implant étant partiellement inséré sur (ou à côté de) la fenêtre ovale, il permet de libérer le PA de manière contrôlée pendant des mois ou des années. Néanmoins, cette intervention est relativement invasive et le bénéfice pour chaque patient doit être évalué en détail.

Cet implant pourra consister d'une matrice polymérique, notamment à base de silicone à cause de ses excellentes propriétés mécaniques et son innocuité.

La mobilité de la dexaméthasone dans une matrice de silicone

Le silicone chargé en principe actif n'est pas seulement utilisé pour traiter les maladies de l'oreille interne, par exemple à partir des électrodes d'un implant cochléaire chargé en dexaméthasone, mais aussi pour traiter des pathologies très diverses telles que le traitement de maladies du vagin, du cœur, de l'œil ou pour améliorer la cicatrisation.

La libération de principe actif à partir de silicone peut être maintenue pendant des années : Du silicone chargé en dexaméthasone a été implanté avec succès dans des pacemakers. Après 10 ans d'implantation, une amélioration du fonctionnement de l'électrode est observée comparativement aux pacemakers non chargés en principe actif.

Pour ajuster la libération du principe actif, plusieurs paramètres peuvent être variés tels que le type de chaînes latérales, l'ajout d'additifs, ou encore le taux de principe actif. De plus, la géométrie et les dimensions du système peuvent avoir une grande influence sur la libération car ils impactent la longueur du « trajet » à parcourir par le principe actif pour être libéré. Ceci

est d'autant plus important de par la nature plutôt hydrophobe du polymère ralentissant la pénétration de l'eau dans la matrice et par conséquent la libération du principe actif. L'ajout d'additifs hydrophiles, comme le polyéthylène glycol, facilite la pénétration de l'eau et donc la libération du principe actif.

Objectif de recherche

L'objectif de ces travaux était de développer de nouveaux implants miniaturisés pour le traitement de maladies telles que la surdité et les acouphènes. Les systèmes sont basés sur le silicone, un polymère biocompatible, chargé en dexaméthasone pour la libération contrôlée de dexaméthasone dans l'oreille interne.

Les principaux objectifs de cette thèse incluent :

(i) La préparation et la caractérisation des matrices chargés en principe actif in vitro afin d'identifier des outils simples pour ajuster le taux de libération. Plusieurs paramètres de formulation ont été évalués : Le taux de polyéthylène glycol ajouté ainsi que la variation du poids moléculaire de ce dernier. De plus, la structure chimique du silicone et son taux initial ont été varié. Les mécanismes de libération ont été élucidés par modélisation mathématique.

(ii) Conception d'implants chargés en dexaméthasone en utilisant le silicone le plus prometteur. Préparation des films et des implants pour les caractériser in vitro.

(iii) Conception d'implants se formant in situ chargés en dexaméthasone en utilisant le silicone le plus prometteur. Préparation des films et des implants pour les caractériser in vitro. La formulation a également été évaluée in vivo en se basant sur un modèle de gerbilles. Le principe actif a été détecté dans la cochlée explantée par microscopie confocale laser.

2. Matériels et méthodes

Préparation des matrices chargées en dexaméthasone :

Films - Silicone pâteux

Les Partie A et B du kit de silicone ont été mélangées séparément puis réunies dans un laminoir (Chef Premier KMC 560/AT970A, Kenwood, Havant, UK). Le principe actif a été introduit petit à petit dans les parties A et B afin d'éviter toute perte. La masse a été mélangée jusqu'à obtenir un mélange homogène. La masse ainsi obtenue a été introduite entre deux couches de Teflon pour ajuster l'épaisseur du film lors de son passage dans le laminoir. La réticulation a été effectuée dans une étuve à 60 °C pendant 24 h.

Films - Silicone liquide

Les Partie A et B du kit de silicone ont été mélangées dans un mortier refroidi par des glaçons (pour ralentir la réticulation). Le principe actif a été introduit petit à petit dans les parties A et B afin d'éviter toute perte. La masse a été mélangée jusqu'à obtenir un mélange homogène. La masse ainsi obtenue a été introduite entre deux couches de Teflon pour ajuster l'épaisseur du film lors de son passage dans le laminoir. La réticulation a été effectuée dans une étuve à 60 °C pendant 24 h.

Pour la préparation des films chargés à la fois en dexaméthasone et en polyéthylène glycol (PEG), le PEG était préalablement mélangé avec le principe actif avant d'introduire ce mélange PEG-dexaméthasone dans le silicone comme décrit ci-dessus.

Les films sans principe actif étaient préparés en conséquence sans ajout de dexaméthasone.

Implants « Ear Cube »

Le mélange silicone liquide-dexaméthasone a été préparé comme décrit ci-dessus et mis en seringue et injecté dans le moule à implants. Après réticulation des implants à 60 °C, les implants ont été démoulés précautionneusement sous macroscope.

Implants se formant in situ

Le mélange PEG-dexaméthasone a été introduit séparément dans les partie A et B du kit de silicone, puis introduit séparément dans une double seringue pour éviter la réticulation

rapide du silicone intervenant par contact entre les 2 parties du silicone. L'implant s'est formé in situ après mélange des deux composants à température ambiante ou in vivo.

Caractérisation in vitro :

- **Etudes de libération**

Les cinétiques de libération du principe actif à partir des formulations en silicone ont été réalisées dans de la périlymphe artificielle (solution aqueuse contenant : 1,2 mmol de chlorure de calcium dihydraté, 2mmol de sulfate de magnesium tétrahydraté, 2,7 mmol de chlorure de potassium, 145 mmol de chlorure de sodium et 5 mmol de HEPES). L'analyse du principe actif a été réalisée par HPLC-UV.

Films

La libération du principe actif à partir des films a été réalisée dans de la périlymphe artificielle à 37 °C (80 tours/min). A des temps prédéfinis, 1 mL du milieu de libération a été prélevé puis remplacé par de la périlymphe artificielle fraîche.

Cellule de diffusion

Un film sans principe actif a été placé dans une cellule de diffusion horizontale pour suivre la diffusion de la dexaméthasone : Le compartiment donneur comportait une solution saturée en principe actif, le compartiment receveur était quant à lui rempli de tampon initialement exempt de principe actif. A des temps prédéfinis, 1 mL du milieu de libération était prélevé puis remplacé par de la périlymphe artificielle fraîche.

Implants « Ear Cube »

Des implants « Ear Cube » ont été placés dans un tube Eppendorf coupé à la moitié de sa hauteur. Un trou de 0,4 mm percé dans le fond du tube permettait d'imiter la situation in vivo (l'implant est destiné a être placé dans l'oreille moyenne et donc est en contact avec la périlymphe au travers d'un trou). Pour maintenir l'implant en place, ce-denier était fixé avec du silicone. Ce tube était fixé dans un deuxième tube intact rempli avec 100 µl de périlymphe artificielle. A des temps prédéfinis, tout le milieu de libération était prélevé puis remplacé par la périlymphe artificielle fraîche.

Implants se formant in situ

Des implants se formant in situ ont été placés dans un tube Eppendorf coupé à la moitié de sa hauteur. Un trou de 0,35 mm percé dans le fond du tube permettait d'imiter la situation in vivo (l'implant est destiné à être placé dans l'oreille moyenne et donc est en contact avec la périlymphe au travers d'un trou). Pour maintenir l'implant en place, ce-denier était fixé avec du silicone. Ce tube était fixé dans un deuxième tube intact rempli avec 100 µl de périlymphe artificielle. A des temps prédéfinis, tout le milieu de libération était prélevé puis remplacé par la périlymphe artificielle fraîche.

- **Caractérisation physico-chimique**

SEM

La morphologie interne des formulations a été caractérisées par Scanning Electron Microscopy (S-4000; Hitachi High-Technologies Europe, Krefeld, Germany). Pour ce faire, le silicone chargé en dexaméthasone était congelé dans de l'azote liquide et brisé en deux pour scanner le point de rupture de la matrice.

DSC

Des implants « Ear Cube » ont été caractérisés par Differential Scanning Calorimetry (DSC Q10, TA Instruments, Guyancourt, France). Les implants étaient coupés (pour éviter un bruit de fond généré par la géométrie inégale de l'implant) et placés dans une coupelle ouverte. La poudre de dexaméthasone était analysée en conséquence. Les échantillons étaient refroidis à -150 °C et chauffés à 280 °C (10 K/min).

X-ray diffraction

Les implants « Ear Cube » ont été analysés par X-ray diffraction (PANalytical, Almelo, Netherlands) en mode transmission sous rotation. Les implants étaient coupés et seulement les cubes étaient placés dans les capillaires pour être analysés.

- **Etudes in vivo**

Les études in vivo ont été réalisées par Mme Julie Sircoglou.

Trois groupes de gerbilles étaient analysés :

▪ 13 gerbilles recevaient des implants se formant in situ. Ils étaient sacrifiés 20 min, 7 et 30 jours après l'implantation.

▪ 2 gerbilles recevaient plusieurs injections de solution de dexaméthasone (intra-tympanique) pour prouver la spécificité de l'anticorps anti-dexaméthasone.

▪ 2 gerbilles ne recevaient pas de traitement (contrôle négatif).

Les implants étaient implantés à côte de l'étrier en faisant un trou de 0,35 mm sous anesthésie générale. La formulation contenait 5 % de polyéthylène glycol 400 et 10 % de dexaméthasone.

Après avoir sacrifié des gerbilles, les cochlées étaient explantées et analysées par microscopie confocale à balayage laser.

3.   Résultats et discussion

La mobilité de la dexaméthasone dans les films

Dans un premier temps, de fins films de silicone chargés en principe actif (PA) ont été préparés et caractérisé in vitro. La libération à partir de ces films peut être ajustée en modifiant le type de silicone (ex : le type des chaînes latérales, degré de réticulation) ou en ajoutant différents quantités de PEG 400 ou 1000.

Dans le cas du silicone liquide, l'ajout de PEG augmente la libération du principe actif. L'ajout de différents ratios de PEG a une plus grande influence sur la libération que la variation du poids moléculaire de PEG :

(i)   L'ajout d'une concentration plus élevée de PEG augmente la vitesse de libération.

(ii)   L'introduction de PEG de poids moléculaire plus élevé augmente la vitesse de libération.

La modélisation mathématique effectuée considère que la diffusion est le principal mécanisme de la libération du principe actif (solutions analytiques et numériques de la 2nde loi de diffusion de Fick) ainsi que la solubilité du principe actif (modèles prenant en compte l'effet des limites de solubilité du principe actif, les processus de dissolution contrôlés par diffusion, les effets de couche stationnaire). L'érosion, le gonflement et la dissolution du polymère peuvent être négligés car le polymère est insoluble et ne gonfle pratiquement pas dans l'eau. L'analyse mathématique est réalisée sur de fins films de silicone chargés en principe actif afin de déterminer rapidement le coefficient de diffusion du principe actif.

Les coefficients de diffusion « apparents » ont été déterminés : pour MED-4011 ils varient de D = 5,51 ± 1,71 à 64,54 ± 0,64 x 10^{-14} cm^2/s, de D = 7,59 ± 0,58 à 72,04 ± 17,96 x 10^{-14} cm^2/s pour le silicone MED-6015 et de D = 22,41 ± 0,16 à 232,41 ± 5,78 x 10^{-14} cm^2/s pour MED-6755 (tous pour les films sans PEG et les films contenants 10 % PEG 1000). Une bonne concordance était observée entre les cinétiques déterminées expérimentalement et calculées théoriquement avec ou sans ajout de PEG. Cela indique que la libération est très probablement contrôlée par diffusion. Il faut noter que la matrice contient des cristaux de PA – ce qui n'est pas pris en compte dans l'équation utilisée. C'est pourquoi le terme coefficient de diffusion « apparent » est utilisé.

Les coefficients de diffusion « apparents » calculés sont conformes aux tendances observées sur les courbes de libération : Le coefficient le plus élevé correspond au film contenant 10 % de PEG 1000.

Les cinétiques de libération des films préparés avec le silicone pâteux augmentent également par ajout de l'agent hydrophile dans la matrice. Par contre, les courbes de libérations calculées théoriquement diffèrent énormément des courbes observées expérimentalement. Les courbes calculées concordent seulement pour les films sans PEG. Ceci est une indication que la libération dans les films chargés en PEG n'est pas seulement contrôlée par diffusion mais d'autres processus interviennent.

La modélisation a également été effectuée sur différents types de silicone et pour modéliser la libération de dexaméthasone à partir des films chargés en 10 à 50 % de PA.

Basé sur ces résultats expérimentaux, le coefficient de diffusion du principe actif a été utilisé pour prédire de manière quantitative l'effet de différents paramètres de formulation et de procédé sur les cinétiques de libération résultantes pour des extrudats. Ces prédictions permettraient de faciliter et surtout d'accélérer l'optimisation de tels implants.

Implant « Ear Cube »

Deux types d'implants ont été préparés en se basant sur les systèmes les plus prometteurs.

Le premier est l'implant miniaturisé « Ear Cube » ayant une forme prédéfinie avec un cube lié à un cylindre. Ce cylindre est en contact avec la périlymphe de l'oreille interne. L'administration sous forme d'implant est moins invasive comparé à un implant cochléaire « classique » mais une cochleostomie est néanmoins nécessaire. L'implant peut être fixé sur la platine de l'étrier ou sur la fenêtre ovale en utilisant un polymère, ex du silicone qui réticule vite, in vivo.

Simlairement aux films présentés précédemment, l'implant paraît opaque et blanc en raison des cristaux de PA piégés dans la matrice. Les cristaux sont bien visibles sur les images SEM.

La DSC et la diffraction des rayons X ont confirmés ces résultats : La courbe DSC des implants « Ear Cube » chargés en dexaméthasone analysés contient un pic correspondant au PA observé avec la poudre seule. La surface du pic confirme que presque tout le PA inséré dans la matrice est présent sous une forme cristalline. Les rayons X confirme ces résultats car la courbe de l'implant non-chargé ne présente pas de pics. Par contre, la courbe observée avec un implant chargé présente des pics de dexaméthasone.

Des films chargés en dexaméthasone ont été préparés pour servir de modèle simplifié pendant le développement de l'implant. Encore une fois, la libération est modélisée en se basant sur une solution analytique de la 2nde loi de diffusion de Fick.

Les courbes théoriques concordent avec les courbes observées expérimentalement. La libération de dexaméthasone était donc contrôlée par diffusion et les coefficients de diffusion « apparents » ont été calculés.

Le transport de dexaméthasone à travers une membrane en silicone a été réalisé pour comparer le coefficient de diffusion calculé pour la cellule de diffusion avec les valeurs calculés pendant la libération de PA à partir des films chargés. Le coefficient de diffusion trouvé dans le silicone non-chargé est de $1,9 \times 10^{-9} \, cm^2/s$. Comparé aux valeurs des films chargés en PA ($3,4$ à $4,9 \times 10^{-14} \, cm^2/s$), la valeur du silicone non-chargé est beaucoup plus haute. La différence peut s'expliquer par la solubilité limitée de la dexaméthasone dans la matrice et la faible quantité de l'eau présente dans les films. Pour prédire la libération de

principe actif, le coefficient de diffusion « apparent » peut malgré tout être utilisé car l'impact sur les valeurs prédites pourrait peut-être être négligeable. Il faut considérer tous les facteurs qui influencent le système choisi.

La libération à partir des implants « Ear Cube » a été prédite en utilisant deux modèles se basant sur les coefficients de diffusion « apparents » observés sur les films chargés :

(i) Un modèle qui considère la libération du PA à partir d'un cylindre.

(ii) Un modèle qui considère la libération seulement à partir d'un cercle en bas du cylindre.

Les calculs faits en utilisant le modèle (i) résultent en plus hautes concentration prédites comparés au modèle (ii) qui prédit des plus faibles concentrations libérés par le cercle. Les deux modèles prédisent une libération très faible pendant les deux premiers mois de la libération : Seulement 0,06 à 1,45 %, ou 0,046 à 2,35 µg dexaméthasone sont libérés selon les deux modèles. La libération in vivo peut donc être contrôlée sur de très longues périodes.

Les implants « Ear Cubes » ont été préparés en réalité et la libération comparée avec les valeurs prédites par les deux modèles. Presque tous les résultats sont situés entre les les cinétiques de libération prédites par les deux modèles. Il faut admettre que les implants libèrent la PA in vivo probablement pas seulement à travers le cylindre. Il est possible que la dexaméthasone soit libérée à partir du cube à travers la fenêtre ovale. Ce phénomène n'était pas simulé avec le setup utilisé. Par conséquent, il est fort probable que la libération in vivo soit plus élevée comparée aux tests in vitro.

L'étude de gonflement sert à exclure le phénomène de changement de dimension qui peut être crucial pour la faisabilité in vivo : Un implant qui gonfle pourrait avoir des effets néfastes pour le patient, notamment douloureux. L'absence de gonflement a été confirmée pour une période d'au moins 60 jours.

Implant se formant in situ

Le second implant est un implant se formant in situ qui s'adapte parfaitement à l'anatomie de l'oreille moyenne en réticulant directement dans l'oreille moyenne. Cet implant est en contact avec l'oreille interne par un orifice.

In vitro, le filme chargé à 10 % de dexaméthasone et de 5 % de PEG 400, montre une libération contrôlée pendant au moins 30 jours. Encore une fois, la libération était contrôlée par diffusion car une solution analytique de la 2nde loi de diffusion de Fick montre des résultats en concordance avec les courbes de libération qui étaient observés in vitro. Le coefficient de diffusion « apparent » est de D = 1.2 x 10^{-11} cm^2/s.

La libération à partir de l'implant est continue pendant la période d'observation. Le taux de dexaméthasone libéré est très faible comparé à la libération à partir des films. Ce phénomène peut s'expliquer par la surface très petite de l'implant en contact avec la périlymphe artificielle.

La microscopie confocale laser a été utilisée pour confirmer la présence des cristaux de dexaméthasone dans les films chargés en PA.

In vivo, la dexaméthasone a été détectée dans la cochlée. En préservant la structure intégrale de la cochlée, l'architecture de la cochlée a pu être observée. Les acquisitions tridimensionnelles permettent d'examiner les cellules de l'oreille interne sous plusieurs points de vue.

Plusieurs témoins non-implantés ou chargés avec les différentes étapes de l'immuno-marquage permettent de prouver la spécificité du marquage.

Les cochlées, explantés après 20 min, 7 jours et 30 jours montrent toutes une fluorescence indiquant que la dexaméthasone est libérée dans l'oreille interne. Le PA peut être détecté déjà 20 min après implantation jusqu'à au moins 30 jours avec une intensité maximale à 7 jours après implantation.

Un zoom sur les cellules ciliées prouve que la dexaméthasone est absorbée par ces cellules – même sur la rangée des cellules ciliées interne le PA peut être détectée.

4. Conclusion

Le traitement de la surdité et des autres maladies de l'oreille interne reste un challenge car l'étiologie de ces maladies reste dans la plupart des cas inconnue. Des thérapies ciblant un traitement local et contrôlé de la cochlée sont actuellement e cours de développement. Les difficultés majeures sont les dimensions très petites de la cochlée et la sensibilité des cellules ciliées envers les changements de pression. Un principe actif tel que la dexaméthasone peut être incorporé dans le polymère et libéré de manière prolongée et homogène dans la périlymphe. Ainsi, la dexaméthasone peut aider à prévenir l'inflammation et la perte de nombreuses cellules ciliées après l'opération. Pour cela, deux types d'implants miniaturisés ont été développés.

Dans la première partie, des films chargés en dexaméthasone ont été préparés pour identifier différentes stratégies permettant d'ajuster les cinétiques de libération in vitro. Pour ce faire, différents types de silicones ont été testés de même que l'ajout d'un agent hydrophile, le PEG. Le taux et la masse moléculaire du PEG ont été variés. Ces différentes stratégies permettent d'atteindre une large gamme de cinétiques de libération.

Ces résultats ont été utilisés pour optimiser la libération de dexaméthasone in vitro à partir des implants « Ear Cube ». Ces implants miniaturisés ont l'avantage d'avoir une forme prédéfinie qui permet aussi de prédire de manière quantitative la libération à partir du cylindre de l'implant inséré sur (ou à côté de) la fenêtre ovale.

Le deuxième implant consiste d'un silicone liquide réticulant très vite quand les deux composés sont mélangés. De plus, la formulation se présente sous forme liquide, et est donc très facile à gérer par le chirurgien avant implantation. Un autre avantage est que cet implant prend la forme de l'oreille du patient, et s'adapte donc parfaitement. La libération in vitro est prolongée pendant au moins 30 jours, ce qui est confirmé par des images de microscopie confocale à balaye laser. La dexaméthasone est détectée après 20 min jusqu'à au moins 30 jours après l'implantation.

Ainsi, les deux implants semblent prometteurs pour contrôler à long terme la libération de dexaméthasone directement dans l'oreille interne. A l'avenir, des études pour évaluer les effets des implants « Ear Cube » seront menées. De plus, ces systèmes pourraient être adaptés pour délivrer d'autres PA, ex : la gentamicine, pour traiter d'autres maladies.

List of Publications

Research Articles

Gehrke, M; Sircoglou, J; Gnansia, D; Tourrel, G; Lacante, E; Vincent, C; Siepmann, J; Siepmann, F (2016) Ear Cubes for Local Controlled Drug Delivery to the Inner Ear. Int. J. Pharm. *Accepted*

Gehrke, M; Sircoglou, J; Vincent, C; Siepmann, J; Siepmann, F (2016) How to adjust dexamethasone mobility in silicone matrices: A quantitative treatment. Eur. J. Pharm. Biopharm. 100, 27-37.

Sircoglou, J; Gehrke, M; Tardivel, M; Siepmann, F; Siepmann, J; Vincent, C (2015) Trans-Oval-Window Implants, A New Approach for Drug Delivery to the Inner Ear: Extended dexamethasone release from silicone-based implants. Otology & Neurotology, 36(10), 1572-1579.

Siepmann, J; Karrout, Y.; Gehrke, M; Penz, FK; Siepmann, F (2013) Predicting drug release from HPMC/lactose tablets. Int. J. Pharm. 441, 826-834.

Oral Communications

Siepmann, J; Gehrke, M; Sircoglou, J; Vincent, C; Siepmann, F (2014) Local Controlled Drug Delivery to the Inner Ear. 1st International AMPTEC Conference (Advanced Materials and Pharmaceutical Technologies), Lille, France.

Gehrke, M; Vincent, C; Siepmann, J; Siepmann, F (2013) Adjustment of drug release of dexamethasone from cochlear implants. 7th Pharmaceutical Solid State Cluster Annual Meeting, Lille, France.

Gehrke, M; Krenzlin, S; Vincent, C; Gnansia, D; Siepmann, F; Siepmann, J (2012) In silico simulation of cochlear implants loaded with dexamethasone. 6th Pharmaceutical Solid State Cluster Annual Meeting, Lisbon, Portugal.

Poster Presentations

Gehrke, M; Verin, J; Gnansia, D; Tourrel, G; Vincent, C; Siepmann, J; Siepmann, F (2016) Hybrid Ear Cubes for Controlled Dexamethasone Delivery to the Inner Ear. 10th World Meeting on Pharmaceutics, Biopharmaceutics and Pharmaceutical Technology, Glasgow, UK.

Gehrke, M; Sircoglou, J; Gnansia, D; Tourrel, G; Vincent, C; Siepmann, J; Siepmann, F (2016) Ear Cubes: A New Approach for Local Controlled Drug Delivery to the Inner Ear. 10th World Meeting on Pharmaceutics, Biopharmaceutics and Pharmaceutical Technology, Glasgow, UK.

Sircoglou, J; Gehrke, M; Tardivel, M; Siepmann, F; Siepmann, J; Vincent, C (2016) In-situ Forming Trans-Oval-Window Implants for Controlled Drug Delivery to the Inner Ear. 10th World Meeting on Pharmaceutics, Biopharmaceutics and Pharmaceutical Technology, Glasgow, UK.

Siepmann, F; Karrout, Y; Gehrke, M; Penz, F; Siepmann, J (2015) Even in the Case of Freely Water-Soluble Drugs Limited Solubility Effects can Play a Major Role in the Control of Drug Release from HPMC Tablets. AAPS Annual Meeting and Exposition, Orlando, USA.

Siepmann, F; Karrout, Y; Gehrke, M; Moussa, E; Penz, F; Siepmann, J (2015) Computer-Aided Design of Controlled Release HPMC:Lactose-based Tablets. AAPS Annual Meeting and Exposition, Orlando, USA.

Gehrke, M; Sircoglou, J; Vincent, C; Siepmann, J; Siepmann, F (2015) Importance of diffusion and limited drug solubility in silicone matrices for cochlear implants. 1st European Conference on Pharmaceutics: Drug Delivery, Reims, France.

Gehrke, M; Vincent, C; Siepmann, J; Siepmann, F (2014) How Dexamethasone release can be adjusted from silicone matrices. 1st International AMPTEC Conference (Advanced Materials and Pharmaceutical Technologies), Lille, France.

Gehrke, M; Vincent, C; Siepmann, J; Siepmann, F (2014) How Dexamethasone release can be adjusted from silicone matrices. 9th World Meeting on Pharmaceutics, Biopharmaceutics and Pharmaceutical Technology, Lisbon, Portugal.

Gehrke, M; Vincent, C; Siepmann, J; Siepmann, F (2013) How to adjust desired drug release kinetics from cochlear implants. 3rd Conference on Innovation in Drug Delivery: Advances in Local Drug Delivery, Pisa, Italy.

Gehrke, M; Vincent, C; Siepmann, J; Siepmann, F (2013) How to adjust desired drug release kinetics from cochlear implants. Forum du Prim " Rencontres de la Chimie, de la Biologie et de la Physique ", Lille, France.

Siepmann, F; Karrout, Y.; Gehrke, M; Penz, FK; Siepmann, J (2013) A simple mathematical model allowing for the prediction of drug release from HPMC/lactose-based controlled release matrix tablets. AAPS Annual Meeting and Exposition, San Antonio, USA.

Gehrke, M; Krenzlin, S; Vincent, C; Gnansia, D; Siepmann, J; Siepmann, F (2012) In silico simulation of cochlear implants loaded with dexamethasone. 4ème réunion annuelle de l'ITS, Lille, France.

Siepmann, F; Karrout, Y.; Gehrke, M; Penz, FK; Siepmann, J (2012) Modeling Drug Release From RetaLac® Tablets: Impact of Drug Solubility. AAPS Annual Meeting and Exposition, Chicago, USA.

Curriculum Vitae

Name   Maria Gehrke

Birth   November 19, 1985 in Berlin, Germany

Nationality   German

Career

Since 2016   Post-Doc at the Université de Lille, France

2012 - 2016   Ph.D. student at the Université de Lille, France
                Subject: "Controlled Release of Dexamethasone to the Inner Ear from silicone-based Implants"
                Supervisor: F. Siepmann, C. Vincent
                Laboratory: INSERM U1008 Controlled Drug Delivery Systems and Biomaterials

2012   License to practice in a Pharmacy

2011   Internship at the Pharmacy Prisma-Apotheke, Berlin, Germany

2010   Internship at the Université de Lille, France
                Subject: "Preparation and characterization of controlled release matrices"
                Supervisor: F. Siepmann, Y. Karrout
                Laboratory: INSERM U1008 Controlled Drug Delivery Systems and Biomaterials

2005 - 2010   Pharmaceutical studies at the Ernst-Moritz-Arndt-Universität Greifswald, Germany

2005   High School Diploma at the Oberschule an der Weide, Berlin, Germany

Voluntary internships

2009   Coordinating Center for Clinical Studies (KKS Charité), Berlin, Germany

2008   Hospital Pharmacy Charité, Berlin, Germany

2006   Pharmacy Apotheke im Friedrichshain, Berlin, Germany

                Hospital Pharmacy Vivantes Klinikum Neukölln, Berlin, Germany

2004   Pharmacy Apotheke am Ostbahnhof, Berlin, Germany

                Hospital Pharmacy Vivantes Klinikum im Friedrichshain, Berlin, Germany

Assistance in organizing Workshops and Symposia

2nd APGI Poorly Soluble Drugs Workshop (Lille, France), 2014 – 150 participants

7th Pharmaceutical Solid State Research Cluster Symposium (Lille, France) 2013 – 200 participants

2nd APGI Coating Workshop (Lille, France), 2013 – 150 participants

Reviewer for scientific Journals

International Journal of Pharmaceutics

Training of pharmaceutical and medical Students

Michaël Risoud: Université de Lille, France
Master student, ENT specialist (12 months)

Jérémy Verin: Université de Lille, France
Research assistant (3 months)

Coralie Lacheretz: Université de Lille, France
Master student, dentist (12 months)

Emmely Lacante: Universiteit Gent, Belgium
Master student, pharmacist (4 months)

Sanja Puric: Univerza V Ljubljani, Slovenia
Master student, pharmacist (4 months)

Julie Sircoglou: Université de Lille, France
Master student, ENT specialist (12 months)

Pierre Stievenard: Université de Lille, France
Internship student (1 month)

Guillaume Dedieu: Université de Lille, France
Internship student (0.5 months)

Linguistic skills

German (mother tongue)

English and French (fluent in spoken and written)

Latin